MECHANISM AND INHIBITION OF THE PHENYLETHYLAMINE OXIDASE FROM *Arthrobacter globiformis*

by

Gregory Alexander Juda

A dissertation submitted in partial fulfillment
of the requirements for the degree

of

Doctor of Philosophy

in

Biochemistry

MONTANA STATE UNIVERSITY
Bozeman, Montana

April 2005

APPROVAL

of a dissertation submitted by

Gregory Alexander Juda

This thesis has been read by each member of the thesis committee and has been found to be satisfactory regarding content, English usage, format, citations, bibliographic style, and consistency, and is ready for submission to the College of Graduate Studies.

David M Dooley

Approved for the Department of Chemistry and Biochemistry

Paul A. Grieco

Approved for the College of Graduate Studies

Bruce R. McLeod

STATEMENT OF PERMISSION TO USE

In presenting this thesis in partial fulfillment of the requirements for a doctoral degree at Montana State University, I agree that the Library shall make it available to borrowers under rules of the Library. I further agree that copying of this dissertation is allowable only for scholarly purposes, consistent with "fair use" as prescribed in the U.S. Copyright Law. Requests for extensive copying or reproduction of this dissertation should be referred to ProQuest Information and Learning, 300 North Zeeb Road, Ann Arbor, Michigan 48106, to whom I have granted "the exclusive right to reproduce and distribute my dissertation in and from microform along with the non-exclusive right to reproduce and distribute my abstract in any format in whole or in part."

Gregory Juda

April 15th, 2005

ACKNOWLEDGEMENTS

This work is dedicated in loving memory of my father Robert H. Juda (1939-2005).

TABLE OF CONTENTS

TABLE OF CONTENTS CONTINUED

LIST OF TABLES

Table Page

LIST OF FIGURES

Figure Page

LIST OF FIGURES CONTINUED

LIST OF FIGURES CONTINUED

ABSTRACT

Copper amine oxidases (CuAOs) catalyze the oxidative deamination of primary amines to the corresponding aldehydes, utilizing O_2 as the oxidant with concomitant production of H_2O_2 and NH_3. The discovery that the human vascular adhesion protein (HVAP-1) is a copper amine oxidase has sparked considerable interest in the mechanism and inhibition of these enzymes. With the potential for therapeutic applications, substantial efforts have been made to determine the molecular factors which govern inhibitor sensitivity and selectivity for copper amine oxidases. In order to contribute to this growing body of knowledge, a series of inhibitors were screened for their ability to inhibit enzymatic catalysis in the phenylethylamine oxidase from *Arthrobacter globiformis* (AGAO). This CuAO was chosen as a model enzyme for these studies due to its ease in expression and purification as a C-terminal *Strep*-tag II fusion protein. This work describes the kinetic and structural characterization of a new class of highly potent, reversible CuAO inhibitors with inhibition constants in the low nanomolar range. In addition, an investigation of the molecular details of copper amine oxidase catalysis is described; in particular, mechanistic studies of the controversial oxidative half reaction. Studies using the monodentate copper ligand cyanide provided the first spectroscopic evidence for cyanohydrin derivitization of the quinone cofactor in AGAO and led to the proposal of a detailed mechanism for inhibition of CuAO catalysis by cyanide. Lastly, the role of copper during the oxidative half-reaction of amine oxidation in AGAO and *Pichia pastoris* lysyl oxidase (PPLO) was investigated using the exogenously added copper ligand azide. This work describes the first examination of the effects of azide on both the oxidative and reductive half-reactions of multiple CuAOs. Azide is the first example of a CuAO inhibitor that significantly reduces the catalytic rate for one half-reaction thereby abolishing the kinetic independence of the other half-reaction. Taken collectively, these results show that in the case of some CuAOs it is experimentally impossible to discern the effects of azide on copper mediated enzymatic reoxidation from the inhibition induced during the reductive half-reaction.

1

INTRODUCTION

Amine oxidases catalyze the oxidative deamination of primary amines to the corresponding aldehydes, utilizing O_2 as the oxidant with concomitant production of H_2O_2 and NH_3. The two classes of amine oxidases present in mammals are the quinone and copper-containing amine oxidases (CuAOs) and the flavin-dependent monoamine oxidases (MAO enzymes; EC 1.4.3.4). MAOs are exclusively found in the outer mitochondrial membrane of virtually all mammalian cell types and oxidize primary, secondary, and tertiary amines either through a single electron transfer mechanism or through a concerted covalent catalysis mechanism, both involving the FAD cofactor [1]. Quinone copper-containing amine oxidases, on the other hand, principally oxidize primary amines. Copper-containing amine oxidases have been actively investigated since their discovery, and are the first examples of enzymes in which a post-translationally modified amino acid side chain is present in the active site, and has a redox role in catalysis [2-5]. Copper-containing amine oxidases may currently be divided into two groups: the TPQ (2,4,5-trihydroxyphenylalanine quinone) containing class (E.C. 1.4.3.6); and the mammalian lysyl oxidase group (E.C. 1.4.3.13), which contain lysyl tyrosylquinone (LTQ) as a cofactor. Recent results have established that the widespread, "semicarbazide-sensitive amine oxidases" are copper enzymes, and also contain TPQ [6-8]. The work presented in this thesis will focus solely on the characterization of the quinone (TPQ) and copper containing amine oxidases. Much of this work is dedicated towards the characterization of the phenethylamine oxidase from *Arthrobacter globiformis* (AGAO), a bacterial enzyme.

Post-Translationally Modified Amino Acid Cofactors

In addition to the twenty encoded amino acids which make up the primary structure of most proteins, it is now widely recognized that some proteins contain additional chemical modification(s) of amino acid side-chains which can serve to diversify the biological functionality of these residues. This process, referred to as post-translational amino acid modification, requires the alteration of an intrinsic, encoded amino acid residue. These modifications are usually required for catalytic activity and the alteration may or may not require the participation of chaperone proteins. Copper amine oxidase, lysyl oxidase, galactose oxidase, methylamine dehydrogenase, cytochrome oxidase, catechol oxidases, nitrile hydratases, and numerous other enzymes are now known to contain modified amino acids in their active sites [9]. In several cases, redox cofactors are generated via crosslinking of amino acid side chains, for example, galactose oxidase (Y-C), lysyl oxidase (Y-K), amine dehydrogenase (W-W), and catechol oxidase (H-C) [9]. Cytochrome *c* oxidase contains a Y-H crosslink, which may function as a new type of cofactor [10], or have a structural role within the heme a_3-Cu_B site, since the crosslinked His residue is a Cu_B ligand [11]. Exploration of the functional and structural consequences of these modifications is an area of intense current interest in protein biochemistry.

Among post-translationally modified amino acid cofactors is a sub-group termed quinones that are specifically derived from oxidation of either tyrosine or tryptophan residues. The identification of 2,4,5-trihydroxy-phenylalanine quinone (TPQ) in 1990 [12], originally believed to be the noncovalently associated cofactor pyrroloquinoline quinone

(PQQ), paved the way for the identification of a series of these quinone cofactors. Four covalently attached amino acid derived quinone cofactors have been identified to date (Figure 1): (1) TPQ of the copper amine oxidases; (2) LTQ found in the copper containing lysyl oxidases; (3) tryptophan tyrptophylquinone (TTQ) present in bacterial methylamine dehydrogenase (EC 1.4.99.3); and (4) cysteine tryptophyl quinone (CTQ) of the bacterial quinohemoprotein amine dehydrogenase.

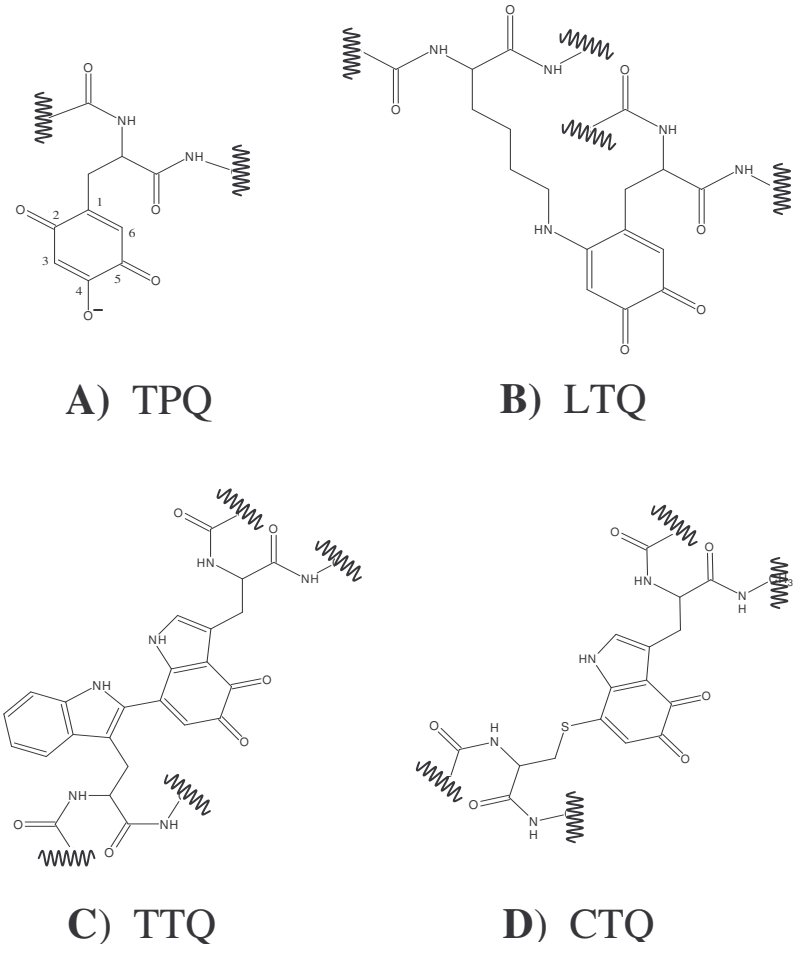

Figure 1: Post-translationally modified amino acid quinone cofactors; A) 2,4,5-trihydroxyphenylalanine quinone, TPQ; B) lysyl tyrosylquinone, LTQ; C) tryptophan tryptophylquinone, TTQ; D) cysteine tryptophyl quinone, CTQ.

Both the formation of TPQ and LTQ are now known to be self processing events, requiring only the presence of apo-unprocessed enzyme, copper, and molecular oxygen [5,13-16]. It is known that in addition to the two structural genes comprising the α and β subunits of methylamine dehydrogenase, biogenesis of TTQ requires the expression of four additional gene products, *mauDEF* and *G* [17]. The formation of CTQ remains less understood as it is not known whether biogenesis proceeds via self processing chemistry or through the participation of additional proteins [18].

Amine Oxidase Physiology

CuAOs have long been known to be widely distributed in nature and have been purified from mammals, plants, and microorganisms [19-22]. With the recent identification of the first archael copper amine oxidase sequence in *Sulfolobus solfataricus* P2, CuAOs are known to be distributed in all three super kingdoms (archael, eubacterial, and eukaryotic). In microorganisms, amine oxidases frequently have a nutritional role in the utilization of primary amines as the sole source of nitrogen or carbon [19,23]. The role of amine oxidases in higher organisms is considerably more complex and diverse. The substrate specificities of amine oxidases depend on the enzyme source but nearly all biogenic primary amines can be substrates, e.g. histamine, cadaverine, putrescine, agmatine, tyramine, tryptamine, dopamine, serotonin, norepinephrine, mescaline, spermine, and spermidine. Because the physiological function of many amine oxidases is the breakdown or transformation of biologically active amines, these enzymes may act as regulators of physiological amine concentrations and, therefore, may participate in numerous biological processes. For example, histamine is a potent effector of the

cardiovascular and gastrointestinal systems, and is directly involved in inflammatory, allergic, and ischemic phenomena [24,25]. Polyamines are implicated in the stimulation and control of cell proliferation, protein and nucleic acid synthesis, growth, and development [26]. Polyamines may also be involved in enzyme regulation; their oxidation products are implicated as inhibitors of cell proliferation and may play a direct role in the immune response [27]. Polyamine and diamine oxidation and interconversion in the brain are implicated in both normal processes and in brain injury in response to several kinds of deleterious stimuli [28,29]. Agmatine, a compound produced *in vivo* via the enzymatic decarboxylation of arginine, has been identified in mammalian brain, kidney and liver tissues, and is believed to act as an endogenous neuromodulator or neurotransmitter [30]. The ability of recombinant human diamine oxidase (rhDAO) to oxidize agmatine *in vitro* [31], coupled with the known expression of hDAO in human kidney, liver, and certain regions of the brain, points to a possible role of hDAO in agmatine metabolism *in vivo*. Furthermore, the finding that histamine is the preferred substrate for rhDAO implicates this enzyme as playing an important role in histamine metabolism [21]. Since biogenic amines serve so many diverse functions, it is not surprising that amine oxidases are widely distributed in mammalian tissues, e.g. brain, plasma, kidney, placenta, and throughout the cardiovascular and gastrointestinal systems.

Semicarbazide-sensitive amine oxidases (SSAOs) have been detected or described in numerous mammalian tissues and are increasingly believed to have multiple physiological roles [32,33]. SSAOs are implicated in the pharmacology and toxicology of biogenic and exogenous amines and their oxidation products. In addition to the biogenic amines listed above, methylamine and aminoacetone, which are not substrates of the flavin-

containing monoamine amine oxidases (MAOs), are now recognized to be physiological substrates for SSAO. Levels of SSAO activity are upregulated in several pathological states including diabetes mellitus, congestive heart failure, hepatic cirrhosis, uremia, and Alzheimer's disease [34-36]. The increased formation of potentially cytotoxic products of amine oxidation by SSAO may contribute to endothelial injury, resulting in the early development of severe atherosclerosis [36]. Human vascular adhesion protein (HVAP-1), which mediates L-selectin dependent lymphocyte adhesion to endothelial cells, has been recently identified as an SSAO [37-39]. It has also been speculated that SSAOs might participate in the regulation of physiological processes through generation of hydrogen peroxide, a well known signaling molecule [34,40]. In this manner, SSAO has been shown to stimulate glucose uptake in adipocytes, believed to be mediated by the generation of H_2O_2 during amine oxidation [35,36,39].

Amine Oxidase Structure

Seven copper-containing amine oxidases structures are known: *Arthrobacter globiformis* phenethylamine oxidase (AGAO; Figure 2) [19], pea seedling amine oxidase (PSAO) [41], *Hansenula polymorpha* amine oxidase (HPAO) [42], *Escherichia coli* amine oxidase (ECAO) [43], *Pichia pastoris* "lysyl" oxidase (PPLO) [44], the amine oxidase from bovine serum (BPAO) [45], and human vascular adhesion protein (VAP-1) (PDB coordinates 1US1) [46].

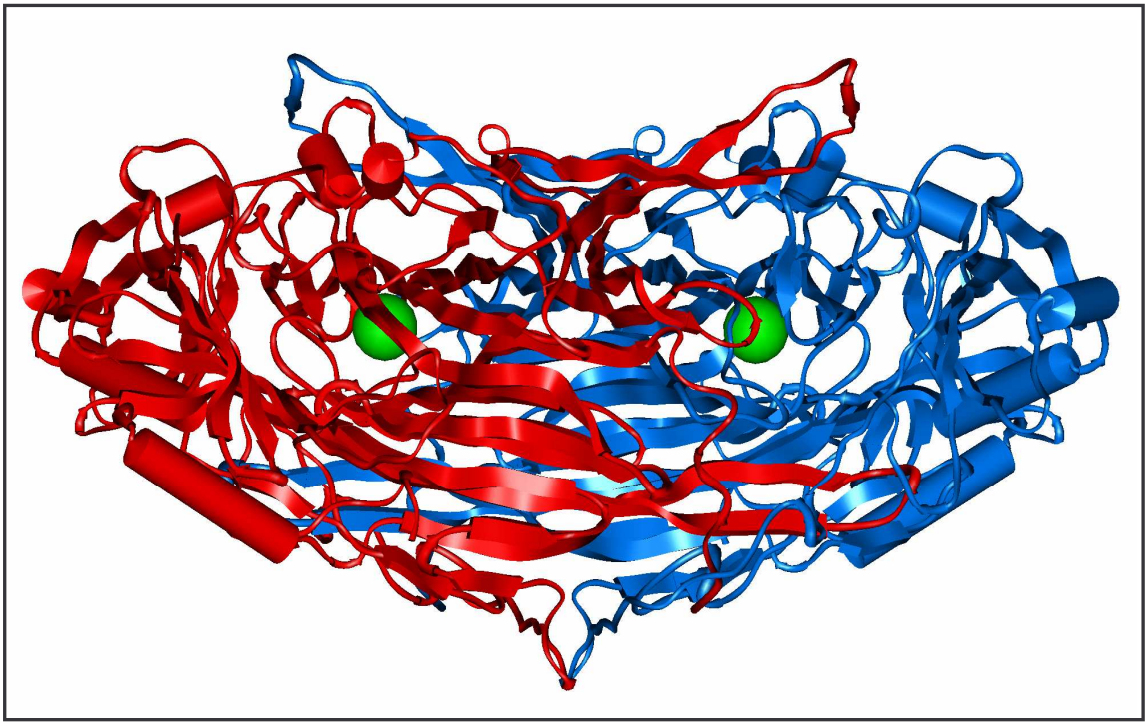

Figure 2: Secondary structure diagram of AGAO dimer as viewed along its 2-fold symmetry axis. Subunits are colored in blue and red with copper shown as a green sphere.

Collectively, the native enzymes share considerable structural homology; all being homodimeric and containing one active site per subunit comprising a single Type II copper ion and the TPQ cofactor (Figure 3; A and C) [47-49]. The Cu(II) ion is 5-coordinate (3 equatorial histidine ligands and 2 H_2O molecules; one equatorial, one axial) in distorted square pyramidal geometry. TPQ is in close proximity to the Cu(II) ion and has been observed in two distinct states: both “on”-copper and “off”-copper (the active state; Figure 3A) [50].

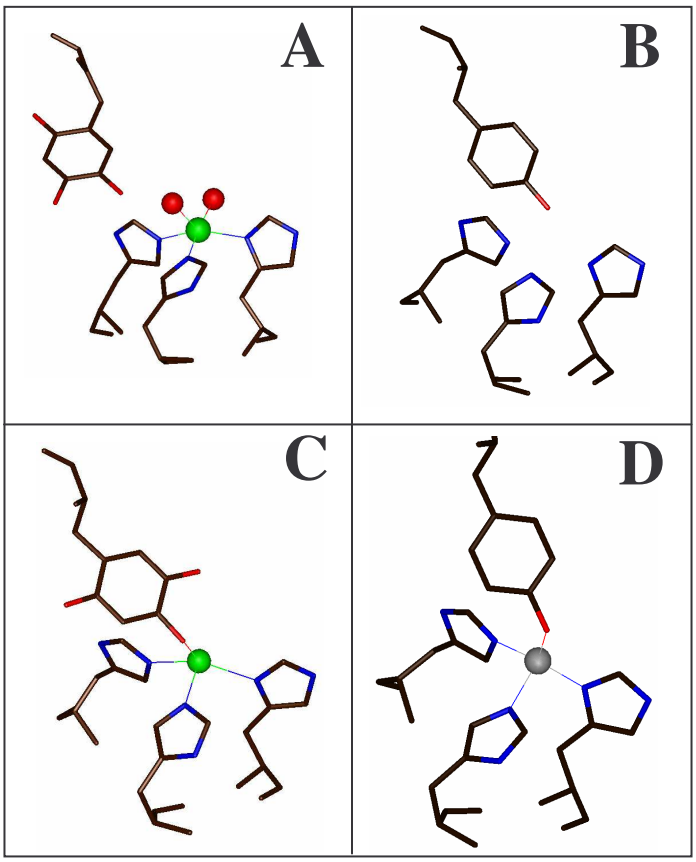

Figure 3: Active site representations of "active" AGAO (A). Apo-AGAO (B). "Inactive" AGAO (C). Zinc-substituted HPAO (D). Panels A, B, C adapted from [19], panel D was taken from [51].

Each monomer is composed of three or four domains (ECAO is the only CuAO with domain 1) with a large, C-terminal β-sandwich catalytic domain [19,43]. A β-ribbon from one subunit extends to the active site channel of the other, and residues at the end of the ribbon form part of the entrance to this channel. These residues vary considerably among amine oxidases [42]. An additional feature of several CuAO structures is the presence of a second-metal binding site located ~ 33 Å from the copper site (Figure 4). These sites are believed to be occupied by Ca(II), Mg(II), Mn(II), or

Zn(II) under physiological conditions. This site appears to be conserved among all CuAOs, and although its function(s) remains elusive, recent results with AGAO point towards a role in proper protein folding. The finding that a point mutation (D440A; see Figure 4) of one of the second metal site ligands in AGAO results in expression of insoluble protein is the first clue as to the possible function of these sites in CuAOs. Expression of this site-directed variant in an *E. coli* host showed recombinant AGAO to be located primarily in inclusion bodies (K. M. Okonski and G. A. Juda unpublished results).

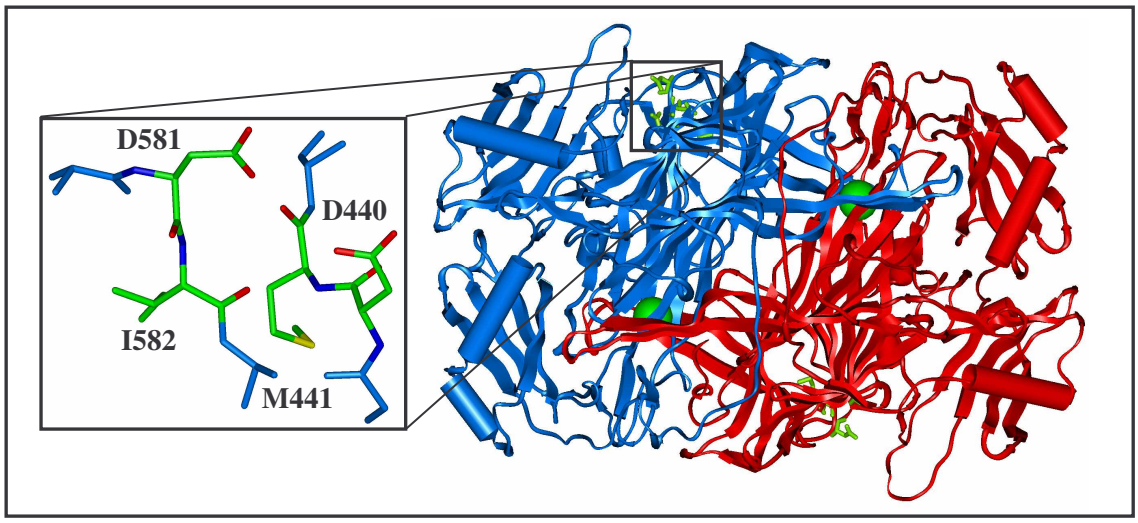

Figure 4**:** Second metal site in AGAO. AGAO dimer viewed along a direction parallel to the 2-fold symmetry axis. Expanded view illustrates the residues comprising the second metal binding site.

As stated above, the overall fold for the known CuAO structures is quite similar, as indicated by the low rms difference (1.4 Å) between the 1178 Cα positions in PSAO and ECAO [41]. Despite the structural similarity in the tertiary folds of these enzymes, a sequence alignment of domain 4 (the catalytic domain) from plant and bacterial sources

indicates sequence identity of less than 35% for all known sequences [8]. However, some trends are apparent. For instance, the plant enzymes share >50% identity and the plasma and SSAO enzymes across species are similar, *e.g*. BPAO and human VAP-1 protein display 82% sequence identity [8]. Furthermore, mammalian DAO sequences are distinct from plasma and SSAO enzymes (hDAO shares only 43% identity with HVAP-1) [8,52]. As a further consequence of these differences in sequence, substantial variations exist with regard to active site dimensions, TPQ accessibility, and in the presence or absence of active site "gate" residues [42,50]. Variances in the channels among CuAOs are believed to be one of the main reasons for observed differences in substrate and inhibitor specificity [53,54]. For example, the active site channel of PPLO is known to be much larger than that for other structurally determined CuAOs and as a result it is the only CuAO known to catalyze peptidyl lysine oxidation [44]. A current area of emphasis in the study of CuAOs is to define the structural bases for the striking variability in the substrate and inhibitor specificities.

TPQ Cofactor Biogenesis

The TPQ cofactor was first identified in 1990 by means of mass spectral analysis, NMR [12], and later confirmed by resonance Raman spectroscopy [55]. This quinone cofactor is now known to be derived from a conserved tyrosine residue present in the consensus sequence T/S–X–X–N–Y(TPQ)–D/E–Y/N requiring only apo-unprocessed enzyme, copper, and molecular oxygen [5,13-15]. Subequently, the work of Dooley and coworkers demonstrated that, at least for AGAO, TPQ is oxidized in a $6e^-$ process consuming 2 mol of O_2 and producing 1 mol of H_2O_2/mol of TPQ formed, yielding the

net stoichiometry of: 2 O_2 + E-Tyr → E-TPQ + H_2O_2 [56]. Furthermore, the rate of H_2O_2 production was approximately equal to the rate of TPQ formation. In the precursor, unprocessed apo-AGAO structure (Figure 3B), Cu(II) and TPQ are not present, but the precursor tyrosine (Y382) is clearly resolved and poised to bind copper serving as an axial ligand [19]. This hypothesis was subsequently supported by the crystal structure of the unprocessed zinc-substituted HPAO (zinc replaced copper) where the tyrosine was directly ligated to the metal [51]. Collectively, these results suggested that the precursor tyrosine is activated by copper during cofactor biogenesis and led Dooley and coworkers to propose a detailed, structure-based mechanism for biogenesis [15].

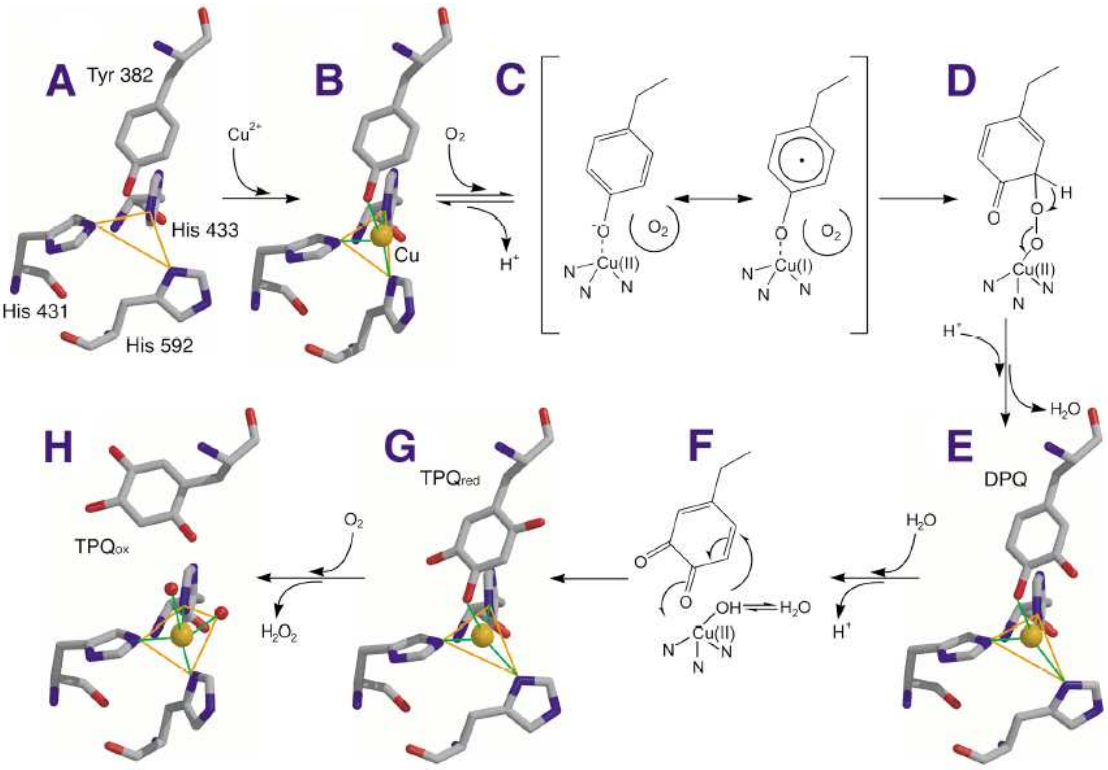

Figure 5: Mechanism of TPQ biogenesis. Stages A, B, E, G, and H represent intermediates that were isolated and their structures determined by X-ray crystallography. Figure was taken from [57].

Strong support for this proposed mechanism was provided by the work of Kim et al. probing biogenesis in AGAO by characterization of freeze-trapped intermediates via X-ray crystallography and single-crystal micro-spectroscopy (Figure 5) [57]. The initial structure reveals the Y382 (TPQ precursor)–Cu complex, as initially proposed by the structural results of apo AGAO (Figure 3B) [19]. Of interest is the relatively long phenolic O···Cu bond length of 2.5 Å, which might be too long for intense LMCT transitions (B). This suggests that the hydroxyl group of Y382 remains protonated, in agreement with previous reports with HPAO, which proposed deprotonation of the precursor Tyr and formation of the LMCT only *after binding of* O_2 [58-61]. O_2 may bind at either the vacant equatorial site at the copper center [19] or at a site adjacent to the Tyr(TPQ) precursor [60]. A recent theoretical study concluded that the O_2 binding energy to the equatorial copper position is more favorable by 11.7 kcal/mol [62]. It has been proposed that only *partial* charge-transfer from the tyrosinate to copper is required to sufficiently activate the phenol ring of Y382 towards nucleophilic attack by O_2 in AGAO [19,63]. Further studies are required to resolve these issues.

The early intermediate structure reveals 3,4-dihydroxyphenylalanine quinone, or dopaquinone (DPQ), coordinated to copper via the O4 atom. Note that the water/hydroxide species bound in the equatorial position (E, 2.1 Å from Cu) would be expected to readily exchange with solvent, consistent with the previous resonance Raman results [64]. The late intermediate structure (G) shows the cofactor to be 2,4,5-trihydroxyphenylalanine (reduced form of TPQ; TPQ_{red}). The copper site remains four coordinate with the three His imidazole nitrogen atoms and the C4 oxygen atom of TPQ_{red}. The final stage structure solved at 100 K clearly shows the oxidized cofactor in a

single, well-defined orientation with the C2=O group directed towards the copper, which displays the 5-coordinate distorted square-pyramidal geometry of three His imidazole nitrogen atoms and two water molecules observed for the resting enzyme (H).

Several studies directed towards determining the role of active site residues during biogenesis have been performed utilizing site-directed mutagenesis. The role of the conserved sequence N-Y-D/E-Y in the histamine oxidase from *Arthrobacter globiformis* (APAO; distinct from the phenylethylamine oxidase from this organism known as AGAO) was probed by generating the variants N401D/Q, D403E/N, and Y404F [65]. The alteration of N401 to an aspartate or glutamine residue produced a 10^3-10^4 fold decrease in the rate of copper-induced TPQ biogenesis, illustrating the importance of this residue in rapid TPQ formation. Likewise a mutation of D403N caused a marked decrease in the rate of biogenesis, however, the variant D403E was able to process TPQ at rates comparable to wild-type enzyme. The results with D403 suggest that this residue is important in maintaining the structural integrity of the active site during biogenesis in AGAO via hydrogen bonding. While mutation of Y404 to phenylalanine had no effect on TPQ biogenesis in this enzyme, significant effects were seen during catalytic turnover, especially in regards to substrate preference. The site-directed variants E406Q and N404D (residues immediately flanking TPQ) in HPAO have indicated that these two residues are not only important for positioning TPQ during catalysis, but also play a key role in determining the overall rate of biogenesis [58,66]. Mutagenesis of Y305 to alanine showed an ~ 800-fold decrease in k_{obs} for TPQ biogenesis versus WT-HPAO, indicating that this residue also helps orient precursor Tyr in a conformation more favorable for biogenesis [67]. In contrast, similar studies

performed in ECAO concluded that mutating the corresponding residue Y369 to a phenylalanine primarily affected k_{cat} during amine oxidation [68]. Although rates of biogenesis were not measured in ECAO, TPQ was found to be fully formed [68]. Taken collectively, these mutational studies illustrate the importance of the conserved sequence T/S–X–X–N–Y(TPQ)–D/E–Y/N and other active site residues in forming the functional TPQ cofactor, and aiding in efficient catalysis. Whether the roles of these residues are similar in other CuAOs remains to be tested.

Amine Oxidase Mechanism

CuAOs from various sources preferentially oxidize a multitude of amine compounds, from short to long chain aliphatic mono- and diamines, including several arylalkylamines [21,42,69]. Catalysis proceeds through a Ping-Pong Bi Bi mechanism divided into two half reactions:

$$E_{ox} + RCH_2NH_2 \leftrightarrow E\text{-}RCH_2NH_2 \rightarrow E_{red} + RCHO \quad (1)$$

$$E_{red} + O_2 + H_2O \rightarrow E_{ox} + H_2O_2 + NH_3 \quad (2)$$

The first half reaction is conventionally known as the reductive half reaction and is detailed in Figure 6, A $\rightarrow$ D. The crucial step is the conversion of the initial quinoneimine "substrate Schiff base" (B, TPQ_{SSB}) to a quinolaldimine "product Schiff base" (C, TPQ_{PSB}), facilitated by proton abstraction from the α carbon of the bound amine substrate by a conserved aspartate acting as a general base [50,70]. Product aldehyde is then readily released by hydrolysis.

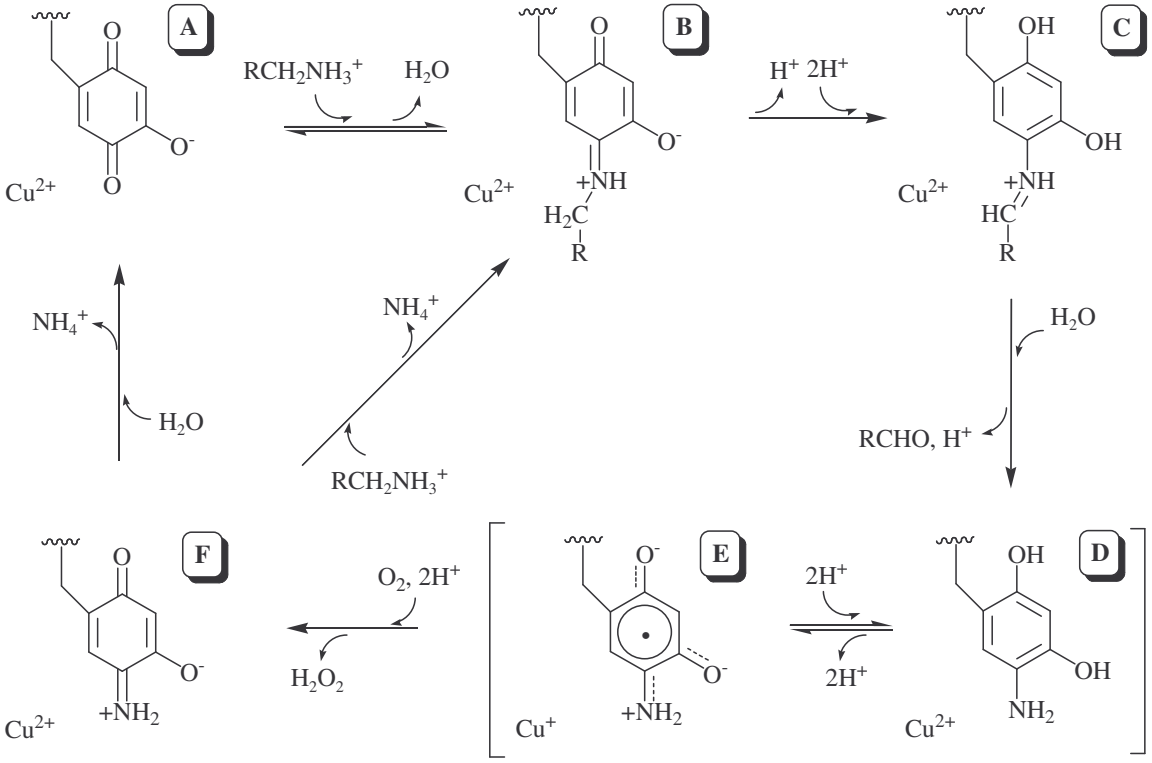

Figure 6**:** Proposed reaction mechanism for the oxidation of amines by copper-containing amine oxidases.

The second half reaction involving reoxidation of the organic cofactor is known as the oxidative half reaction, and is diagrammed in steps D → A (Figure 6). Upon release of aldehyde, the reduced enzyme exists as an equilibrium between a Cu(II)-aminoresorcinol (D, TPQ_{amr}) and a Cu(I)-semiquinone (E, TPQ_{sq}) state. Reduction of O_2 to H_2O_2 yields an iminoquinone species (F, TPQ_{imq}), which hydrolyzes to liberate NH_3 and the resting cofactor (**A**, TPQ_{ox}) [19]. Model chemistry has suggested the release of NH_3 may also occur through a transimination reaction between substrate and the iminoquinone, generating the substrate Schiff base (F → B) [71,72].

Proton abstraction in most CuAOs by the active site base has been shown to be stereospecific, with stereospecificity varying depending on the enzyme source, and in some cases the identity of the substrate [50,73-75]. While an enzyme-substrate complex has not yet been crystallographically characterized at stage B, a structure of a 2-hydrazinopyridine (2-HP) adduct of TPQ has been solved [50]. This structure showed that C5 must be positioned near the active site base ("off" copper orientation), with O2 of TPQ being positioned closest to the copper ion (via hydrogen bonding to the axial water) [50]. In addition to this structure, the structures of AGAO adducts with benzylhydrazine and tranylcypromine, two compounds that are also trapped at stage B have been solved. Collectively, these structures have shed light on the structural changes that occur upon substrate binding. Evidence from the crystal structures and kinetic studies of the site-directed variants of D383 (D383A, D383N, D383E) in ECAO, have shown that the catalytic base performs the key step of proton abstraction during catalysis and also assists in substrate binding [70,76]. Another residue implicated in positioning TPQ-derived intermediates during turnover is the conserved Tyr residue (Y284 in AGAO; Y369 in ECAO; Y305 in HPAO), that hydrogen bonds with O4 of TPQ in the ECAO-2HP structure [50], positioning TPQ in the productive conformation [68].

The mechanism for enzyme reoxidation (Eq. 2) is not definitively established and might vary among CuAOs. Based on the detection of appreciable quantities of Cu(I)-TPQ_{sq} present in substrate reduced CuAOs from various sources [77], as well as chemical precedence of Cu(I)-O_2 reactivity, Dooley and coworkers proposed that Cu(I)-TPQ_{sq} reacts with O_2 with the first electron reduction of dioxygen coming directly from Cu(I). The reaction mechanism proposed by our laboratory is illustrated in Figure 7, A$\rightarrow$ D.

This hypothesis was supported by temperature jump relaxation measurements on APAO [78] and PSAO [79] which showed that the electron transfer between the TPQ cofactor and the copper center occurs in a sufficiently rapid manner to make the Cu(I)-TPQ_{sq} moiety a kinetically competent intermediate during catalytic turnover. However, an obligatory role for a Cu(I)-semiquinone intermediate has not been established, and other viable mechanisms have been suggested [62,80].

An examination of ^{18}O isotope effects on the oxidative half-reaction of BPAO demonstrated that the first electron transfer to O_2 was the rate-limiting step in this enzyme [80]. Furthermore, solvent viscosity had no effect on the rate of enzymatic reoxidation [80], suggesting that O_2 must prebind to the enzyme prior to its reduction [80,81]. It should be noted that if these results are applicable to other CuAOs, they are consistent with all of the proposed reoxidation mechanisms to date. This prebinding of oxygen was subsequently hypothesized to take place in a proteinaceous, hydrophobic pocket near TPQ comprised of the residues Y407, L425, and M634 (HPAO numbering) [81]. Based on the observation that Co(II)-substituted HPAO was active and displayed a k_{cat} close to that of the native Cu(II) enzyme near pH 7, Klinman and coworkers argued that the first electron transfer to dioxygen occurs directly from TPQ_{amr} and suggested copper reduction is not essential for catalysis but rather the role of copper is to stabilize reduced oxygen species. The differences in the kinetics of the Co(II)-enzyme compared to the Cu(II) enzyme are attributed to a much larger K_M for O_2 [82,83]. This difference in oxygen binding affinity for the nonmetal site is believed to arise from a change in the net charge at the adjacent metal site from +1 (cupric hydroxide) in wild-type HPAO to +2 (cobaltous

H_2O) in the cobalt substituted enzyme. Based on these results, the alternative reaction mechanism illustrated in Figure 7 (A2-D) was proposed.

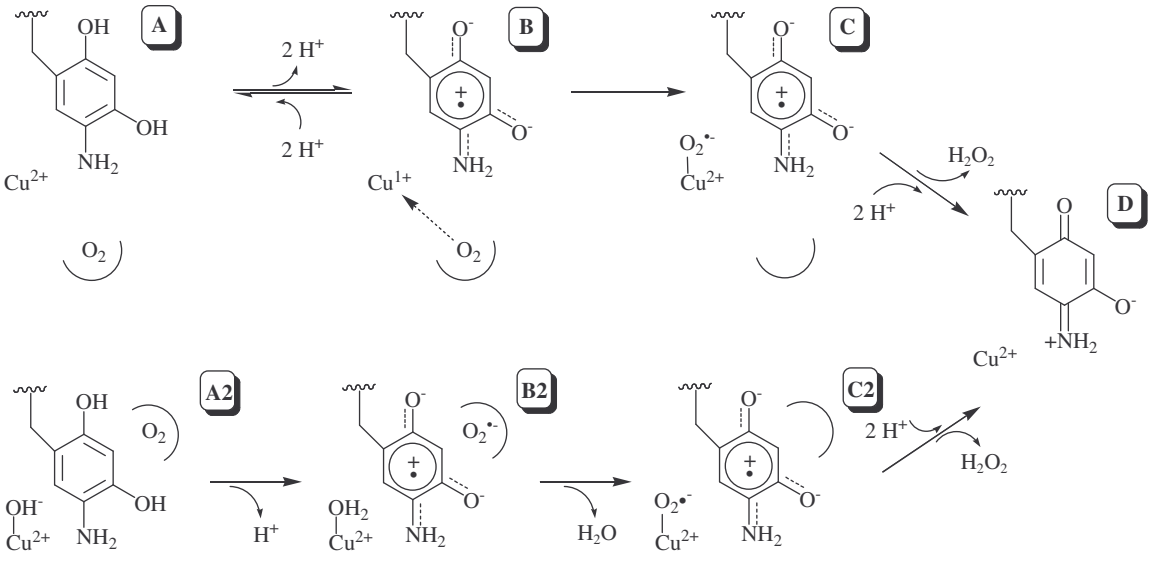

Figure 7: Expanded sequence of possible CuAO reoxidation mechanisms. A→D represents the pathway proposed by Dooley and coworkers. A2→D represents the catalytic steps proposed by Klinman and coworkers.

Exogenous ligands, such as azide, inhibit the reoxidation (Eq. 2) of CuAOs with the type of inhibition varying, depending on the enzyme source. Azide was found to exhibit noncompetitive inhibition with respect to O_2 in HPAO, which was interpreted in terms of prebound O_2 reacting directly with TPQ_{amr} [60]. This result is in direct support of the mechanism proposed by Klinman. In contrast, two earlier studies concluded that azide displayed competitive inhibition with respect to substrate O_2 in the copper amine oxidase from porcine plasma (PPAO) which is consistent with O_2 reacting with copper [84,85]. It should be noted that the crystallographic results of a separate study, where both NO and a reduced oxygen intermediate bind between copper and TPQ, are

consistent with either mechanistic possibility [86]. The nitric oxide complex of substrate-reduced ECAO revealed that NO was bound close to copper replacing the axial water at 2.4 Å and an angle of 117° [86]. The oxygen atom of NO was hydrogen bonded to the protonated O2 of TPQ, consistent with a Cu(II)-NO-aminoquinol structure. Electron density attributed to a dioxygen species was resolved in the structure of crystallized ECAO aerobically exposed to excess substrate; dioxygen occupied a position similar to that of NO. The O_2 moiety was bound in a side-on conformation and was assigned as peroxide, with TPQ in the iminoquinone state. Given the ligand binding site in the peroxide and NO complexes, *electron transfer from Cu(I) or* TPQ_{amr} *are both plausible*. There was no evidence for dioxygen binding in the hydrophobic site proposed earlier [60].

In order to test the hypothesis that dioxygen prebinds in the active site of CuAOs prior to its reduction, our laboratory, in collaboration with Professor Hans C. Freeman and coworkers (University of Sidney, Australia), collected X-ray diffraction data at 1.7-2.2 Å resolution for crystals of three CuAOs under a high pressure of xenon gas [87]. Xenon has been used in this manner as a probe for potential hydrophobic binding pockets since 1965 when myoglobin crystals were found to form stable adducts when exposed to Xe gas under pressure [88]. Examination of the Xe derivatized structures of AGAO (Figure 8), PPLO, and PSAO revealed unexpectedly that only one xenon binding site is observed in more than one structure, and this site is common to all three. This consensus site is the Xe site closest to the copper center and is located ~7.5 Å from the copper center and ~ 9.5 Å from the C^{β} atom of TPQ (Figure 8). Electron transfer from either the copper atom or the TPQ cofactor would require substantial migration of the O_2 molecule

(4-6 Å), however, the most direct trajectory for the O_2 molecule towards the active site would require an initial close approach to copper. Interestingly, a Xe derivative of BPAO identified this same potential dioxygen binding site within the active site [45]. It is worth mention that no evidence of Xe binding in the potential hydrophobic dioxygen binding site proposed for HPAO was seen in any of these crystal structures.

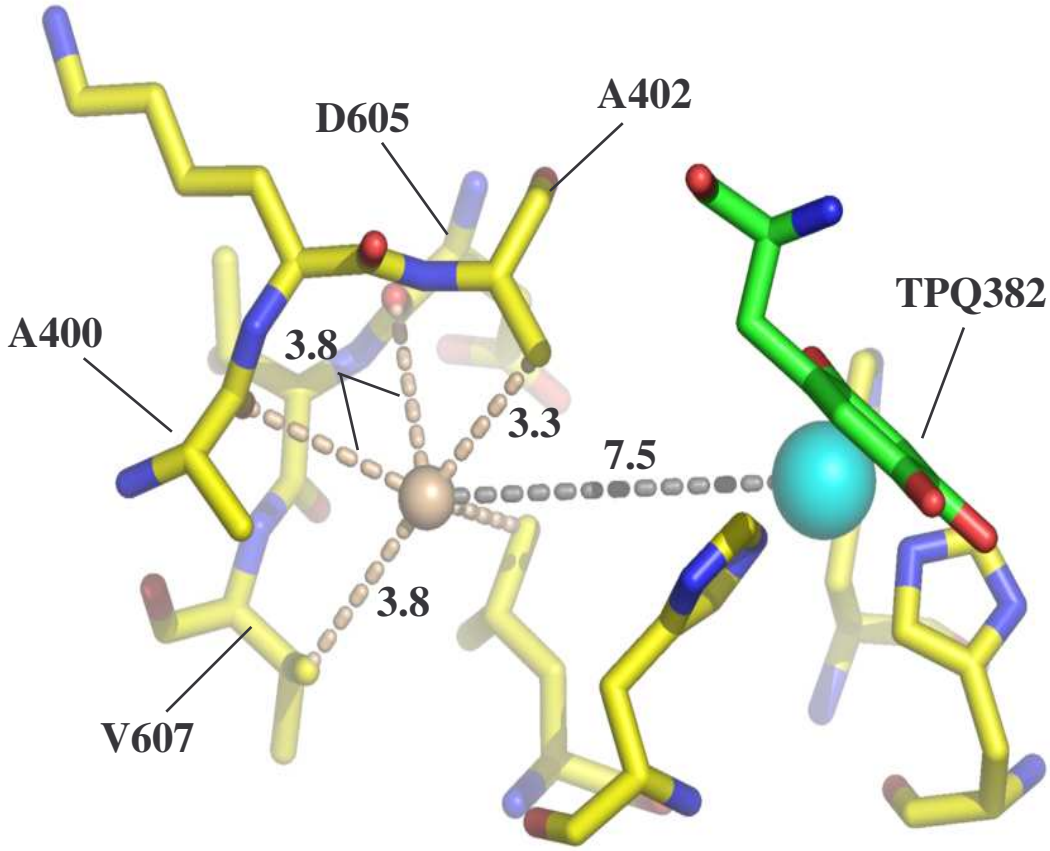

Figure 8: The main Xe binding site in AGAO. Copper is shown as an aqua colored sphere, while Xe is represented as a cream colored sphere. Distances and residues of interest are labeled.

Two recent studies of metal substituted AGAO provided valuable insight into the role of copper in the oxidative half-reaction, and illustrated the mechanistic variability among CuAOs [89,90]. Stopped-flow studies of substrate reduced AGAO showed that reduced AGAO reacted very rapidly with O_2 (< 1ms), forming a Cu-peroxy species (λ_{max} = 410 nm). The results were consistent with either Cu(I)-TPQ_{sq} or Cu(II)-TPQ_{amr} reacting rapidly with O_2, or with rapid $1e^-$ transfer from TPQ_{amr} to Cu(II). Formation of the charge delocalized, oxidized TPQ was proposed to be the rate-determining step in the oxidative half-reaction of AGAO [90]. In marked contrast to the reports on HPAO [82,83], Co(II) and Ni(II) reconstituted forms of AGAO had K_M values for amine and O_2 substrates that were essentially identical to the native enzyme; however, k_{cat} values for Co(II)- and Ni(II)-AGAO were ~ 1 sec^{-1}, as compared to 110 sec^{-1} for Cu(II)-AGAO [89]. Metal substituted AGAO and HPAO differ in two critical aspects: (i) Compared to other metal ion substituted enzymes, the Co(II) forms display the most activity in both AGAO and HPAO, but the levels of recovery vary substantially (2% in AGAO and 19% in HPAO, relative to the native copper enzymes); (ii) The major cause of the reduced activity in HPAO was the large increase in K_M for O_2, whereas it is the substantial decrease in k_{cat} in AGAO, with $K_M(O_2)$ remaining unchanged. X-ray crystal structures of Co(II)- and Ni(II)-AGAO established that the hydrogen-bonding network in the active site was preserved [89]. The coordination of both Co(II) and Ni(II) was octahedral, with the addition of another H_2O molecule as a ligand. The results indicate that the low catalytic activities of Co(II)- and Ni(II)-AGAO were associated with impaired efficiency of the oxidative half-reaction. Rate constants for reoxidation (measured by decay of the TPQ_{amr}) were 0.18 s^{-1} and 0.17 s^{-1} for Co(II)-and Ni(II)-AGAO, respectively, *and*

conclusively show that the initial reaction with O_2 is substantially slower in the metal substituted enzymes. These reported k_{obs} values probably underestimate the true rate constants; nonetheless, it is clear that oxidation of TPQ_{amr} and subsequent formation of TPQ_{imq} occurs over 20 seconds, a rate which is two orders of magnitude slower than the Cu(II) enzyme. The rate acceleration of the initial reaction of substrate-reduced enzyme with O_2 observed for the native copper enzyme was regarded as consistent with the participation of a reactive Cu(I) semiquinone, but cannot be regarded as conclusive. Kishishita et al. propose that copper plays an essential role in catalyzing electron transfer between TPQ_{amr} and O_2, at least in part by acting as a binding site for reduced dioxygen species to be efficiently protonated and released [89].

In lentil seedling amine oxidase (LSAO) neither Ni(II) nor Zn(II) substituted LSAO displayed any catalytic activity, while Co(II)-LSAO displayed minor (7%) activity relative to the wild-type enzyme [91]. Detailed mechanistic studies of LSAO concluded that the reoxidation of the reduced enzyme at pH 7 proceeded mainly through the reaction of the Cu(I)-TPQ_{sq} with O_2, with a rate constant of 1.56×10^7 $M^{-1}s^{-1}$ [92]. This rate constant is consistent with the rapid intramolecular electron transfer rate of 20,000 s^{-1} from TPQ_{red} to Cu(II) obtained from the closely related enzyme PSAO [79]. Taken together, these data suggest that *enzymes from different sources may utilize distinct mechanisms to reoxidize the reduced quinone species* [60,89]. It also must be acknowledged that the fundamental difference between the proposed mechanisms for the oxidative half-reaction may ultimately be a relatively subtle one concerning the timing between the electron-transfer step relative to the migration of O_2 from its initial binding site to the metal ion. Nevertheless, these mechanistic issues are important ones, with

implications for dioxygen reactivity in other enzyme systems, and surely warrant further investigation.

Research Goals

In order to efficiently carry out biochemical, kinetic, spectroscopic, and structural studies of a particular protein, a consistent means of protein expression and purification is needed to supply milligram quantities of homogeneous protein. One goal of this research project is to accelerate the current protocol for the purification of a copper amine oxidase from the soil bacterium *Arthrobacter globiformis* (AGAO) in order to provide a substantial quantity of this protein for such studies. This work describes the development of a revised purification protocol for a fusion construct of this protein utilizing the *Strep*-tag II affinity purification system. The purification of AGAO using this protocol served as the source for all experiments utilizing this protein that are detailed in the pages that follow.

A second goal of this work is to contribute to the growing body of knowledge concerning the molecular factors which control substrate specificity and recognition as well as inhibitor selectivity among CuAOs. This work describes the kinetic and structural characterization of an exciting new class of highly potent CuAO inhibitors with inhibition constants in the low nanomolar range.

Lastly, an investigation of the molecular details of copper amine oxidase catalysis is intended; in particular, mechanistic studies on the controversial oxidative half reaction. Experiments outlined concern the interaction of the monodentate copper ligands cyanide

and azide with multiple CuAOs and the implications with regards to a comprehensive catalytic mechanism for amine oxidation.

CONSTRUCTION, OVEREXPRESSION, AND PURIFICATION OF *Arthrobacter globiformis* AMINE OXIDASE *STREP*-TAG II FUSION PROTEIN

Introduction

In order to carry out detailed structural, kinetic, and spectroscopic studies on an enzyme in a timely fashion, it is imperative to have a consistent source of protein expression and be able to carry out large-scale purification of that protein in a timely manner. Along these lines, we set out to reduce the time required for the purification of a CuAO from the soil bacterium *Arthrobacter globiformis* (AGAO, accession number U03517). This protein has played a major role in laying a foundation for the understanding of both the mechanism of amine oxidation and TPQ biogenesis owing to the vast array of biochemical, kinetic, spectroscopic, and structural work amassed utilizing AGAO to date. Recent work with AGAO in our laboratory has established the exact stoichiometry of copper and O_2 required for TPQ biogenesis [56], and provided spectroscopic and kinetic information concerning TPQ formation [15].

AGAO is an attractive target for mechanistic and structural investigations of the mature enzyme and of its biogenesis owing to the availability of structures of both the mature and the apo enzymes [19]. Moreover, its expression in *E. coli* will facilitate the use of site-directed mutagenesis to explore these issues. Expression of AGAO was first accomplished in *E. coli* using a pET-3c expression vector from Novagen (Madison, WI) as described by Tanizawa *et al.* [93]. This expression clone was generously provided by Professor Katsuyuki Tanizawa and protein purification was previously accomplished in our laboratory using a modified protocol based on that described by Shimizu *et al.* [94],

which involved the use of two successive ion-exchange steps followed by gel filtration. This procedure proved to be quite lengthy, requiring 6 days for a given protein preparation. In order to facilitate the rapid, large-scale purification of both native, apo, and site-directed variants of AGAO, the *Strep*-tag II affinity peptide purification system (Genosys Biotechnologies Inc., The Woodlands, TX) was implemented.

The *Strep*-tag II is an eight amino acid peptide having the sequence NH_2-WSHPQFEK-COOH that can be engineered to either the N- or C-terminus of a protein to allow for its one-step purification under mild buffer conditions using an immobilized variant of streptavidin called StrepTactin [95]. More recently, immobilization of StrepTactin on a POROS 20 or POROS 50 carrier has allowed for StrepTactin chromatography to be performed at elevated pressures using FPLC (Pharmacia Biotech) or BioCAD^{TM} (PerSeptive Biosystems) workstations. Herein is reported the overexpression and purification of recombinant AGAO-*Strep*-tag II fusion protein in *E. coli*. AGAO-*Strep*-tag II fusion protein purification using StrepTactin POROS chromatography at elevated pressures is described in detail and can now be accomplished in 2 days. Detailed characterization of the AGAO-*Strep*-tag II protein established that the fusion protein displays essentially identical turnover and active-site properties as wild-type AGAO. This methodology should be very robust for the purification of site-directed variants of AGAO. Moreover, inspection of the published crystal structures of amine oxidases suggests that the C-terminal *Strep*-tag methodology should be generally applicable to amine oxidase purification because the C-termini of all six published structures are readily accessible and distant from the active sites and the substrate recognition channels.

Materials and Methods

Cloning of AGAO-*Strep*-tag II Fusion Protein

Figure 9 summarizes the cloning strategy described below. The entire coding sequence for AGAO was lifted from the pPEAO2 construct (Tanizawa *et al.* [93]) by PCR using primer-adapters containing newly-engineered BsaI sites (forward primer: 5'-GACCATGGTCTCAAATGACGC-CCTCCACTATCCAAAC; reverse primer: 5'-GACCATGGTCTCAGCGCTGCCG-TGGCAGTGGGAGCC). The pASK-IBA3 vector (Genosys Biotechnologies Inc.) and PCR product were then digested with BsaI (New England Biolabs, Beverly, MA) and the resulting fragments ligated to form expression vector pAGAO1 (Figure 9a).

Since the expression levels of AGAO using construct pAGAO1 were not nearly as high as observed previously using the pPEAO2 construct, it was desirable to engineer the C-terminal portion of the coding sequence including the *Strep*-tag II back into the original pet vector (Figure 9). The C-terminal portion from pAGAO1, including the *Strep*-tag II sequence (~190 base pairs), was lifted from the pAGAO1 construct by PCR using a forward primer-adapter containing an XcmI site (5'-CAGCTACCATCATGCCGGTGGAC) and a reverse primer-adapter containing a newly engineered BlpI site located downstream of the stop codon (5'-GAAGCTCAGCCACTTCACAGGTCAAGCTT). The PCR product (Figure 9b) and pPEAO2 were digested using BlpI and XcmI (New England Biolabs) and the resulting fragments ligated with T4 DNA ligase (New England Biolabs). Electrocompetent *E. coli* expression strain BL21(DE3) (Novagen) was transformed with the ligation product and

presence of the new construct was confirmed by PCR screening of colonies. DNA sequence analysis was performed using an ABI PRISM BigDye Terminator Cycle Sequencing Ready Reaction Kit from PE Applied Biosystems (Foster City, CA). The expression plasmid constructed was designated pAGAO2 (Figure 9c).

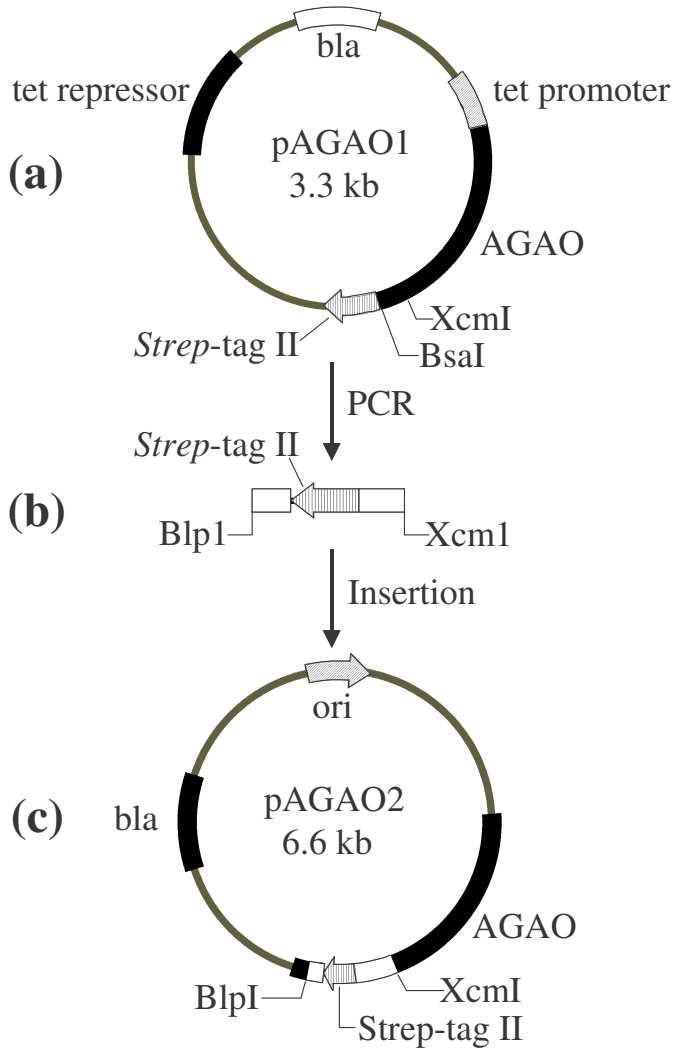

Figure 9: Cloning strategy used to construct pAGAO2 as described in the text. (a) pASK-IBA3 vector containing AGAO coding sequence; (b) PCR product containing C-terminal portion of AGAO coding sequence and *Strep*-tag II; (c) Final pet3c expression construct containin full AGAO coding sequence with *Strep*-tag II.

Cell Growth and Expression

E. coli strain BL21 DE3/pAGAO2 was streaked onto a Luria-Bertani (LB) (Ampicillin 100 μg/mL) plate and allowed to incubate at 37° C overnight. Single colonies were used to innoculate four 2.5 mL LB (carbenicillin 100 μg/mL) cultures which were grown in a 37° C shaking incubator (200 rpm). Cells were allowed to grow to an OD_{600} of ~1 and subsequently used to innoculate four 50 mL LB (carbenicillin 100 μg/mL) culture flasks which were also grown at 37° C with shaking (200 rpm). When the cells had reached an OD_{600} of ~0.7 the cells were centrifuged and the cell pellets resuspended in 2.5 mL of LB media. These resuspended cells were used to innoculate four 500 mL LB (carbenicillin 100 μg/mL) cultures which were grown at 37° C with shaking. Cells were induced at an OD_{600} of 1 by addition of IPTG to a final concentration of 0.34 mM and moved to a room temperature (25° C) platform shaker (150 rpm). Cell cultures were harvested 9 hours after induction. Harvested cell pellets were resuspended in 0.1 M Tris-HCl, pH 8.0, at a ratio of 10:1 (vol:wt).

StrepTactin Column Packing and Handling

StrepTactin POROS media was received from Genosys Biotechnologies Inc. in the form of a 2 mL slurry (suspended in 100 mM Tris-HCl, pH 8.0, 1 mM EDTA, 0.02% NaN_3). A StrepTactin POROS PEEK column (4.6 mm x 100 mm) was packed on a BioCAD *SPRINT* (PerSeptive Biosystems) workstation with the media using a POROS Self-Pack packing device. The column was packed using equilibration buffer (100 mM Tris-HCl, pH 8.0) at sufficient pressure (400 psi) to allow for the manufacturer's recommended flow rate (2-4 mL/min) for protein purification, and a maximum column

pressure limit of 340 psi was set in the BioCAD purification method. Once equilibrated the column was stored at 4 °C.

Purification of AGAO

During protein purification, all steps were carried out on ice or in a cold room unless otherwise noted. PMSF was added to the harvested cell suspensions to a final concentration of 0.1 mg/mL immediately prior to sonication. After cell disruption, the sonicate was centrifuged at 15,000 rpm (Sorvall ss34 rotor) and the supernatant retained. A post-lysis incubation was then performed by adding $CuSO_4$ to the supernatant to a final concentration of 1 mM (30° C for 1 hour with 100 rpm shaking). The purpose of this step was to saturate the enzyme with copper in order to obtain a maximum level of copper loading, processing, and enzyme activity. After copper incubation, the sample was ultracentrifuged for 1 hour (45,000 rpm in a Beckman 50TI rotor). The supernatant was pooled and run through a 0.2 µm syringe filter prior to loading onto a DEAE Sepharose Fast Flow column (9.6 cm^2 x 8 cm) equilibrated with 0.1 M Tris-HCl, pH 8.0 buffer. The protein-bound column was washed with ~700 mL of 0.1 M Tris-HCl, pH 8.0, and the absorbance of the wash was monitored at 280 nm to determine completion of the wash step. Bound protein was batch eluted using 150 mL of 0.1 M Tris-HCl, pH 8.0, containing 0.5 M KCl. A total of three 50 mL fractions were collected with AGAO found to have eluted almost exclusively in fraction 2. This fraction was then run over a StrepTactin POROS PEEK column (4.6 mm x 100 mm) at elevated pressure using a BioCAD *SPRINT* perfusion chromatography system. The column was kept at room temperature with all buffers and fractions kept on ice. The method for this affinity

chromatography described by the manufacturer's protocol was used for each run of the column and upon regeneration, the column was ready for additional runs [95].

Fractions containing purified AGAO using the StrepTactin column were identified by measuring the absorbance at 280 nm. These fractions were pooled, dialyzed against 4 × 1 L of 50 mM HEPES, pH 7.0, for 12 hours (changing buffer every 3 h), and assayed for specific activity. The dialyzed protein was then concentrated for storage at -80° C using a Millipore Ultrafree-15 centrifugal filter (50 kDa molecular weight cut off). Activity assays were performed on all fractions by spectrophotometrically monitoring H_2O_2 production, coupled to the oxidation of 2,2'-azinobis(3-ethylbenzthiazoline-6-sulfonic acid) by horseradish peroxidase (Sigma, St. Louis, MO) as described previously [96]. Specific activity is reported as micromoles of product per minute per milligram.

Protein Characterization

Copper analysis by flame atomic absorption spectroscopy was performed using a Buck Scientific Model 210 VGP. Phenylhydrazine titrations of AGAO were conducted as previously described [97] by monitoring the increase in absorbance at 450 nm. All UV and visible absorption data were acquired using either a Hewlett-Packard model 8452A or 8453 diode-array spectrophotometer. CD data were recorded using a JASCO J-710 spectropolarimeter and resonance Raman spectroscopy was performed on a Spex Triplemate spectrometer equipped with a CCD detector, featuring excitation by a Coherent argon-ion laser.

Results

Using the StrepTactin POROS column a total of 50 mg of recombinant AGAO were purified from 2 L of *E. coli* culture in two major steps: (1) a DEAE Sepharose as an initial clean-up of the centrifuged extract; followed by (2) StrepTactin POROS chromatography on a BioCad workstation. The recombinant AGAO-*Strep*-tag II protein was purified to homogeneity as judged by SDS-PAGE (Figure 10). Table 1 shows the results of a typical two-step purification of AGAO from 2 L of culture, with the pure pooled fractions accounting for 53% of the total activity units loaded onto the column (DEAE fraction 2).

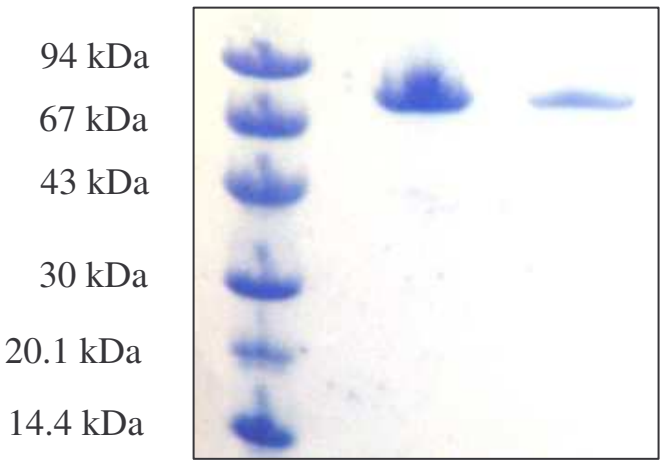

Figure 10: 8-25% gradient SDS PAGE gel analysis of purified AGAO. Left lane, molecular mass standards (Pharmacia); center lane, recombinant AGAO-*Strep*-tag II protein (1.6 mg/mL); right lane, recombinant AGAO-*Strep*-tag II protein (0.38 mg/mL).

Table 1: Purification of Recombinant AGAO-*Strep*tag II Fusion Protein

Step	Protein (mg)	Total activity units	Specific Activity[a]	% Yield	Fold Purification
Crude Extract	2385	2085	0.874	100	
DEAE Sepharose	782	1606	2.05	77	2.3
StrepTactin POROS	50	851	16.9	41	19

[a] $\mu mol\ min^{-1}\ mg^{-1}$

During development of the purification procedure, we observed that higher pressures were needed in order to sustain the same flow rates after the StrepTactin POROS column was used several times. Increasing the pump pressure in order to maintain a desired flow rate may be used as long as the pressure limit of the column is not exceeded. However, decreased flow rates were prevented (or minimized) by ultracentrifuging the extract, followed by a 0.2 μm syringe filtration of the protein sample, prior to loading onto the StrepTactin POROS column. Removal of any insoluble membrane or protein aggregates that did bind to the media can be accomplished by treatment of the Streptacin POROS column with up to 1 M guanadine HCl in accordance with the manufacturer's protocol.

Table 2: Kinetic Comparison of Tagged vs. Wild-Type AGAO (for benzylamine)

Protein	V_{max} (ΔA_{250}/min)	K_M (μM)	k_{cat} (sec^{-1})	k_{cat}/K_M ($sec^{-1}\mu M^{-1}$)
WT AGAO	0.039 ± 0.002	42 ± 4.9	0.52	0.013
Tagged AGAO	0.040 ± 0.002	42 ± 3.6	0.47	0.011

After purification, the tagged AGAO was extensively characterized in order to establish that it was spectroscopically and kinetically identical to wild-type AGAO. Turnover kinetics (Table 2) were obtained using the canonical amine oxidase substrate

benzylamine, with the rates measured by directly monitoring benzaldehyde production at 250 nm [98,99]. Wild-type enzyme and the AGAO-*Strep*-tag II fusion protein are kinetically indistinguishable within experimental error. Atomic absorption spectroscopy was used to determine the copper content of the purified AGAO-*Strep*-tag II fusion protein. The stoichiometry of copper was found to be 1.94 Cu atoms/dimer AGAO, which is consistent with the wild-type stoichiometry [94]. Phenylhydrazine titrations are routinely used to assess the TPQ content of amine oxidases [97], and this reagent reacts specifically with the oxidized form of the quinone cofactor. The results of such an analysis of the purified, tagged AGAO revealed the presence of 1.3 phenylhydrazine reactive TPQs/protein dimer.

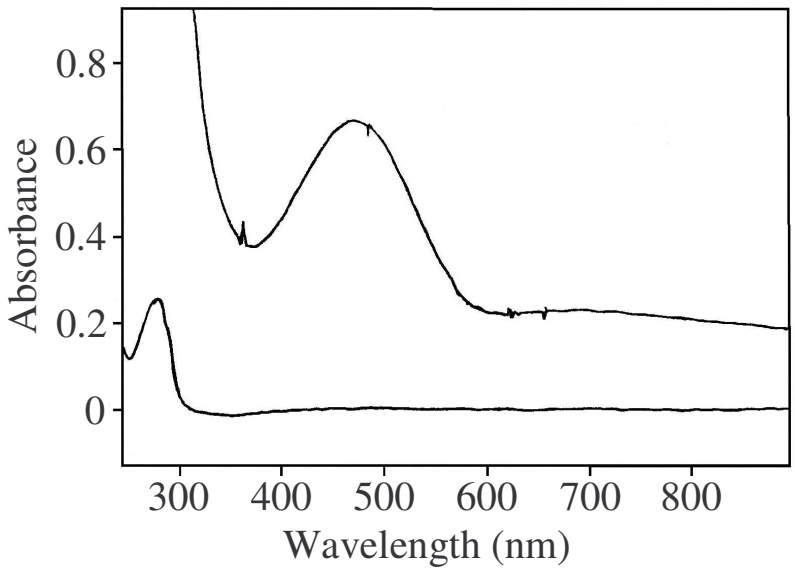

Figure 11: Optical spectra of AGAO-*Strep*-tag II protein. Upper spectrum representing TPQ (480 nm) absorbance band of AGAO (19.6 mg/mL); lower spectrum representing protein (280 nm) absorbance band of AGAO (0.2 mg/mL). Spectra are offset for clarity.

The integrity of the active site of the tagged AGAO was evaluated using a variety of spectroscopic techniques previously shown to be sensitive to the structure and bonding of active-site Cu(II) and TPQ, and the active-site microenvironment. The absorption spectrum of the purified AGAO displayed the characteristic protein maximum at 280 nm (with a small shoulder around 290 nm), and an exceptionally well-resolved band at 480 nm (Figure 11) associated with oxidized TPQ. Previous spectroscopic studies of amine oxidases demonstrated that CD spectroscopy resolves electronic transitions of both Cu(II) and TPQ. CD spectra of the AGAO-*Strep*-tag II and wild-type AGAO proteins are shown in Figure 12. Clearly all the transitions of the wild-type protein are also present in the tagged enzyme at the same energies. Also, the intensities of the transitions are quite similar, with the exception of the band at 310 nm. The proximity of this band to the intense transitions associated with aromatic residues tends to make its intensity somewhat variable and sensitive to the presence of minor impurities. Notably, the (-) band at 715 nm arises from Cu(II) ligand-field (*d-d*) transitions so the similarity of this band between the two proteins is consistent with essentially identical Cu(II) site structures. Another powerful probe of the active-site structures of amine oxidases is resonance Raman spectroscopy [100]. Resonance Raman data for the wild-type and tagged AGAO are presented in Figure 13. All of the observed bands are associated with vibrational modes of the TPQ moiety; the frequencies and relative intensities of the bands in the 1200 – 1700 cm^{-1} region are significantly influenced by the environment of the quinone. Hence, the near identity of these spectra provides strong support for the proposition that the *Strep*-tag II peptide does not perturb the structure of the AGAO active site TPQ.

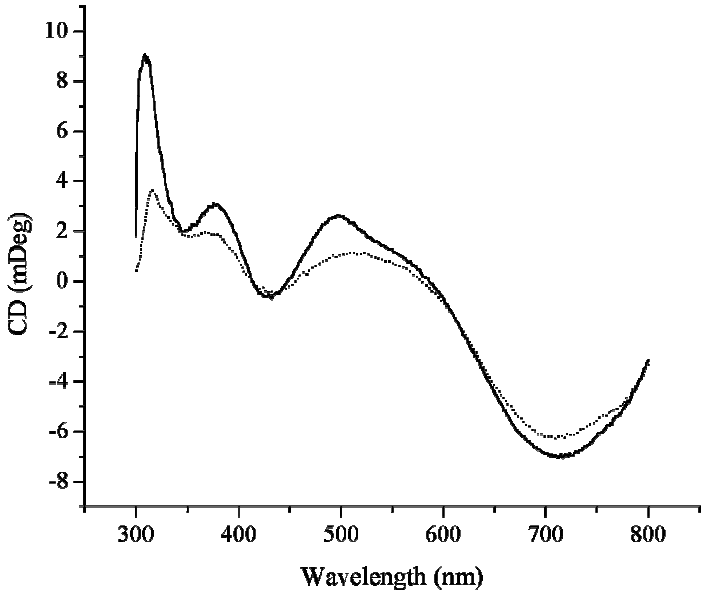

Figure 12: Circular dichroism spectra of wild-type AGAO and AGAO-*Strep*-tag II proteins. Solid line, AGAO-*Strep*-tag II protein (0.079 mM); dotted line, wild-type AGAO (0.076 mM).

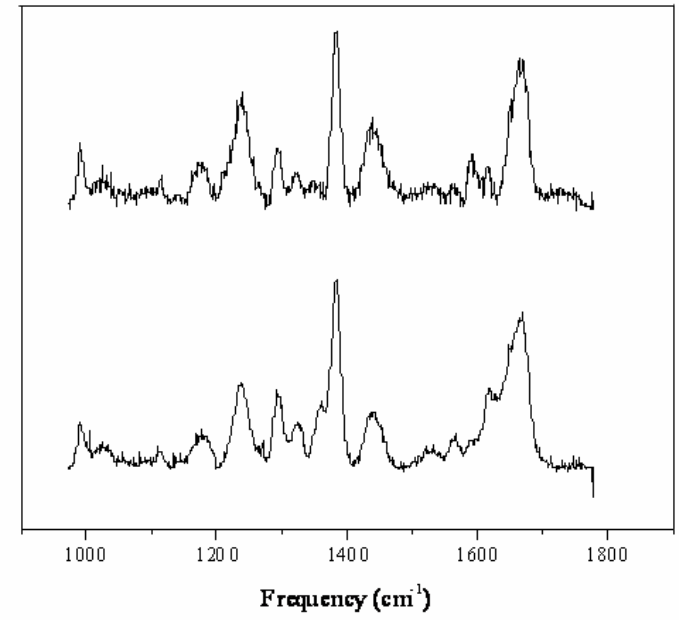

Figure 13: Resonance Raman spectra of wild-type AGAO and AGAO-*Strep*-tag II proteins obtained with 514.5 nm excitation at 298 K. Upper spectrum, AGAO-*Strep*-tag II (1.38 mM); lower spectrum, wild type AGAO (0.99 mM).

Discussion

AGAO was initially "tagged" by insertion of the AGAO coding sequence into a Genosys *tet*-vector (pASK-IBA3) that contained the sequence for a C-terminal *Strep*-tag II. This vector (pAGAO1) was under the control of the promoter/operator from the *tetA* resistance gene, which can be fully induced by adding anhydrotetracycline at a level where it is ineffective as an antibiotic. However, expression levels of the pAGAO1 construct based on SDS-PAGE analysis were found to be considerably less than that previously observed for the pPEAO2 construct (unpublished results). Accordingly, the *Strep*-tag II sequence was engineered into the pPEAO2 plasmid (pET-3c (Novagen) expression vector containing the AGAO coding sequence), previously shown to exhibit high levels of AGAO expression in our laboratory. Although the purification procedure described herein is straightforward, discussion of some additional details may be helpful. As provided by the manufacturer, the StrepTactin column resin volume has a limited binding capacity (4-5 mg per run for AGAO), thereby requiring multiple cycles to load all of the tagged protein to be purified (DEAE fraction 2). If an appropriate chromatography workstation is available, multiple runs are a convenient and cost-effective procedure. To obtain the 50 mg of protein (Table 1), a total of 11 runs over the 1.7 mL StrepTactin column were needed. Seven runs were required to load all of fraction 2 from the DEAE Sepharose column onto the StrepTactin column. Any fractions collected during column loading or washing that contained amine oxidase activity were pooled, concentrated, and dialyzed and then re-applied to the StrepTactin column. For the purification summarized in Table 1, four additional runs were required. *Strep*-tagged

amine oxidase was sufficiently stable such that rechromatographed protein samples behaved identically to the original sample. Because the StrepTactin POROS media is expensive and has a limited lifetime (up to 40 runs), it is desirable to balance the number of column runs required and the amount of material needed to achieve a particular column capacity. A factor that must be considered is the subunit composition of the protein. Since both subunits of the amine oxidase dimer are labeled with the *Strep*-tag II, one enzyme molecule may occupy two binding sites on the affinity column. Binding capacities higher than those obtained in this work would therefore be expected for monomeric proteins.

Purified AGAO-*Strep*-tag II fusion protein had a specific activity of 17 units/mg toward 2-phenylethylamine. Previous purification and characterization of the wild-type AGAO reported values for specific activity as high as 20.8 units/mg toward 2-phenylethylamine [94]. Results of a phenylhydrazine titration indicate a quantity of 1.3 TPQs/dimer of the *Strep*-tagged AGAO. This ratio is slightly lower than the 1.5 TPQs/dimer of wild-type AGAO previously reported [94], which is completely consistent with the dependence of the specific activity on the amount of titratable TPQ present in the active site [97]. Although substoichiometric amounts of TPQ were observed for the tagged protein, the optical spectrum is consistent with TPQ in a fully oxidized form [86]. Specific activities of individual fractions varied considerably and the specific activity of 17 units/mg reported herein was determined for the final pool of all fractions found to contain purified AGAO-*Strep*-tag II fusion protein. Previous work with *E. coli* amine oxidase (ECAO) has also demonstrated variability in the determined quantity of TPQ/dimer, dependent on the enzyme preparation used [101]. This led to the suggestion

that the observed variance in TPQ processing and specific activity could be attributable to the processing system in the recombinant strain and the conditions used during overexpression.

The purified AGAO-*Strep*-tag II fusion protein was shown to exhibit nearly identical characteristics to wild-type AGAO. Kinetic characterization of both the tagged AGAO and wild-type AGAO indicated no significant perturbation of k_{cat} or K_M with respect to substrate benzylamine. The copper content as determined by atomic absorption spectroscopy was found to be 1.94 Cu atoms/dimer of AGAO, as expected for a dimeric protein containing one mononuclear copper atom per subunit. Obtaining the correct copper content for the recombinant, overexpressed protein appears to be an advantage of expression in prokaryotic host organisms; tightly-bound zinc has been reported for two heterologously-expressed amine oxidases in eukaryotic cells [102].

The optical spectra of the AGAO-*Strep*-tag II protein showing the TPQ absorbance band (480 nm) is represented in Figure 11. This spectrum is consistent with AGAO that has a high degree of homogeneity and relatively consistent TPQ processing in the active site (for reviews of TPQ biogenesis see [5,15,19, 57,103]). Detailed analysis of absorption spectra of overexpressed ECAO suggested that incompletely processed TPQ, or biogenesis side products, might contribute spurious intensity on the high-energy side of the TPQ electronic absorption band [101]. In contrast, unmodified tyrosine residues would not be expected to absorb in this region. Thus the apparent bandwidth of the TPQ transition may reflect the degree to which tyrosine oxidation, once initiated, is carried through to TPQ. The CD and resonance Raman spectra data presented in Figures 12 and 13 are both consistent with previously published results [64], and confirm the

integrity of the AGAO active site. Taken collectively, the kinetics data and spectroscopic results argue strongly that the fusion of the *Strep*-tag II polypeptide to the C-terminus of AGAO has not resulted in any significant perturbation of the active site environment.

Conclusions

The *Strep*-tag II affinity purification system has proven useful for the large-scale, rapid purification of AGAO, and significantly reduced the time required to purify AGAO compared to earlier protocols. This procedure can be readily adapted to both smaller and larger scales, and is likely to be generally applicable for the purification of this widespread class of enzyme. The purification of *Strep*-tag II fusion proteins from eukaryotic expression hosts has proven to be equally successful, having been accomplished in both yeast and SF9-cells. The advantages of protein purification using StrepTactin POROS media, over alternative StrepTactin medias such as StrepTactin Sepharose, include higher binding capacity, faster separation, and increased column life.

The work reported herein has been published in *Journal of Protein Expression and Purification* [104]. Since the development of the purification protocol reported herein, over one gram of AGAO has been purified in our laboratory and has served as the basis for numerous kinetic, spectroscopic, and structural studies to date [54,87,105-107]. It should be noted that subsequent to this work appearing in press, two modifications to the overall protocol were made: 1) a larger column volume of Streptactin POROS (10 mL) is now used for increased binding capacity; and 2) the pAGAO2 construct has been transformed into a strain of *E. coli* in which two of the three genes encoding for catalase have been disrupted (for description see Appendix A). The latter modification has

eliminated catalase contamination during protein purification, a feature common to most CuAO protein preparations.

NANOSECOND ELECTRON TUNNELING WIRES AS NOVEL INHIBITORS OF A COPPER AMINE OXIDASE FROM *Arthrobacter globiformis*

Introduction

Our laboratory initiated a collaboration with Professor Harry B. Gray and coworkers (California Institute of Technology) in an attempt to measure the reduction potential of the TPQ cofactor in AGAO. The strategy was to bind an electrode–coupled, diethylaniline-terminated oligo-(phenyl-ethynyl)-thiol (DEA-OPE-SH) wire (Figure 14) in the AGAO substrate channel, thus providing a conduit for electron transfer between gold-bead electrodes and the buried TPQ [106]. Inhibition studies indicated that diethylanaline was a strong inhibitor of phenethylamine turnover in AGAO, suggesting that the DEA terminus of the wire acts as a protein specific functionality. Following functionalization with the DEA-OPE-SH wire, gold bead electrodes were incubated with purified AGAO. Cyclic voltammetry of the absorbed protein on electrodes that had been modified in this fashion showed a reversible $2e^-$, $2H^+$ reduction of TPQ at -140 mV versus SCE in phosphate buffer, pH 7, *which is the first direct determination of the TPQ redox potential in CuAOs*. This reduction potential is in agreement with that published for quinone model complexes [108].

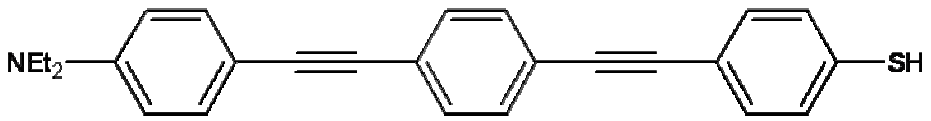

Figure 14: Structure of the diethylaniline-terminated oligo-(phenyl-ethynyl)-thiol (DEA-OPE-SH) wire described in text.

These studies were extended to the development of a fluorescent probe (Figure 15A) for the copper amine oxidase AGAO. The design of this compound (called Ru11Q) was centered on allowing the amine terminus to bind in the active site channel of AGAO, thereby blocking its interaction with the 4-4'-diphenyl-2,2'-bipyridyl-coordinated Ru(II) terminus, and relieving the intramolecular fluorescence quenching. The two ends of the molecule were connected by a flexible 11 hydrocarbon tether which allowed for the interaction of the termini when free in solution. This strategy was very successful and the initial compound is considered an excellent lead for the development of high sensitivity, *in vivo* probes for the presence of CuAOs. However, the diphenyl-bipyridine ligands proved to be very hydrophobic and as a result, concentrated stocks of the compound would only remain soluble in organic solvent. To circumvent the solubility issue, two bipyridine ligands were used to coordinate the ruthenium metal center (Figure 15B). This compound, initially synthesized with an 11 hydrocarbon tether (called Rubpy11Q), proved to be soluble in both water and buffer solutions at millimolar concentrations. Further, this compound was found to exhibit potent competitive inhibition with respect to substrate benzylamine in AGAO, supporting the hypothesis that the tertiary amine portion of the molecule binds in the active site channel. The effectiveness of this inhibitor was unanticipated, with a calculated K_i in the low nanomolar range. In order to investigate what properties of this compound were responsible for the observed potency, a series of variants of this compound were assessed as AGAO inhhibitors. These were based on the design principle of varying the "linker" between the substrate analogue functionality and the surface group to obtain a "best fit" within the active-site channel.

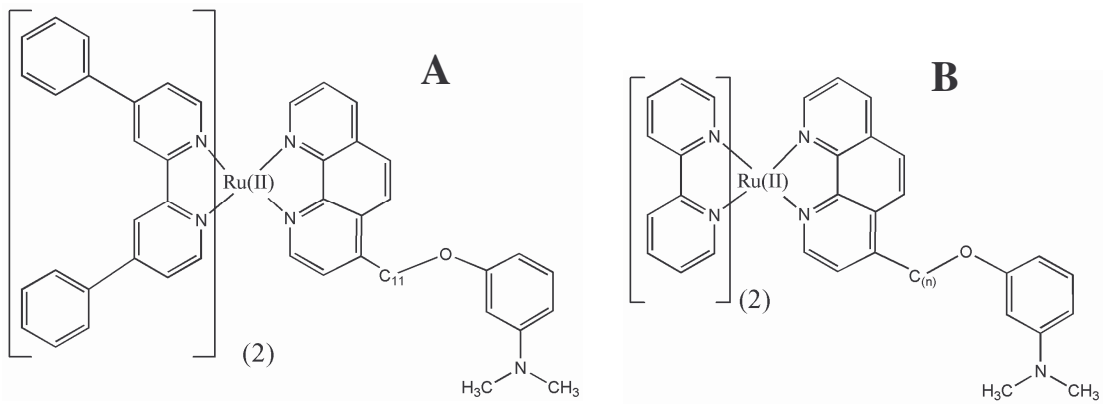

Figure 15: Structures of ruthenium probes. (A) Water insoluble Ru11Q fluorescent probe. (B) Generic structure for water soluble RubpyQ series of inhibitors.

Materials and Methods

AGAO was purified as described previously [104]. Amine oxidase activity was determined by monitoring benzaldehyde production over the course of 3 minutes (at 25 °C) at 250 nm using an extinction coefficient of 12,800 $M^{-1}cm^{-1}$ [99]. Kinetic analysis involved first equilibrating each enzyme with a given amount of inhibitor for one minute under magnetic stirring, followed by addition of substrate benzylamine to initiate each assay. Assays were at least run in duplicate, most often triplicate, at varying inhibitor concentrations and data were fit to the Michaelis-Menten equation using Origin 7.0 software (Microcal, MA, USA). Error bars on each plot represent the standard deviation of the rate at a particular substrate concentration. Steady-state kinetic data were collected on a Hewlett-Packard 8453 diode-array spectrophotometer equipped with a thermostatted cell chamber connected to an Endocal RTE-5 circulating water bath. Inhibitor stocks of the bipyridine coordinated ruthenium probes were prepared using ε_{455} = 14,500 $M^{-1}cm^{-1}$.

All inhibitors with the exception of N,N-dimethyl-m-anisidine (Acros Organics) were synthesized by Harry B. Gray and coworkers at California Institute of Technology, Pasadena, CA. N,N-dimethyl-m-anisidine was distilled prior to its use to remove potential impurities. Inhibitor stocks of N,N-dimethyl-m-anisidine were made up in acetonitrile.

Results

Table 3: Inhibition constants for Rubpy variants

Inhibitor	K_i
(1) C11Q	92 ± 11 nM
(2) C9Q	92 ± 9 nM
(3) C6Q	80 ± 11 nM
(4) C5Q	43 ± 1.5 nM
(5) C4Q	37 ± 3 nM
(6) C1Q	300 ± 18 nM
(7) C4-phenyl	680 ± 35 nM
(8) N,N-dimethyl-m-anisidine	8 ± 1 μM

Characterization of Ru11Q (Figure 15A) indicated this compound to be a very potent classical noncompetitive inhibitor of AGAO with respect to substrate benzylamine, having a calculated K_i of ~200 nM (data not shown). This result was surprising since it was expected that the tertiary amine terminus of the molecule would not be recognized by the active site channel of AGAO, given that this class of enzymes acts on primary amines. A modification of the Ru(II) ligands of this molecule gave rise to a series of water soluble compounds for which a generic structure is illustrated in Figure 15B. Table 3 lists the calculated inhibition constants for this series of compounds. All of the inhibitors listed in Table 3 exhibited clean competitive inhibition with respect

to substrate amine, indicating that they bind in the substrate channel, or otherwise interfere with substrate amine binding. It should be noted that inhibition by these compounds was found to be completely reversible upon dialysis. In order to provide definitive proof that these inhibitors are indeed binding within the substrate channel, we have solved the X-ray crystal structure of the AGAO-C4 inhibitor complex (Figure 16), in collaboration with Professor Hans C. Freeman (University of Sidney). This structure has provided definitive proof of the tertiary amine terminus binding in the active site channel, in close proximity (2.94 Å) to the TPQ cofactor.

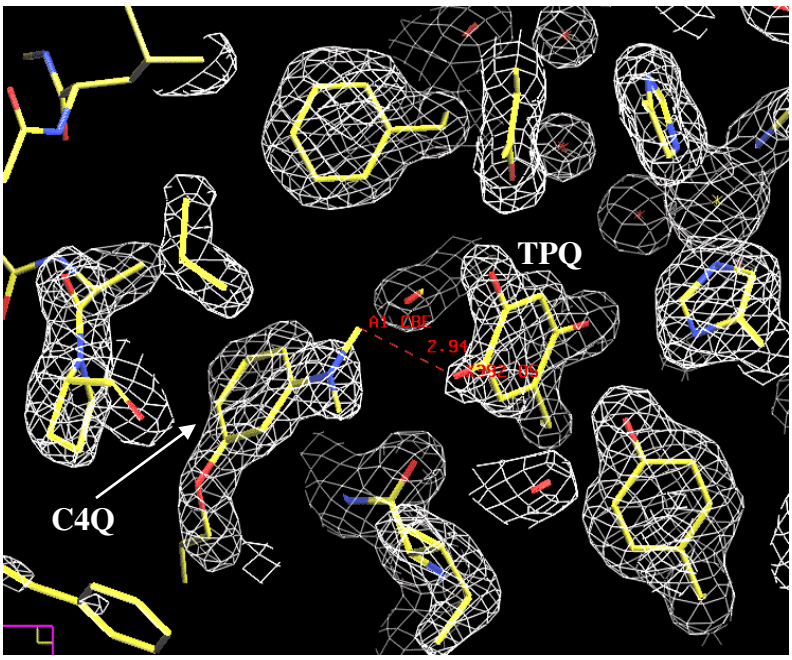

Figure 16: Crystal structure of AGAO-Rubpy-C4Q complex. Active site view illustrating the C4Q inhibitor bound within close proximity to the TPQ cofactor. Red text shows a distance of 2.94 Å from inhibitor to the TPQ cofactor.

From an examination of the inhibition constants reported in Table 3, it can be seen that the potency of the inhibition by this class of compounds increases as the length of the

hydrocarbon tether is decreased, with the Rubpy-C4Q compound being the most effective inhibitor characterized. As the hydrocarbon linker is shortened to one carbon, however, the inhibition constant goes up, indicating that the Rubpy-C1Q compound is not as tightly associated with AGAO as the Rubpy-C4Q compound. In addition to varying the length of the hydrocarbon linker, two additional compounds (Figure 17A, B) were characterized with regards to their inhibition of AGAO in order to provide information concerning what structural features of these compounds are responsible for the tight interaction with AGAO.

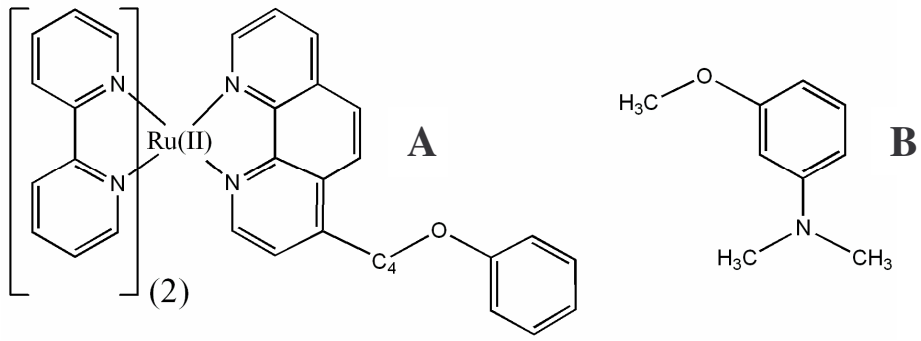

Figure 17: Structures of Rubpy C4-phenyl **(A)** and N,N-dimethyl-m-anisidine **(B).**

Interestingly, the Rubpy-C4-phenyl variant shows competitive inhibition with respect to substrate benzylamine with a calculated K_i in the high nanomolar range. This result was unexpected given the considerable differences between the phenyl terminus of this molecule and traditional primary amine substrates. The N,N-dimethyl-m-anisidine was also shown to be a competitive inhibitor with a K_i in the low micromolar range (Table 3). Since stocks of this compound were made up in acetonitrile, it was necessary to run control assays in the presence of acetonitrile in order to exclude possible inhibition arising from this solvent. Acetonitrile was shown not to affect the rate of amine oxidation. Kinetic characterization of all compounds in Table 3 is shown in Figures 18-33.

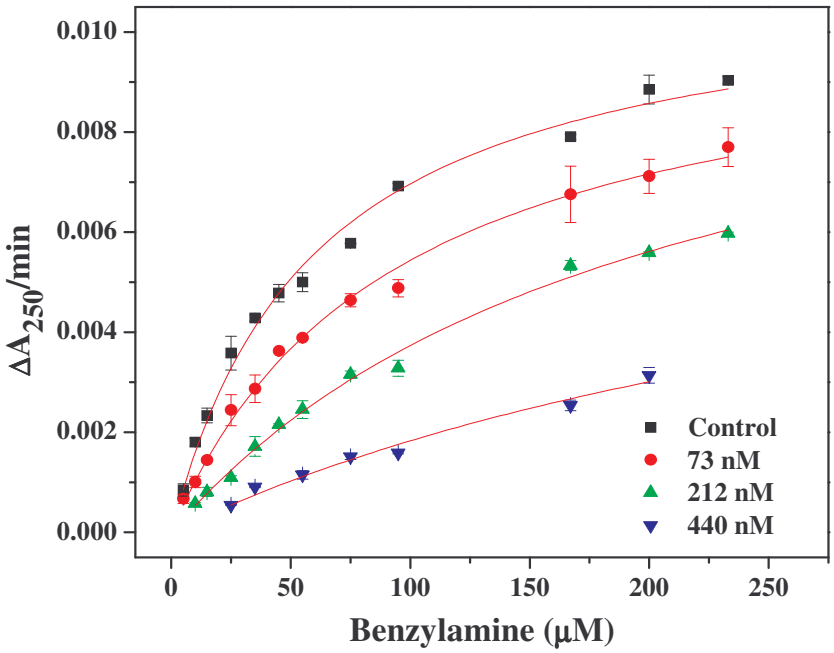

Figure 18: Inhibition kinetics of Rubpy-C11Q with AGAO. Data fit to Michaelis-Menten model. Inset shows the concentration of inhibitor used for each curve.

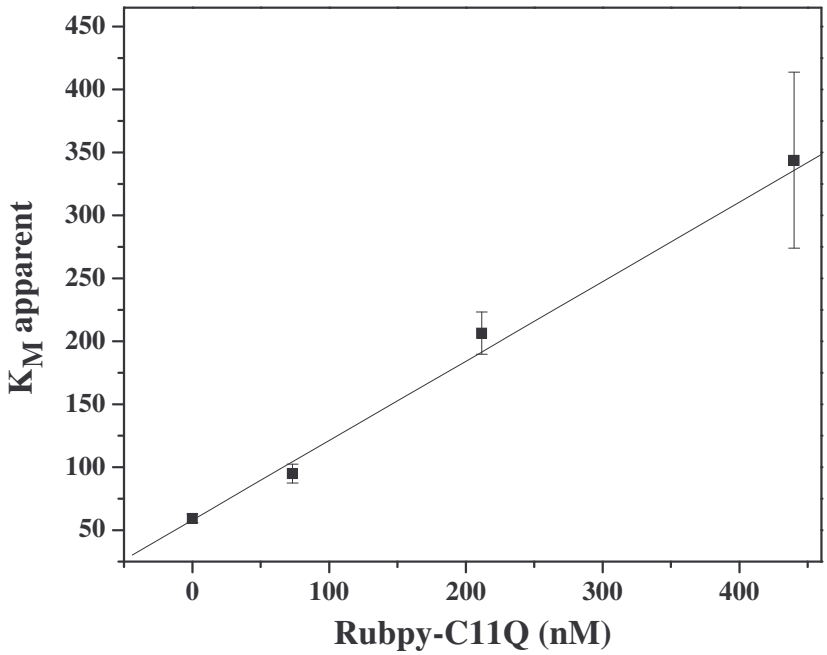

Figure 19: K_i plot for Rubpy-C11Q. Treatment of kinetic data for a competitive inhibitor according to Segel [109]. K_i is calculated from a linear plot of $K_{Mapparent}$ vs. [I] where the x-intercept is equal to $-K_i$.

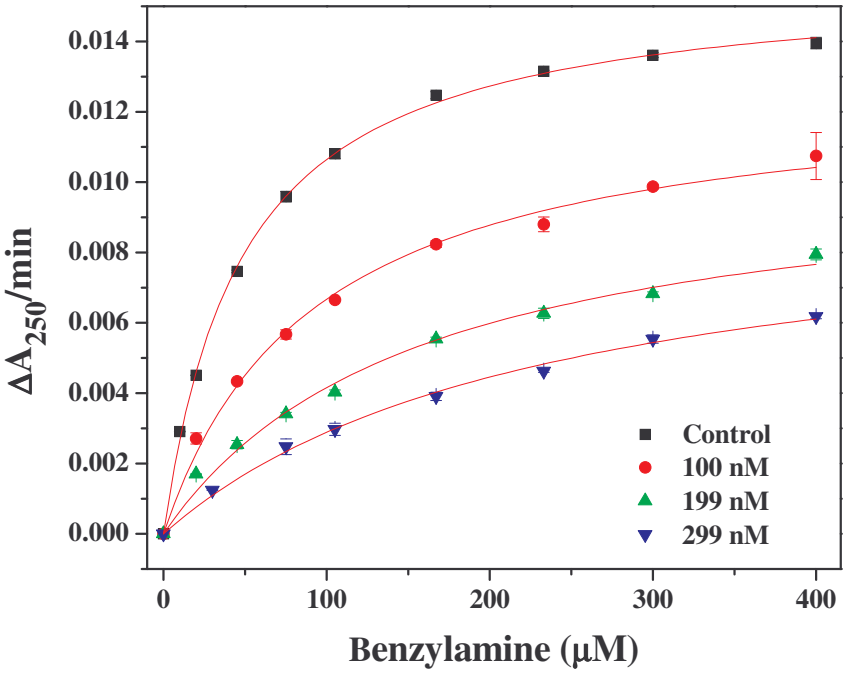

Figure 20: Inhibition kinetics of Rubpy-C9Q with AGAO. Data fit to Michaelis-Menten model. Inset shows the concentration of inhibitor used for each curve.

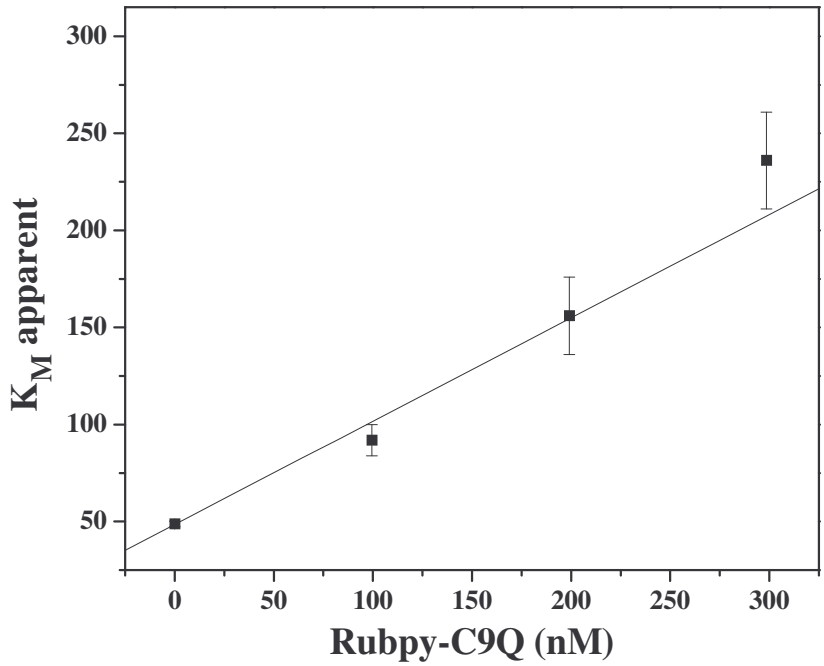

Figure 21: K_i determination for Rubpy-C9Q.

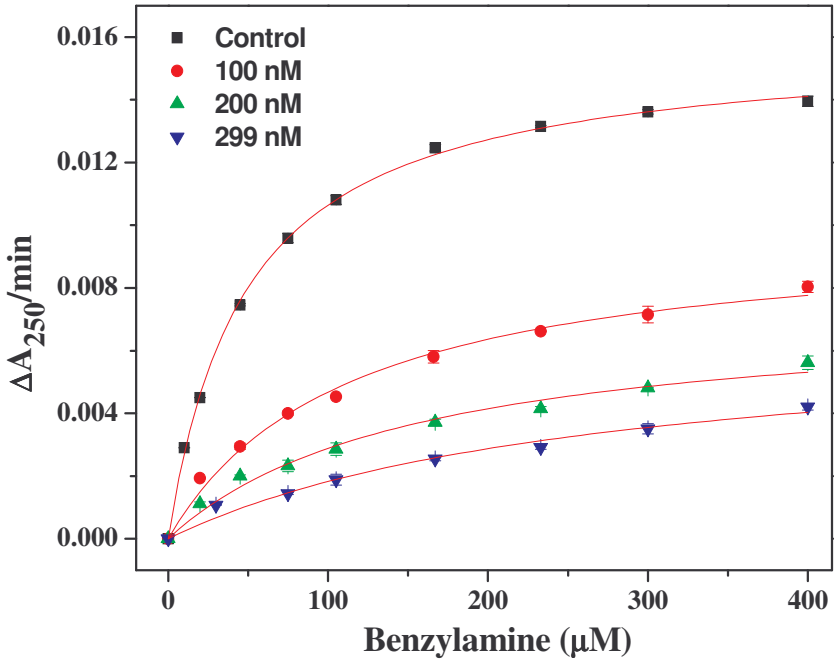

Figure 22: Inhibition kinetics of Rubpy-C6Q with AGAO. Data fit to Michaelis-Menten model. Inset shows the concentration of inhibitor used for each curve.

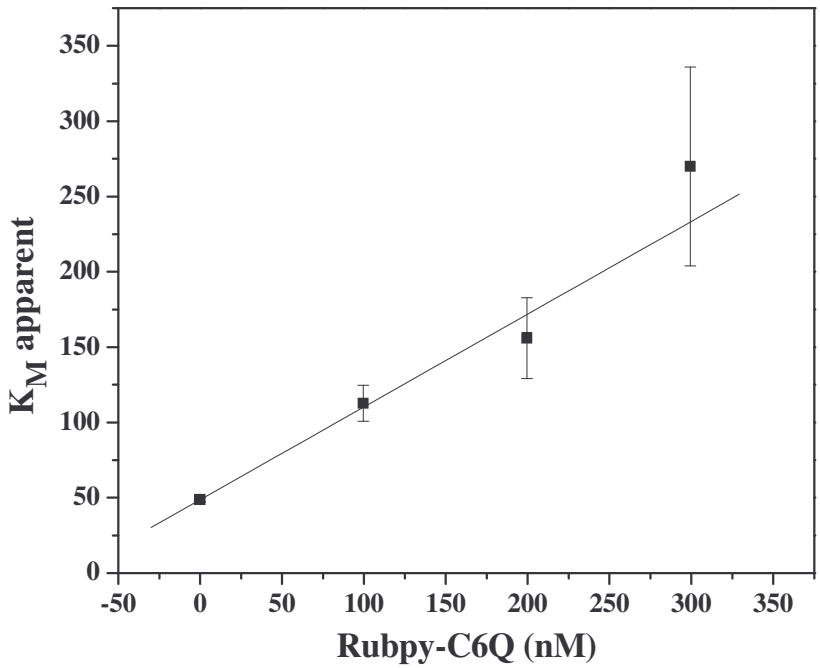

Figure 23: K_i determination for Rubpy-C6Q.

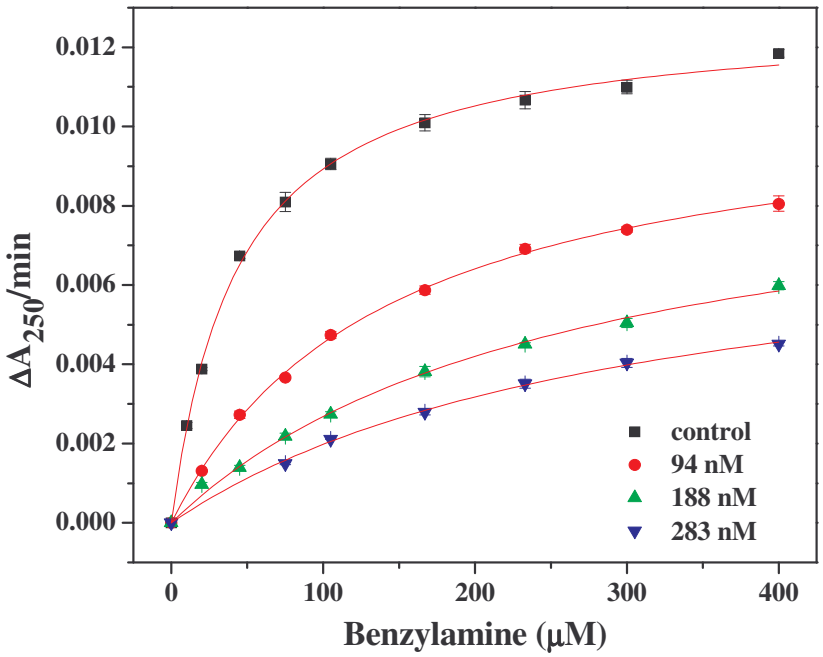

Figure 24: Inhibition kinetics of Rubpy-C5Q with AGAO. Data fit to Michaelis-Menten model. Inset shows the concentration of inhibitor used for each curve.

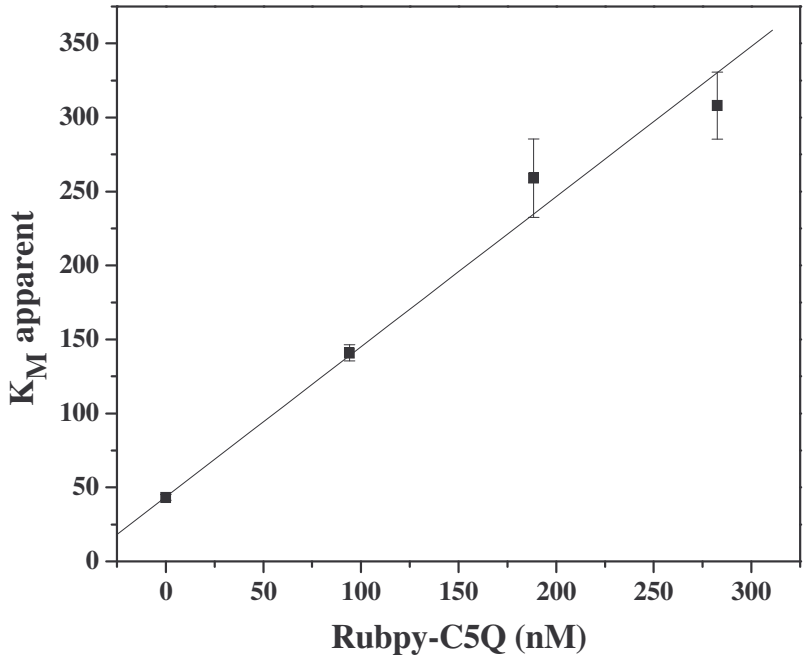

Figure 25: K_i determination for Rubpy-C5Q.

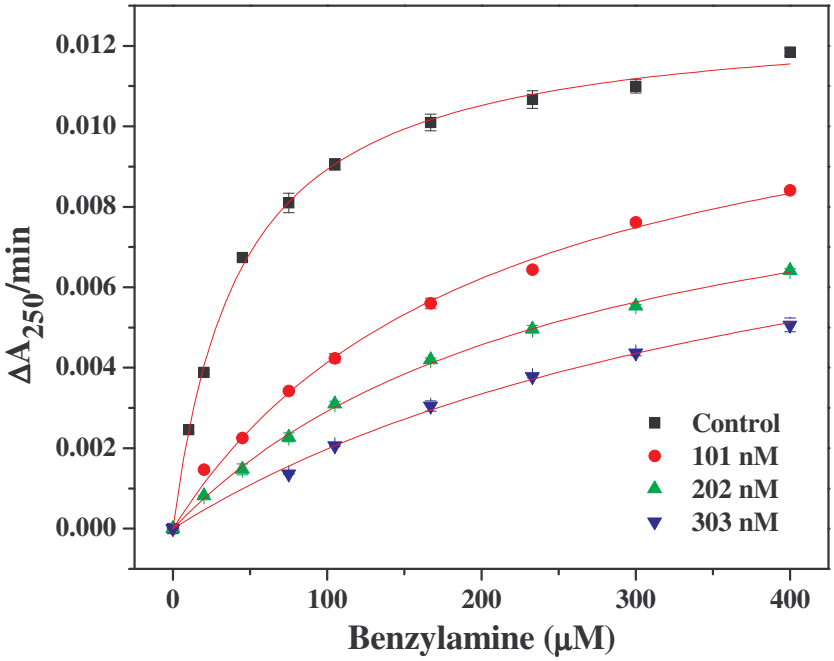

Figure 26: Inhibition kinetics of Rubpy-C4Q with AGAO. Data fit to Michaelis-Menten model. Inset shows the concentration of inhibitor used for each curve.

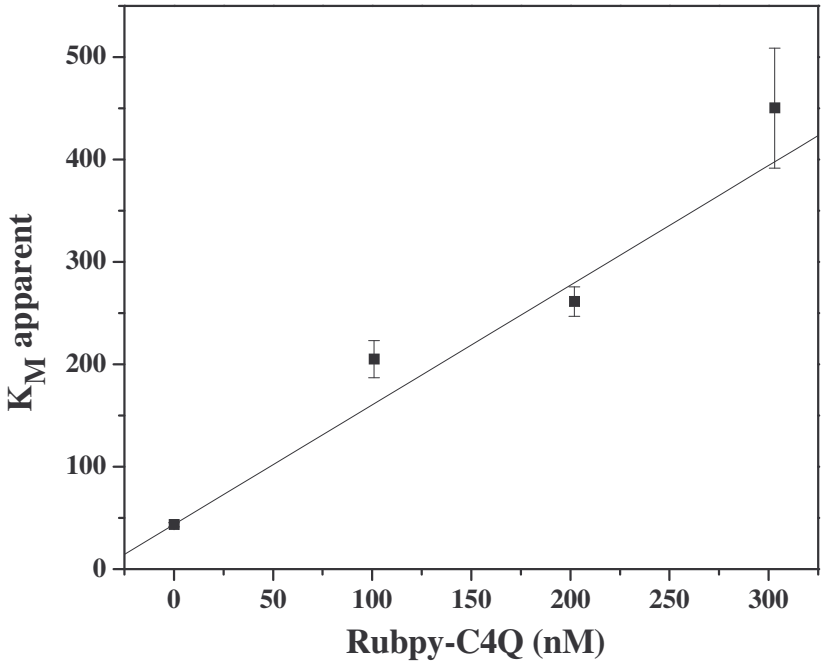

Figure 27: K_i determination for Rubpy-C4Q.

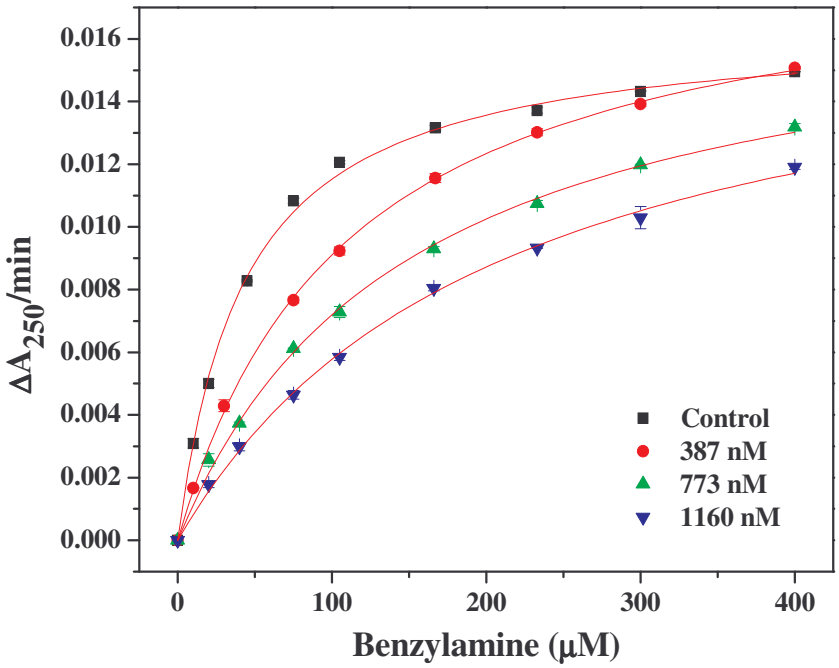

Figure 28: Inhibition kinetics of Rubpy-C1Q with AGAO. Data fit to Michaelis-Menten model. Inset shows the concentration of inhibitor used for each curve.

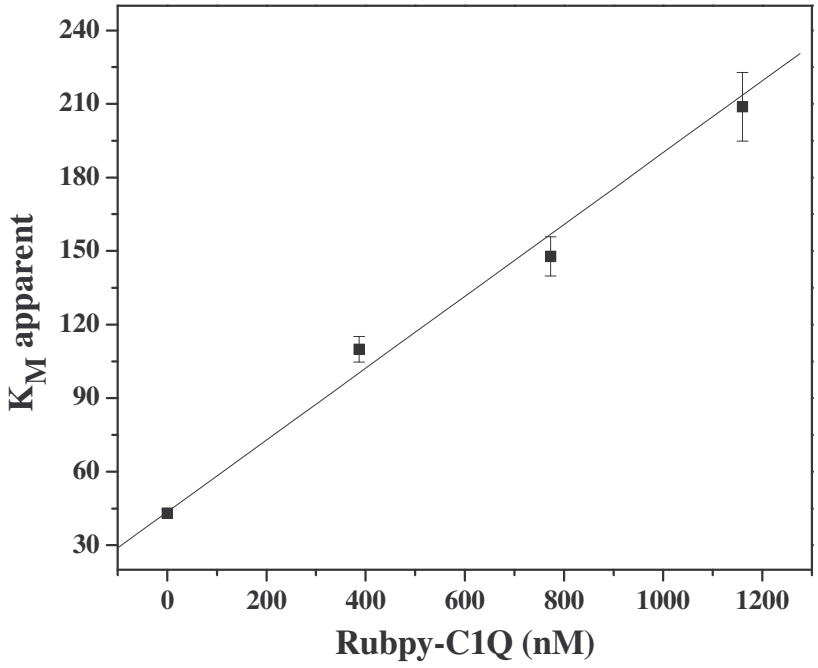

Figure 29: K_i determination for Rubpy-C1Q.

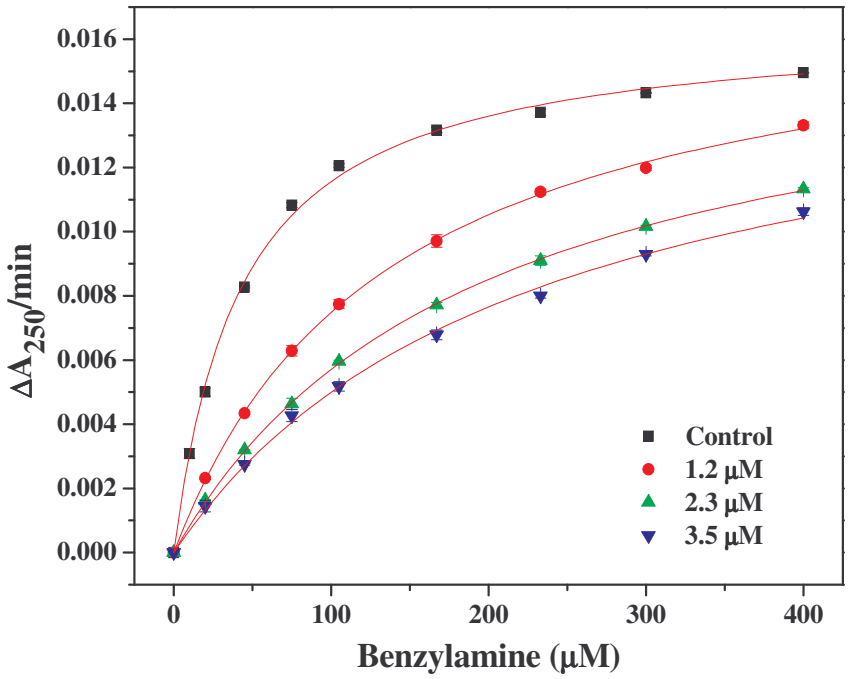

Figure 30: Inhibition kinetics of Rubpy-C4-phenyl with AGAO. Data fit to Michaelis-Menten model. Inset shows the concentration of inhibitor used for each curve.

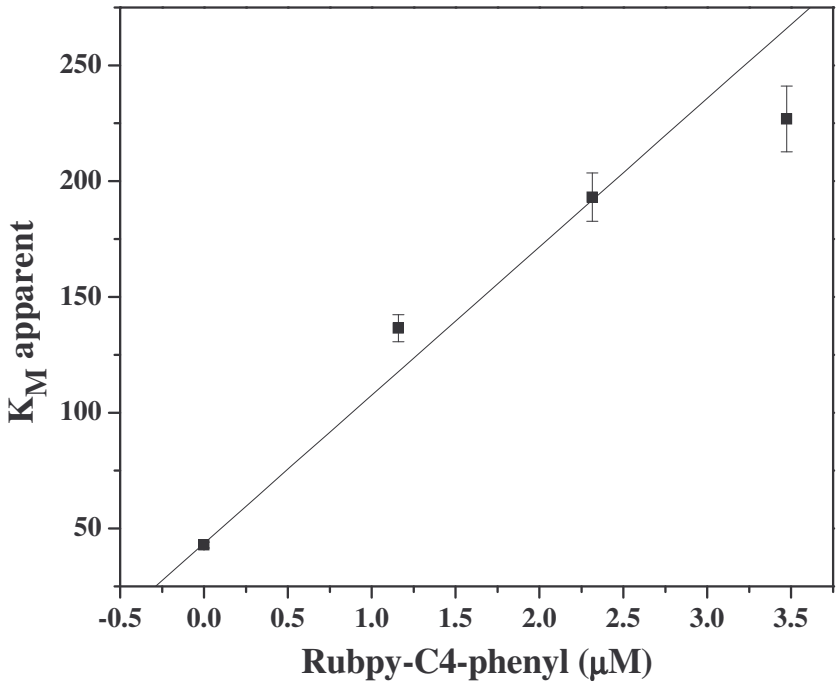

Figure 31: K_i determination for Rubpy-C4-phenyl.

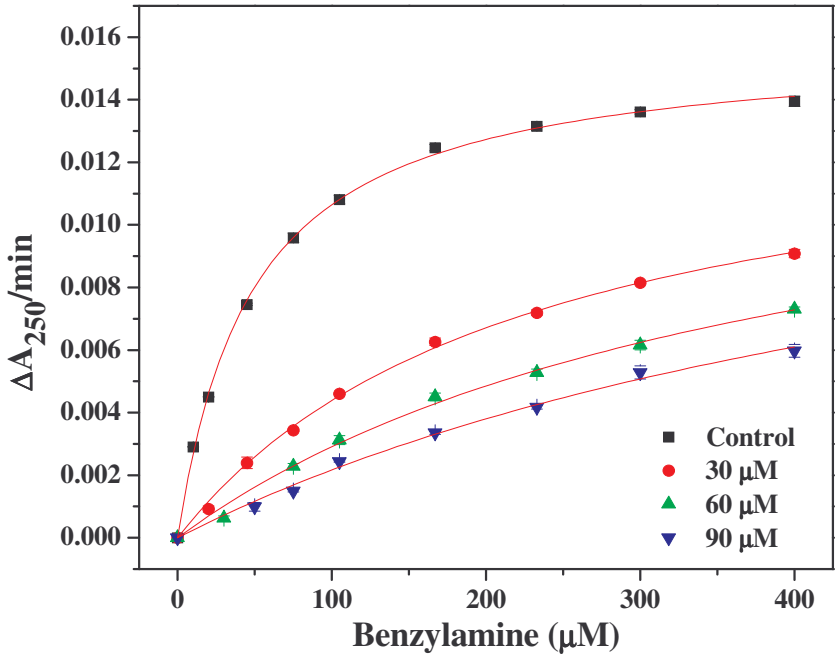

Figure 32: Inhibition kinetics of N,N-dimethyl-m-anisidine with AGAO. Data fit to Michaelis-Menten model. Inset shows the concentration of inhibitor used for each curve.

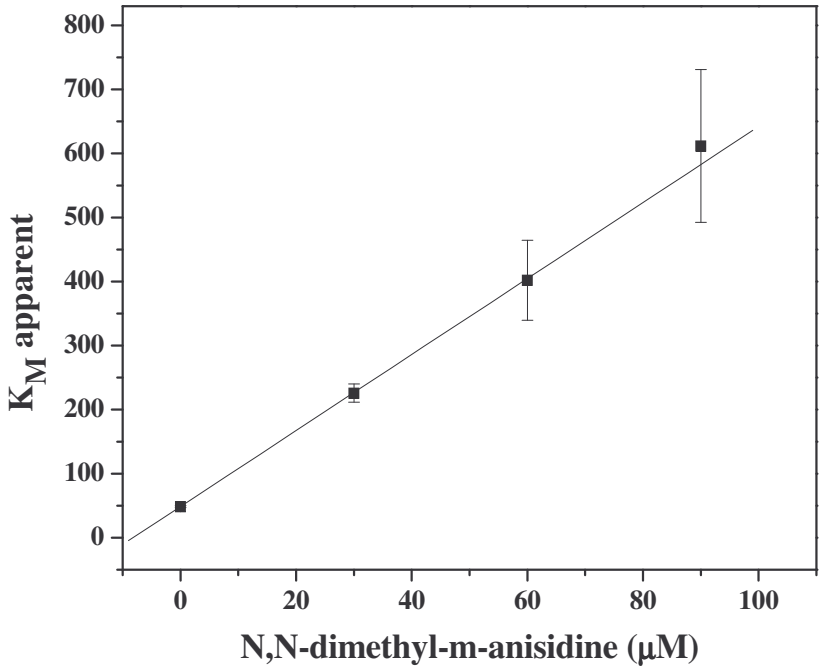

Figure 33: K_i determination for N,N-dimethyl-m-anisidine.

Discussion

Investigation into the inhibition of copper amine oxidases has increased in recent years with the identification of at least three human copper amine oxidases [21,110,111]. Pentamidine and related diamidines are front line therapeutics in the treatment of *Pneumocystis carinii* pneumonia (PCP) and other types of fungal or protozoal infections in immunosuppressed patients, such as those with AIDS [112-115]. Recently, Elmore and Dooley demonstrated that pentamidine is an extrememly potent inhibitor of rhDAO *in vitro* [31], thus supporting the hypothesis that some of the deleterious side effects of pentamidine administration may be related to its inhibition of diamine oxidase in the patient. Diamidines and numerous other compounds with guanyl functional groups are potent inhibitors of amine oxidases [112,115-117]. Furthermore, numerous inhibitors of amine oxidases and amine metabolism have shown promising antileukemic, antitumor, antifungal, and antiprotozoal activity [116-124]. With the number of potential inhibitors of this class of enzymes, it is of primary interest to identify the molecular factors which govern inhibitor potency and selectivity.

Recently, work in our laboratory has actively investigated the interaction of different inhibitors with six copper amine oxidases [53,54,105,125]. These studies have emphasized the importance of intrinsic structural differences between the active sites of CuAOs which in turn affects reactivity with a given inhibitor. In addition, recent results suggest that it may be feasible to design selective mechanism-based inhibitors of copper amine oxidases. The results of the computer modeling of 4-(2-naphthyloxy)-2-butyn-1-amine into the AGAO active site as a Schiff base derivative indicated the presence of a

hydrophobic pocket in the active site channel [53]. Several aromatic rings outline this pocket and are positioned to possibly form π-stacking interactions with inhibitors or substrates. The structural and kinetic results of an investigation into the interaction of a family of 4-(aryloxy)-2-butynamines with AGAO provided support for this hypothesis [54]. In this study, it was proposed that van der Waals interactions between this hydrophobic pocket and a given inhibitor may play a key role in determining the overall potency of inhibition.

The results reported herein provide an exciting new lead for the development of highly potent, reversible inhibitors of CuAOs. These inhibitors (Table 3), which exhibit an unexpected level of potency, bind to the active site channel of AGAO with the tertiary amine terminus in close proximity to the active site cofactor (Figure 16). It was shown that as the hydrocarbon linker in these compounds is shortened, the inhibition constant decreases. However, as the length of the hydrocarbon linker is further decreased to one carbon, the calculated inhibition constant rises dramatically, indicating a decreased affinity of the Rubpy-C1Q for AGAO, compared with a hydrocarbon linker containing at least four carbons. These results illustrate the feasibility of designing highly potent inhibitors of CuAOs based on small subtleties in structure to obtain the "best fit" within the CuAO active site channel. It is reasonable to assume that the hydrocarbon linker is responsible for a tight interaction with the active site channel of AGAO, which has been shown to be charged near the surface of the protein and become increasingly hydrophobic near the base of the channel as the active site is approached [19,53,54]. A striking finding of these studies is that even in the absence of the tertiary amine functionality, as in the case of the Rubpy-C4-phenyl inhibitor (Figure 17A), the phenyl terminus still binds and inhibits with a

nanomolar inhibition constant. This non-covalent association could be the result of π-stacking interactions within the active site, as the base of the substrate channel is known to contain numerous aromatic residues which could potentially interact with an inhibitor [53]. These residues may also be important for substrate recognition in AGAO, as it is well documented that the aromatic substrate β-phenylethylamine is the preferred substrate of this enzyme during turnover [94]. The fact that the inhibition constant for N,N-dimethyl-m-anisidine, which lacks a hydrocarbon linker, is two orders of magnitude greater than that for the Rubpy-C4Q thru Rubpy-C11Q series of inhibitors illustrates the importance of this hydrophobic, hydrocarbon portion of the molecule in interacting with the active site channel of AGAO.

Conclusions

A series of highly potent AGAO inhibitors (Table 3) have been developed in collaboration with Professor Harry B. Gray and coworkers. The results of structural analysis have shown these inhibitors to bind in the active site channel of AGAO with the amine terminus in close proximity to TPQ. N,N-dimethyl-m-anisidine (Figure 17B) has an inhibition constant in the micromolar range, as compared to low nanomolar for Rubpy-C4Q, indicating the hydrocarbon linker is responsible for increasing the potency of this class of inhibitors. In addition, characterization of Rubpy-C4-phen, which lacks the tertiary amine moiety at its terminus, illustrates the importance of this amine functionality for the tight interaction of these compounds with AGAO. It is likely that the non-covalent binding of these inhibitors to AGAO is governed by the extent of

favorable van der Waals and hydrophobic interactions between the compound and the residues lining the active site channel of the enzyme.

These compounds have only been screened for their inhibition efficacy against AGAO to date, however, it is necessary to perform inhibition profiles of these compounds with other amine oxidases to test the generality of these findings. These studies will provide information concerning the overall selectivity of this class of inhibitors. Given the results reported herein it is not unreasonable to envision the design of a copper amine oxidase inhibitor with picomolar affinity. Determining what functional groups on these inhibitors confer the highest level of potency of inhibition should set the course for design of future potent and selective amine oxidase inhibitors.

CYANIDE AS A COPPER AND QUINONE-DIRECTED INHIBITOR OF A COPPER AMINE OXIDASE FROM *Arthrobacter globiformis*: EVIDENCE FOR BOTH COPPER COORDINATION AND CYANOHYDRIN DERIVITIZATION OF THE QUINONE COFACTOR

Introduction

Monodentate ligands such as N_3^-, SCN^-, and CN^- replace the equatorial water ligand of copper and have all been described as inhibitors against O_2-mediated quinone regeneration and amine oxidation [84,126-128]. These ligands preferentially bind copper, and their monodentate coordination generally precludes removal of copper from the enzyme. Thus, investigation of the electronic and mechanistic effects of ligand-substitution reactions provide very useful probes of active site structure and catalytic mechanism of copper-containing amine oxidases [127-130].

Cyanide inhibition has been described as competitive [85], non-competitive [84], and mixed [129] with respect to substrate dioxygen. Implications concern whether or not O_2 binds in an off-metal, proteinaceous site as indicated by the noncompetitive inhibition of N_3^- with respect to O_2 in HPAO [60]. Cyanide has classically been described as a mixed or uncompetitive inhibitor versus substrate amine [84,129]. A previous study demonstrates that azide and cyanide effects on catalysis for several CuAOs can be rationalized in terms of copper coordination by these exogenous ligands and their effects on the internal redox equilibrium TPQ_{amr}-Cu(II) $\leftrightarrow$ TPQ_{sq}-Cu(I) [128]. In addition, inhibition due to cyanide has been proposed to arise from both Cu(I) coordination and TPQ-cyanohydrin formation [84,129,130]. As reported in the case of pyrroloquinoline

quinone (PQQ), cyanohydrin derivatization resulted in competitive inhibition versus substrate glucose in glucose dehydrogenase [131]. Even though cyanide readily and reversibly reacts with quinones, no direct spectroscopic evidence for cyanohydrin derivatization of TPQ has been observed in CuAOs [128,132], despite a report indicating slight perturbations in the absorption spectrum of PKAO upon addition of CN^- [129]. This work describes the first direct spectroscopic evidence, using both model and enzyme systems, for cyanohydrin derivatization of TPQ and outlines the mechanism for CN^- inhibition against substrate amine in *Arthrobacter globiformis* amine oxidase.

Materials and Methods

Protein Preparation

Arthrobacter globiformis amine oxidase was purified as described previously [104]. Only protein of the highest quality was utilized for experimentation (at least 1.4 TPQ/dimer). Protein concentrations were calculated using extinction coefficients at 280 nm as previously reported for AGAO [93], and using an extinction coefficient of 2,500 $M^{-1}cm^{-1}$ for TPQ [72].

Spectroscopic Characterization

UV and visible absorption data were acquired utilizing a Cary 6000i UV/vis/NIR spectrophotometer (Varian, Australia) connected to a Cary dual cell Peltier accessory for temperature control. All spectroscopic data were collected at 25 °C in 100 mM phosphate buffer, pH 7.2, and analyzed using Origin 7.0 software (Microcal, MA, USA).

Samples of AGAO (85.1 μM) were titrated with NaN_3 (Fisher) stock solution (1.5 M NaN_3 in 0.1 M KPO_4, pH 7.2) and the absorbance was monitored at 388 nm to determine K_d values for the Cu(II)-N_3^- complex in this enzyme. Following addition and thorough mixing of each aliquot, five minutes were allowed for equilibration before taking spectra. Longer incubation times yielded no significant increases in absorbance of the LMCT band. The ΔA at 388 nm was plotted versus azide concentration and the data were fit to a second order equation in order to determine the K_d value for the Cu-N_3^- complex.

In order to determine the K_d for the Cu(II)-CN^- complex in AGAO, a sample of enzyme that was preequilibrated with near saturating amounts of N_3^- was then titrated with a stock solution of NaCN (Fluka Biochemika) using the method as described by He et al. [129]. All cyanide stock solutions (0.025 – 1.0 M) were prepared prior to each experiment using NaCN in 100 mM KPO_4 buffer, pH 7.2, and were kept anaerobic during the course of experimentation. AGAO (51 μM) was incubated with 600 mM N_3^- for 30 min at 25 °C in the dark prior to the first addition of NaCN. NaCN was then added in small aliquots to a final concentration of 66 mM, allowing 10 min between subsequent additions, and the ΔA at 388 nm was monitored as azide was displaced from Cu(II) by cyanide. The ratio of the two equilibrium constants (K_{CN^-} to K_{N3^-}) was then determined by linear least squares analysis according to the equation [129]:

$$-(A - A_O)/(A - A_Z) = (K_{CN^-}/K_{N3^-}) \times ([CN^-]/[N_3^-])$$

where A is the absorbance at 388 nm, and A_O and A_Z are the absorbance values at the beginning and end of the experiment, respectively.

A buffered sample (0.1 M KPO_4, pH 7.2) of wild-type AGAO was titrated with cyanide in order to determine if any spectroscopic alterations of the native TPQ chromophore occurred. AGAO (18.1 μM) was titrated with ~1 – 2 mM additions of CN^- up to a final concentration of 100 mM, allowing 5 minutes equilibration between additions. Spectroscopic changes were monitored at both 345 nm and 500 nm.

Kinetic Characterization

The effect of cyanide on enzymatic catalysis was investigated for AGAO. All kinetic data were collected at 25 °C in 100 mM phosphate buffer, pH 7.2. Kinetic analysis involved first equilibrating the enzyme with a given amount of cyanide for 5 min under magnetic stirring, followed by addition of substrate benzylamine to initiate each assay. Amine oxidase activity was determined by monitoring benzaldehyde production over the course of 3 minutes at 250 nm using an extinction coefficient of 12,800 $M^{-1}cm^{-1}$ [99]. Assays were at least run in duplicate, most often triplicate at varying cyanide concentrations and data were fit to the Michaelis-Menten equation using Origin 7.0 software (Microcal, MA, USA). Error bars on each plot represent the standard deviation of the rate at a particular substrate concentration. All steady-state kinetic data were collected on a Hewlett-Packard 8453 diode-array spectrophotometer equipped with a thermostatted cell chamber connected to an Endocal RTE-5 circulating water bath.

Results

Cyanide as a Cu(II)-Directed Ligand

The K_d for Cu(II)-N_3^- complex in AGAO was found to be 247 ± 22 mM (K_{eq} = 4.05 ± 0.36 M^{-1}; ε_{388} = 1970 $M^{-1}cm^{-1}$) as determined by monitoring the formation of the LMCT band at 388 nm. This value represents the average obtained from a second orderfit and a reciprocal plot of $1/\Delta A_{388\ nm}$ vs. $1/[N_3^-]$ utilizing the raw data. Determining a K_d value for the Cu(II)-CN^- complex is more difficult given that there exists no LMCT band in the visible region. AGAO was therefore titrated with cyanide following preincubation with near saturating amounts of azide, as established by He et al. [129]. As seen in Figure 34, CN^- binding to Cu(II) was indirectly determined by monitoring the decrease in absorbance at 388 nm due to the displacement of N_3^- by CN^-. Linear least-squares analysis (Figure 35) of ΔA versus cyanide concentration produced a K_d value of 2.9 ± 0.4 mM (K_{eq} = 347 ± 48 M^{-1}) for AGAO. Spectroscopic and kinetic analysis following extensive dialysis of the protein sample (four exchanges against 1 L of 100 mM KPO_4, pH 7.2) showed complete recovery of the native TPQ_{ox} absorbance feature and full restoration of activity.

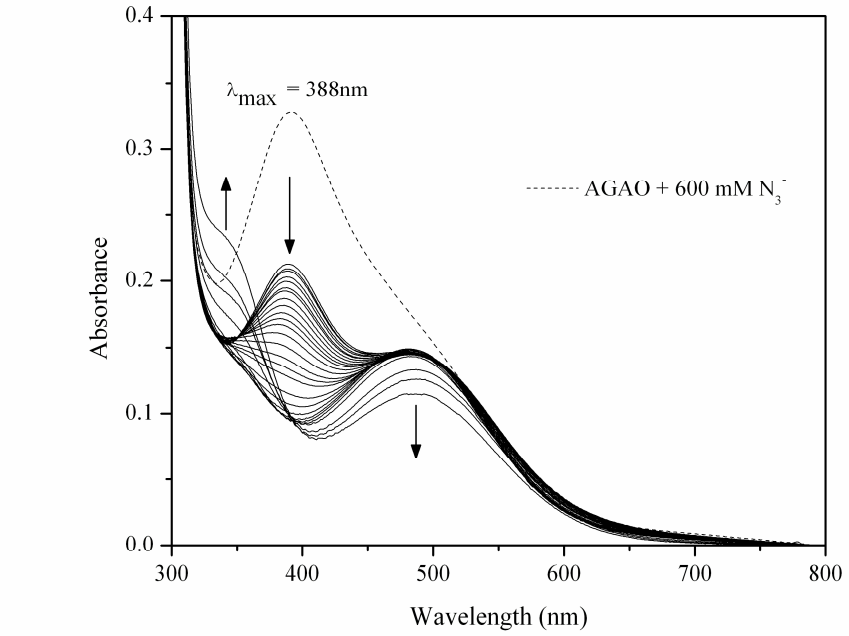

Figure 34: Cyanide as a Cu(II)-directed ligand in AGAO. CN^- displacement of azide bound to copper monitored via the decrease in the Cu(II)-N_3^- LMCT band as described in text. NaCN added in small aliquots (~1-10 mM) to final a final concentration of 66 mM.

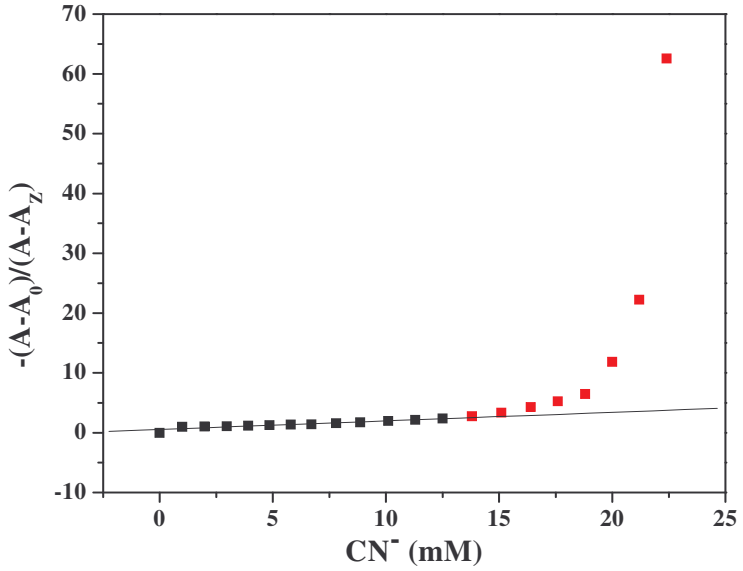

Figure 35: Linear least-squares analysis of the displacement of N_3^- from Cu(II) by CN^-. Data was analyzed according to: $-(A - A_O)/(A - A_Z) = (K_{CN^-}/K_{N3^-}) \bullet ([CN^-]/[N_3^-])$ as described in text. Data points in red were masked for linear the analysis.

During addition of cyanide, azide was observed to be titrated off cleanly up to a concentration of 25 mM CN^- (Figure 34), establishing that CN^- preferentially reacts with Cu(II) rather than the TPQ cofactor in this enzyme. Interestingly, at higher concentrations of cyanide (26 – 66 mM), a spectral feature with a λ_{max} of about 340 nm began to grow in with successive additions of cyanide. The appearance of the 340 nm shoulder was isosbestic with the disappearance of the TPQ_{ox} feature at 480 nm, suggesting a possible derivitization of the TPQ cofactor.

Cyanohydrin Derivatization of the Native Quinone Cofactor

To focus more directly on the spectroscopic feature near 340 nm (Figure 34) and eliminate the complexity of azide displacement, wild-type AGAO (18.1 μM) was titrated with cyanide. Figure 36 illustrates the results of this titration up to a final cyanide concentration of 71 mM. Absorbance at 480 nm (TPQ_{ox}) was seen to decrease at relatively high concentrations of cyanide (30–100 mM), with the formation of a species with a shoulder at 340 nm. This behavior is similar to that seen during the displacement of azide with cyanide in AGAO (Figure 34), however, the intensities of the spectral features are reduced compared with the titration in the presence of azide. Possible reasons for this are discussed below. It should be noted that formation of the ~345 nm species was observed to be rapid (less than 3 min). Additionally, it was determined that pH did not remain constant in this experiment even in the presence of 0.1 M KPO_4, pH 7.2. The pH of the 100 mM cyanide stock was measured to be 9.5, with the pH in the enzyme titration experiment gradually shifting to a more basic pH (final pH ~8.5). The protein sample was extensively dialyzed following titration (four exchanges against 1 L

of 100 mM KPO_4, pH 7.2) and kinetically and spectroscopically analyzed. The native TPQ_{ox} chromophore was observed to completely return and activity was fully restored to control levels.

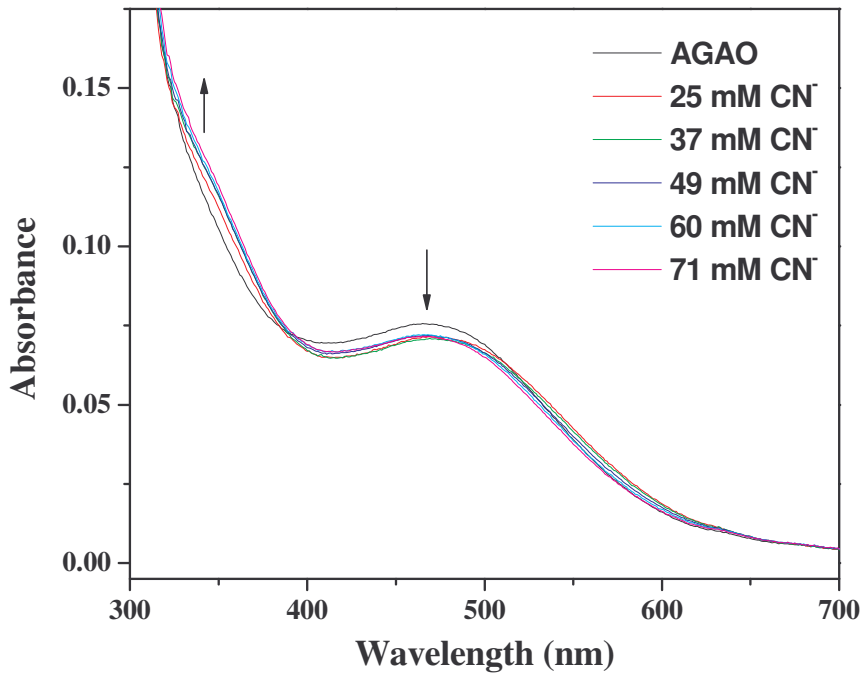

Figure 36: Cyanohydrin derivatization of the native quinone cofactor in AGAO (18.1 μM). NaCN added in ~12 mM additions to a final CN^- concentration of 71 mM.

The Effect of Cyanide on Amine Oxidation

The effects of cyanide on enzymatic catalysis were examined for AGAO. Data analysis revealed that V_{max} and K_{Mapp} decreased as cyanide concentration increased, indicating that cyanide was an uncompetitive inhibitor versus substrate benzylamine (Figure 37). Treatment of the data according to Segel (1975) [109] produced the reciprocal plot seen in Figure 38. The calculated K_i value with respect to substrate benzylamine was 1.05 ± 0.13 mM for AGAO. Control inhibition studies were performed

using NaCl in order to determine whether there were any inhibitory effects that could be attributed to either ionic strength or the presence of Na^+ or Cl^-. No inhibition of AGAO was observed to occur at levels up to 300 mM NaCl.

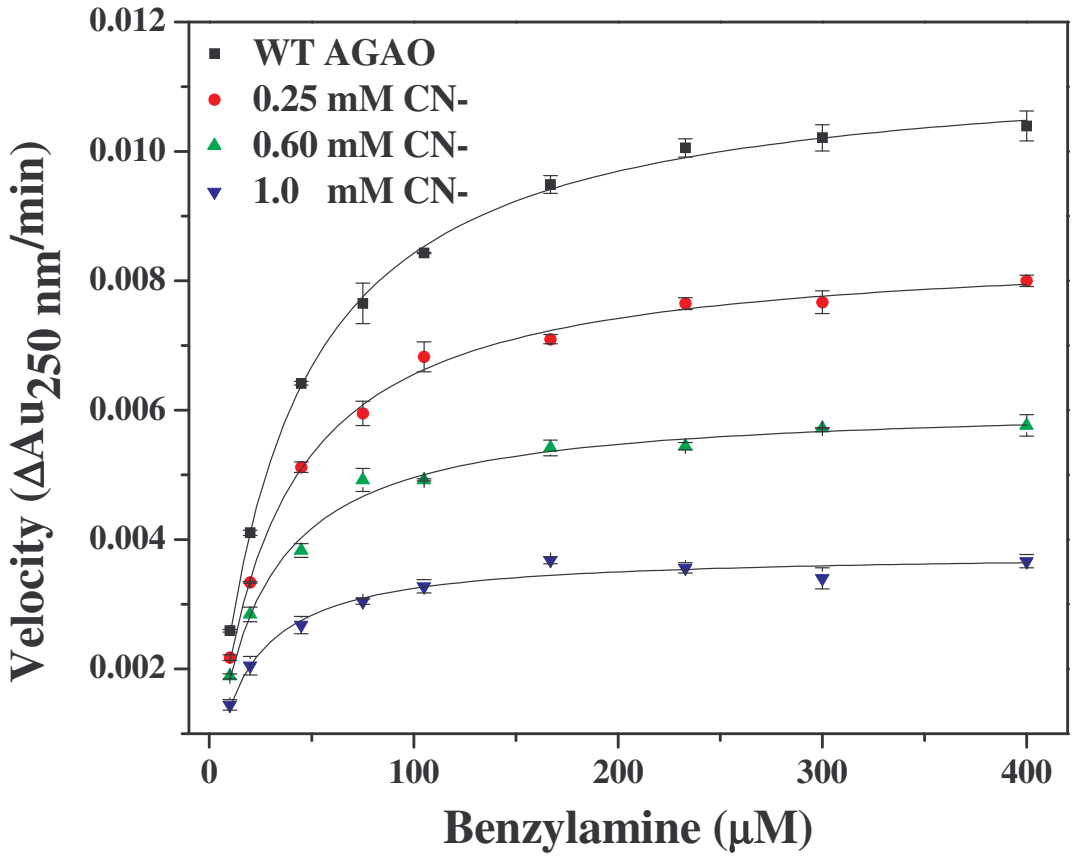

Figure 37: The effect of cyanide on amine oxidation for AGAO. Plots represent initial rates of reaction versus substrate benyzlamine concentration at various cyanide concentrations. All data curves were fit to the Michaelis-Menten equation.

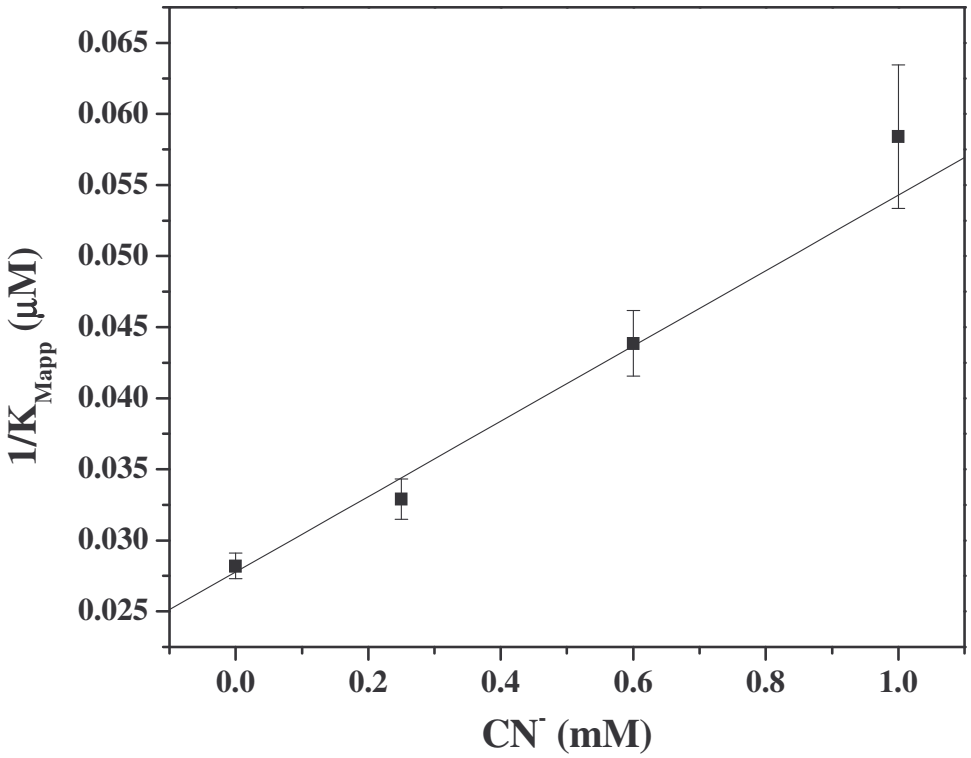

Figure 38: K_i plot for AGAO with CN^- as an uncompetitive inhibitor. Plot represents $1/K_{Mapp}$ vs [Inhibitor] for treatment of uncompetitive inhibition as described in [109].

Discussion

Cyanide has traditionally been used to probe the electronic environment of the copper center, in both the oxidized and substrate reduced forms of CuAOs [84,85,128,129,132]. This research has been primarily concerned with determining how catalysis is affected relative to substrate amine and O_2. The ligand substitution chemistry of cyanide is comparable among CuAOs, preferentially displacing a water molecule at the equatorial, as opposed to the axial position [84,127]. Consequences are reflected in the reactivity of the quinone cofactor and the copper ion, however, variability in the nature of inhibition exists among CuAOs from different sources [84,85,129]. An early

report by Barker et al. (1979) [84] with PPAO interpreted the observed inhibition patterns (uncompetitive versus benzylamine; non-competitive versus O_2) as CN^- ligating copper and reacting with active site carbonyl groups. This explanation was supported by a subsequent study with BPAO and PKAO [129]; however, no evidence for cyanohydrin formation was discovered in a report by McGuirl et al. (1997) [128]. The latter study led to the proposal that the main mechanism of inhibition was the stabilization of Cu(I) by CN^-, thereby preventing reaction with O_2 during reoxidization of the reduced enzyme. Herein, direct spectroscopic evidence for cyanohydrin derivatization of the quinone cofactor in AGAO is described. Furthermore, a mechanism for CN^- inhibition against substrate amine in *Arthrobacter globiformis* amine oxidase is presented. These results were published in conjunction with similar studies using the enzyme PSAO as well as a thorough investigation of the TPQ model chemistry with regards to cyanohydrin formation [107].

TPQ-Cyanohydrin Formation

Interaction of AGAO with CN^- is featured by a reversible conversion of the native TPQ chromophore to a moiety with an absorbance at ~340 nm (Figures 34 and 36). Similar results were obtained with PSAO, for which cyanohydrin derivitization of the TPQ cofactor resulted in a species absorbing at 345 nm [107]. Cyanide addition to TPQ in both AGAO and PSAO was concluded to occur exclusively at TPQ(C5) by virtue of its reversibility (dialysis results in return of the TPQ_{ox} absorbance band and full recovery of activity) and the similarity of the absorbance for the C5 cyanohydrin TPQ model **1** chromophore (Figure 39) [107]. This indicates that CN^- reversibly binds in the active

sites of both these CuAOs at CN^- concentrations up to 100 mM (AGAO) and 50 mM (PSAO). The observation in the model chemistry that irreversible addition of CN^- occurred at C1 rather than C5 of TPQ at high pH [107] was surprising given the steric bulk (*tert*-butyl group) at this position, and raises the question as to whether this could occur in an enzyme system. Although no evidence was obtained for addition of CN^- to C1 in the cases of AGAO and PSAO, addition at TPQ(C1) might occur in other CuAOs if the steric and conformational consequences of C1 addition can be accommodated by the active site.

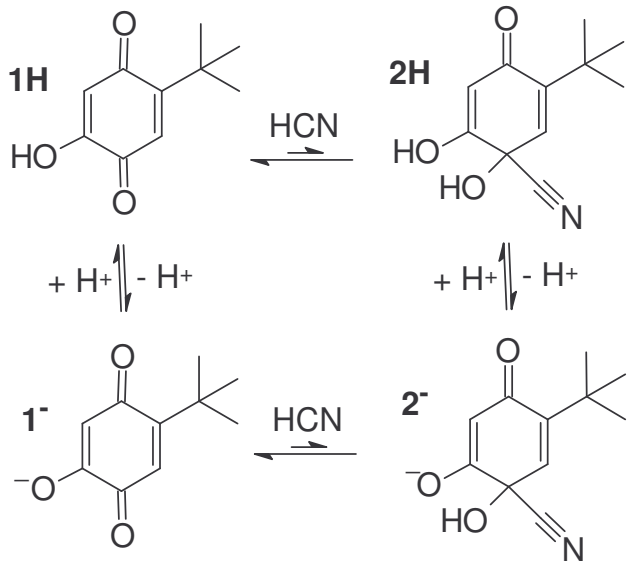

Figure 39: TPQ model chemistry with cyanide. (1H) TPQ model 5-*tert*-butyl-2-hydroxy-1,4-benzoquinone and (1^-) its enolate form. (2H) The C5 cyanohydrin form of the TPQ model compound and (2^-) its enolate form.

Certainly, there should be differences between CuAOs also in the likelihood of cyanohydrin formation at C5. In AGAO, cyanohydrin formation is observed to form at concentrations of cyanide which are an order of magnitude greater (~26 mM; Figure 34)

than concentrations required to derivatize TPQox in PSAO (~700 μM) [107]. Interestingly, the extent of cyanohydrin formation in AGAO appears to be greater in the presence of azide (Figure 34) than in the absence of azide (Figure 36), suggesting that ligand substitution at the Cu(II) center could affect the reactivity of TPQ_{ox} towards CN^-. Substantial evidence exists concerning how either ligand substitution at copper or TPQ modification influences the reactivity and spectroscopic properties of the other cofactor [128,129,133-136]. These results suggest that microenvironmental differences between the active sites of different CuAOs may be responsible for the reactivity of the C5 carbonyl of TPQ towards cyanide. Furthermore, the finding in the model system that cyanide adduction is favored more in DMSO than in water indicates that the equilibrium is quite sensitive to environmental effects [107]. Although one might surmise that the active site of PSAO is more hydrophobic and that the active site of AGAO is more hydrophilic, the much greater ease of cyanohydrin formation in PSAO may also arise from specific hydrogen-bonding or other non-covalent interactions within the active site that stabilize the adduct relative to the starting carbonyl.

Cyanohydrin derivatization of TPQ was examined by EPR and resonance Raman spectroscopies for APAO and PKAO in a previous report by Dooley and coworkers [128], concluding that CN^- was not bound to either TPQ_{sq} or TPQ_{amr}. For the EPR experiments, CN^- isotopes were added *following* anaerobic substrate reduction of the enzymes, and yet we now know that CN^- interacts only with TPQ_{ox}. The lack of any observed effects suggests that APAO, like AGAO, does not as readily form the TPQ-CN adduct.

Mechanism of CN^- interaction with AGAO and PSAO

Cyanide displays uncompetitive inhibition towards turnover of amine substrate in both AGAO (Figure 37) and PSAO [107] with K_i values of 1.05 ± 0.13 mM (AGAO) and 648 ± 77 μM (PSAO), respectively, meaning that inactivation arises when CN^- binds to the substrate reduced form of the enzyme (ES complex or E_{red}) [137]. Although CN^- interacts with both TPQ_{ox} and Cu(II) in the resting enzymes, uncompetitive inhibition suggests that cyanohydrin formation, which would be expected to result in competitive inhibition of substrate turnover, is not primarily responsible for the observed inhibition. The finding that inhibition arises when CN^- interacts with E_{red} is consistent with the report by McGuirl et al. (1997) [128], where stabilization of Cu(I) against reaction with O_2 was attributed to be the source of inactivation.

In an effort to confirm this, the K_d for the Cu(I)-CN^- complex in PSAO was determined to be 302 ± 82 μM [107]. However, due to the difficulties with this experiment, an anaerobic substrate reduced CN^- titration of AGAO was not attempted. With this in mind, it is only appropriate to make the following qualitative statements: 1) the affinity (K_d) of CN^- for Cu(I) is an order of magnitude greater than the K_d of CN^- for Cu(II) in PSAO; and 2) the magnitude of K_d for this association is of similar magnitude to the calculated inhibition constant (K_i) for CN^- inhibition of amine oxidation in PSAO, relative to substrate amine. Higher affinity of CN^- for Cu(I) over Cu(II) is expected owing to metal to ligand π* back bonding [138], which is more extensive for the electron rich d^{10} Cu(I) relative to d^9 Cu(II). Classical uncompetitive inhibition, it seems, does not appear to be a completely accurate description of the interaction of CN^- with these

enzymes, especially given the disparity between the K_i values for AGAO and PSAO with substrate amine and the K_d for the Cu(I)-CN^- complex in PSAO, as these values should be approximately equal if the sole mechanism of inhibition was due to Cu(I) complexation. A possible explanation for the difference in these values could arise from the difficulty in obtaining an accurate K_d for the Cu(I)-CN^- complex. A more likely explanation, however, is that the K_i is a result of Cu(I) complexation as well as TPQ-cyanohydrin formation, a result more consistent with noncompetitive inhibition where I binds to E and ES and S binds to E and EI [137]. This behavior may help to explain why cyanide has been classically described as a mixed and/or uncompetitive inhibitor with respect to substrate amine for several CuAOs, especially at relatively high CN^- concentrations.

It is understandable why it may be difficult to discern the true mode of inhibition towards substrate amine for a set of CuAOs, especially owing to the finding that cyanohydrin formation occurs in such varying affinities between AGAO and PSAO. In this study, only a very small subset of the quinone cofactors present would be modified at the concentrations of CN^- used in the kinetic analysis. Substantial inhibition is observed at 1 mM CN^- in the kinetic experiments (Figure 37), an effect which is inconsistent with the level of TPQ-CN formation. These results taken collectively lend support to the idea that the dominant mode of inhibition towards amine oxidation is indeed uncompetitive with CN^- stabilizing Cu(I). For PSAO, the observation of the slow reoxidation of TPQ_{sq} to TPQ_{ox} in the presence of CN^- [107] is consistent with this scheme and concurs with previous reports [77,128-130,132].

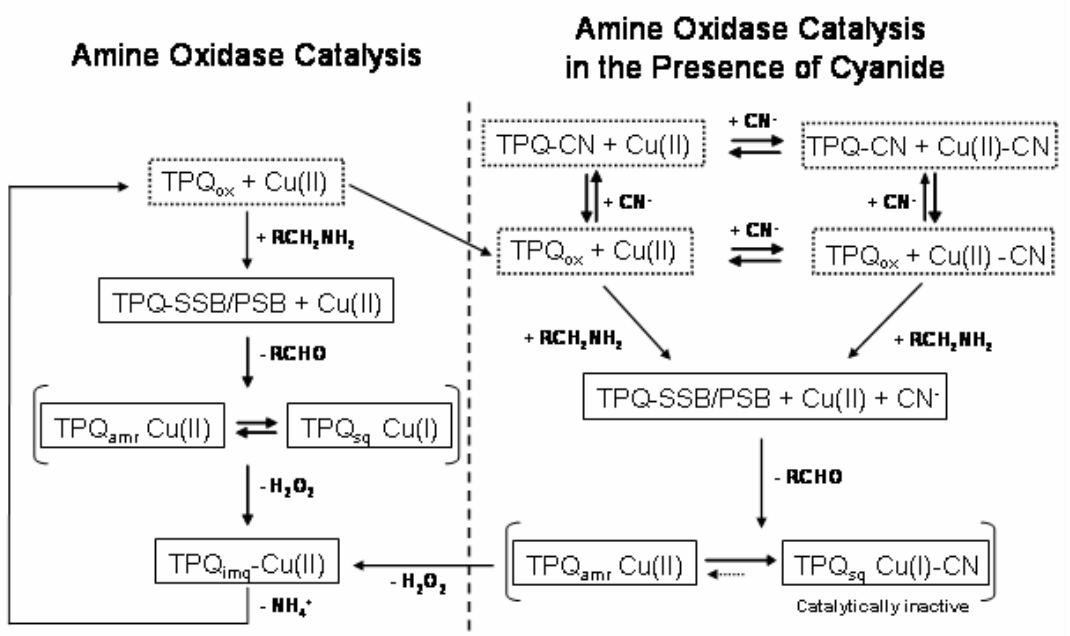

Figure 40: Proposed mechanism of CN^- inhibition of CuAO catalysis. The left panel indicates normal catalysis, as also shown in Figure 6 of this work. Abbreviations are given in the text

Substrate analogs (phenylhydrazine) and presumably substrates react with unmodified TPQ cofactors at similar rates in the presence and absence of CN^-. TPQ cofactors modified by cyanide, however, cannot react directly with substrate amine. Therefore, conversion back to TPQ_{ox} through perturbation of the TPQ-CN $\leftrightarrow$ TPQ_{ox} equilibrium, as mediated by binding of amine to TPQ_{ox}, becomes the determining factor for reactivity with amine substrate. This is supported by results with PSAO indicating that complete phenylhydrazine reactivity is slowed by a factor of ~4 when CN^- is present during the titration [107]. Consequently, preequilibration with CN^- yields a group of derivatized cofactors which do not rapidly react with substrate amine. Based on these

results, a scheme for catalytic turnover of amine substrate in the presence of cyanide was developed (Figure 40).

Conclusions

In summary, the results presented here and in conjunction with those reported in [107] provide the first unequivocal spectroscopic evidence, using both model and enzyme systems, for cyanohydrin derivatization of the quinone cofactor. Cyanide addition to TPQ in both AGAO and PSAO was concluded to occur exclusively at TPQ(C5). The observation in the model chemistry that addition of CN^- can also occur at TPQ(C1) at high [CN^-] [107] raises the question as to whether this addition might occur in other CuAOs if the steric and conformational consequences could be accommodated by the active site. The finding that cyanohydrin formation occurs so much more readily in PSAO than in AGAO is remarkable and suggests there are profound differences in the dielectric microenvironment and/or the availability of nearby active site residues with non-covalent interaction potential, in the vicinity of the TPQ(C5) carbonyl between the two enzymes. Nonetheless, this type of interaction does not play a significant role in the mechanism of inhibition towards substrate amine in either enzyme. Stabilization of Cu(I) by CN^- appears to act as the dominant mode of inhibition, presumably acting in direct competition with O_2 for binding to Cu(I), thereby preventing reoxidation of the reduced enzyme [128,129]. It has been argued that the TPQ_{sq}-Cu(I) species is off-pathway. In this case, CN^- ligation of Cu(I) would then be expected to perturb the equilibrium with the on-pathway, TPQ_{amr}-Cu(II) moiety. Furthermore, cyanide complexation to copper may disrupt electrostatic interactions between copper and reduced dioxygen species, as

implicated as being potentially significant in O_2 affinity [83]. However, given the greater similarity between the K_i value for inhibition of substrate amine (648 ± 77 μM) and the K_d for the Cu(I)-CN^- complex (302 ± 82 μM), relative to the K_d for the Cu(II)-CN^- complex (3.4 ± 0.3 mM) in PSAO [107], the data suggest that Cu(I)-TPQ_{sq} is likely a catalytically competent intermediate in PSAO. Whether dioxygen is reduced via Cu(I) in AGAO remains ambiguous.

A COMPERATIVE STUDY OF THE BINDING AND INHIBITION OF TWO COPPER CONTAINING AMINE OXIDASES BY AZIDE: IMPLICATIONS FOR THE ROLE OF COPPER DURING THE OXIDATIVE HALF-REACTION

Introduction

It is well established that CuAO catalysis proceeds through a Ping-Pong Bi Bi mechanism divided into two half-reactions [163]:

$$E_{ox} + RCH_2NH_2 \leftrightarrow E\text{-}RCH_2NH_2 \rightarrow E_{red} + RCHO \quad (1)$$

$$E_{red} + O_2 + H_2O \rightarrow E_{ox} + H_2O_2 + NH_3 \quad (2)$$

The first half-reaction is conventionally known as the reductive half-reaction and is detailed in chapter 1 of this work (Figure 6, A $\rightarrow$ D). The second half-reaction involving reoxidation of the organic cofactor is known as the oxidative half-reaction, and is diagrammed in Figure 6, D $\rightarrow$ A. The principal unresolved issue in CuAO catalysis is the precise role of copper during enzymatic reoxidation, as outlined in Figure 7. We have suggested that, at least in certain cases, the first electron reduction of dioxygen occurs via Cu(I), resulting in a Cu(II) bound superoxide species (Figure 7, A $\rightarrow$ C) [77,107]. This proposal is supported by the ample precedence among copper-containing metalloproteins for the reactivity of three-coordinate Cu(I) sites with dioxygen [139-142]. In addition, this mechanism circumvents the well-known spin conversion problem associated with two-electron reductions of oxygen [143]. A detailed kinetic study of the catalytic intermediates in LSAO provided direct support for this mechanism [92,144]. Recently, a

kinetic and structural study of a metal substituted CuAO from *Arthrobacter globiformis* suggested two possible reoxidation mechanisms [89]. In one, the initial electron transfer to dioxygen comes directly from the TPQ_{amr} species and the reduction of Cu(II) is not required. The role of Cu(II) in this mechanism is to bind the superoxide anion and facilitate the second electron transfer from the one electron reduced cofactor. However, this study also points out that the rate enhancement for reoxidation observed in the native, copper containing enzyme compared with the metal-substituted forms is consistent with reduction of Cu(II) to Cu(I), thereby implicating the Cu(I)-TPQ_{sq} species as a catalytically viable intermediate [89].

Substantial research on the CuAO from *Hansenula polymorpha* (HPAO) has led to the proposal that copper reduction is not essential for regeneration of the resting cofactor, leading to the suggestion of an alternative reaction pathway (Figure 7, A2 $\rightarrow$ C2) [60,82,83]. These studies suggest that dioxygen receives the first electron directly from TPQ_{amr} (A2 $\rightarrow$ B2; rate limiting step), with the superoxide species subsequently migrating to Cu(II) (B2 $\rightarrow$ C2) [72]. An essential feature of this mechanism is that the copper-bound axial water serves as a proton source in TPQ reduction, resulting in a Cu(II)-OH^- species. It is believed that following the first electron transfer to O_2, the pK_a of TPQ_{sq} is perturbed in a way to allow for rapid proton transfer back to the metal bound hydroxide species forming H_2O. The metal bound water would then be expected to undergo rapid substitution with superoxide anion [72]. In addition to these proposals, a theoretical study utilizing density functional theory has implicated the paramagnetic copper center in the triplet (T) $\rightarrow$ singlet (S) spin transition of the reduced quinone

cofactor, thus facilitating electron transfer directly from TPQ_{amr} to dioxygen [145]. Finally, a structural study of the steady-state intermediate that accumulates in ECAO upon aerobic exposure to excess β-phenylethylamine indicated the presence of a reduced dioxygen species bound axially to copper and equidistant to the copper and TPQ cofactor, consistent with electron transfer to dioxygen occurring from either Cu(I) or TPQ_{amr} [61,86]. In light of these mechanistic questions, it is clear that detailed kinetics and spectroscopic experiments of structurally characterized CuAOs are required to examine the possibility of mechanistic variability among CuAOs.

The monodentate ligands N_3^- and CN^- are known to replace the equatorial water ligand of copper and have been described as inhibitors against O_2-mediated quinone regeneration and amine oxidation [84,126-128]. These ligands preferentially bind copper, and their monodentate coordination generally precludes removal of copper from the enzyme. Thus, investigation of the electronic and mechanistic effects of ligand-substitution reactions provide insight into both active site structure and the catalytic mechanism of copper-containing amine oxidases [127-130]. A previous study demonstrated that azide and cyanide effects on catalysis for several CuAOs can be rationalized in terms of copper coordination by these exogenous ligands and their effects on the internal redox equilibrium TPQ_{amr}-Cu(II) $\leftrightharpoons$ TPQ_{sq}-Cu(I) [128]. Recently we have published a detailed spectroscopic and kinetic report on the interaction of cyanide with two CuAOs [107].

In CuAOs, the mode of inhibition by azide with respect to substrate amine has previously been reported to be uncompetitive [146,147], however, mounting evidence

suggests that the mode of inhibition varies depending on the enzyme source. In the oxidative half-reaction, azide inhibition has been described as competitive with respect to O_2 in pig plasma amine oxidase (PPAO) [84,85] and noncompetitive with respect to O_2 in HPAO [60]. Although the results from inhibition experiments conducted under turnover conditions are not unambiguous, the data provide and important foundation for assessing possible mechanisms, and in this case can provide an informative test of hypotheses for the role of copper in the reaction of reduced CuAOs with O_2. Herein, a detailed spectroscopic and kinetic characterization of the interaction of azide with respect to both the reductive and oxidative half-reactions in the copper-containing amine oxidases AGAO and PPLO is presented. The results are discussed in light of the outcome of similar studies with rhDAO and PSAO.

Materials and Methods

Enzyme Purification and Isolation

AGAO and PPLO were purified as described previously [104,148]. Protein concentrations were calculated using extinction coefficients at 280 nm as previously reported for AGAO [93] and PPLO [148], and using an extinction coefficient of 2,500 $M^{-1}cm^{-1}$ for TPQ [72]. All experiments for AGAO were carried out in 100 mM potassium phosphate buffer, pH 7.2, while those for PPLO were performed in 50 mM HEPES buffer, pH 7.0.

Azide Titrations of Oxidized Amine Oxidases

A sample of AGAO (85 μM) in 100 mM phosphate buffer, pH 7.2 was titrated with a 1.5 – 2.5 M stock of NaN_3 (Fisher Chemicals, NJ, USA) to a final concentration of 900 mM and the LMCT band for the Cu(II)-N_3^- complexes was monitored at 388 nm. A sample of PPLO (39.3 μM) in 50 mM HEPES, pH 7.0, was titrated with a 5 M NaN_3 stock solution in 50 mM HEPES buffer, pH 7.0. The Cu(II)-N_3^- LMCT band was monitored at 385 nm.

All sodium azide stocks were made fresh immediately prior to use and were adjusted to the respective experimental pH values as listed above. Following addition and thorough mixing of each titration aliquot, 2 – 3 min was allowed for equilibration before recording spectra. Longer incubation times yielded no significant increases in the respective LMCT bands. UV and visible absorption data were acquired utilizing a Cary 6000i UV/vis/NIR spectrophotometer (Varian, Australia) connected to a Cary dual cell Peltier accessory for temperature control. Absorbance data were analyzed using Origin 7.0 software (Microcal, MA, USA). The ΔA of the respective LMCT bands were plotted versus azide concentration and the data were fit to a second order equation in order to determine respective K_d values for the Cu(II)-N_3^- complex. All titrations of AGAO, and PPLO were performed at 30 °C.

Azide Titrations of Substrate-Reduced Amine Oxidases

In order to determine if the affinity of azide for copper was altered in the substrate-reduced form of the enzymes, samples of PPLO (50 μM) and AGAO (25 μM) were purged with Argon passed through a vanadium bubbler, HCO_3, H_2O setup

[107,149] and then reduced with a ~5 fold excess (over active site concentration) of substrate benzylamine. Stocks of benzylamine and azide were made anaerobic by purging with argon preceding introduction to the protein samples. As previously described, a glucose, glucose oxidase, catalase solution was added to the protein sample prior to addition of substrate to ensure that anaerobic conditions were maintained throughout the titration [107]. The ΔA of the respective LMCT bands were determined from difference spectra and plotted versus azide concentration to determine respective K_d values for the Cu(II)-N_3^- complex using a second order equation.

Azide Inhibition of the Reductive Half-reaction

In order to determine the effects of azide upon the first half-reaction (Eq. 1), kinetic characterization was determined at three different azide concentrations for AGAO and PPLO. Substrate O_2 was kept at near saturating amounts (~ 185 μM dissolved O_2) while substrate amine was varied below and above respective K_M values for each enzyme. The preferred amine substrate varied depending on the enzyme source, with *β*-phenylethylamine being used for AGAO, and benzylamine for PPLO. Ionic strength was controlled for all kinetic assays (both those for the reductive and oxidative half-reactions) by addition of either potassium chloride for PPLO or potassium sulfate for AGAO. KCl and K_2SO_4 were determined to have no inhibitory affect on respective CuAO activity, as determined through a series of control assays conducted prior to experimentation (data not shown). Assays (including those described below for the oxidative half-reaction) for AGAO were performed at a controlled ionic strength of 440 mM by varying the ratio of azide to K_2SO_4. Likewise, all assays for PPLO were conducted at an ionic strength of

150 mM, supplemented by KCl. The factor controlling ionic strength was determined by the amount of azide required to achieve adequate levels of inhibition. It is important to point out that the rate changes observed with increasing NaN_3 (up to 250 mM) appear to be specific and not to reflect a general salt effect [107].

The rate of β-phenylethylamine oxidation by AGAO was monitored using a horseradish peroxidase (HRP)-ABTS (2,2'-azino-bis(3-ethyl)benzthiazoline-6-sulfonic acid) coupled assay. HRP reacts with the H_2O_2 produced through CuAO catalytic activity and produces an activated form which in turn oxidizes ABTS to produce a chromophore with λ_{max} at 414 nm [96]. For PPLO, amine oxidase activity was determined by monitoring benzaldehyde production over the course of 3 min at 250 nm using an extinction coefficient of 12,800 $M^{-1}cm^{-1}$ [99].

Kinetic analysis involved first equilibrating each enzyme with a given amount of azide for two minutes under magnetic stirring, followed by addition of substrate amine to initiate each assay. Assays were at least run in duplicate, most often triplicate at varying azide concentrations and data were fit to the Michaelis-Menten equation using Origin 7.0 software (Microcal, MA, USA). Error bars on each plot represent the standard deviation of the rate at a particular substrate concentration. Steady-state kinetic data were collected on a Hewlett-Packard 8453 diode-array spectrophotometer equipped with a thermostatted cell chamber connected to an Endocal RTE-5 circulating water bath. All steady-state kinetic data for AGAO and PPLO were conducted at 30 °C.

Azide Inhibition of the Oxidative Half-reaction

In order to determine the effects of azide on the oxidative half-reaction of amine oxidation (Eq. 2), levels of substrate amine were kept at saturating amounts while substrate O_2 was varied. Rates of oxygen uptake in the presence of varying amounts of azide were determined using an Instech (Plymouth Meeting, PA) model 125/05 Clark-type oxygen electrode interfaced to a single channel Instech model 103 oxygen electrode amplifier. All assays were conducted at 30 °C in a thermostatted, 680 µL sealed batch cell equipped with an Instech model 103 magnetic stirring mechanism. The ionic strength of all assays was adjusted to identical levels as described for the reductive half-reaction (see above). Levels of amine substrate varied given the respective K_M values for the different enzymes with 50 µM and 200 µM β-phenylethylamine used for AGAO and 460 µM benzylamine utilized for PPLO.

The following procedure was used for each enzyme with the only difference being the composition of the buffer and the ionic strength. Buffer was made at the appropriate ionic strength and allowed to equilibrate overnight in a 30 °C H_2O bath. Substrate amine was then freshly added to the temperature and air-equilibrated buffer, which was subsequently divided into two flasks. The first flask was left exposed to air while the second flask was purged with Ar passed through a vanadium bubbler, HCO_3, H_2O setup [149] for at least 1 hour. Mixtures of air-equilibrated and anaerobic buffer were then injected into the cell chamber via gas tight syringes to achieve a desired level of dissolved O_2, as monitored using the Clark-type oxygen electrode. When desired levels of dissolved O_2 were reached, the output reading was monitored for a period of 10

seconds to ensure there was no electrode drift (Figure 41). Assays were then initiated by addition of 2 – 3 μL of respective enzyme samples via a gas tight syringe. Initiation of kinetic assays by addition of enzyme could be accomplished due to the fact that azide binding in CuAOs has been shown to be rapid [60,107,128].

Substantial efforts were made in order to ensure the reproducibility of experimental rates. For each kinetic curve obtained, over a range of oxygen concentrations, a minimum of 14 – 20 data points were collected. Each data point represents the rate of oxygen depletion from the assay chamber, determined from a fit of the change in dissolved oxygen levels over time (Figure 41). Reported error bars arise from the standard error associated with the linear fits to the initial reaction rate data. In several cases, rates of O_2 consumption were obtained on consecutive days at the same concentrations of dissolved oxygen, and in each case examined the respective rates were within error of one another. Data were fit to the Michaelis-Menten equation using Origin 7.0 software (Microcal, MA, USA).

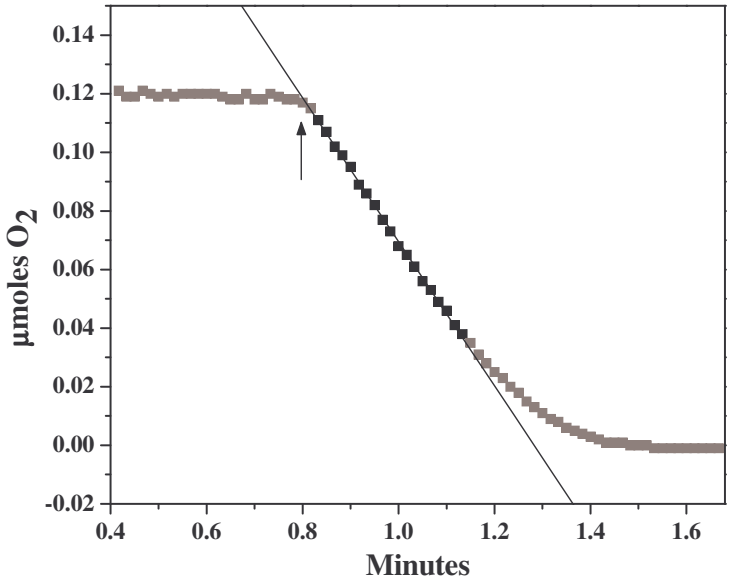

Figure 41: Representative oxygen consumption kinetics followed in the assay chamber. Trace represents an AGAO control assay initiated at 177 µM O_2. Arrow indicates the point at which enzyme was injected into the chamber. Black squares (■) represent data points used to calculate rates of oxygen consumption. Grey squares (■) represent data points not included in linear fits.

Results

Azide as a Cu(II)-Directed Ligand in Oxidized Amine Oxidases

Respective λ_{max} values for the LMCT bands for Cu(II)-N_3^- complexes were found to be 388 nm for AGAO ($\varepsilon_{388} \cong 2000\ M^{-1}cm^{-1}$; Figure 42) and 385 nm for PPLO (Figure 43). The experimentally determined K_d values for the Cu(II)-N_3^- complexes in these enzymes are 213 ± 18 mM for AGAO and 153 ± 16 mM for PPLO (Table 4). In addition, Table 4 reports K_d values for the Cu(II)-N_3^- complexes in rhDAO and PSAO for comparison as reported in [150]. The K_d values determined for the Cu(II)-N_3^- complex in AGAO is in close agreement with that previously reported at 25 ºC [107].

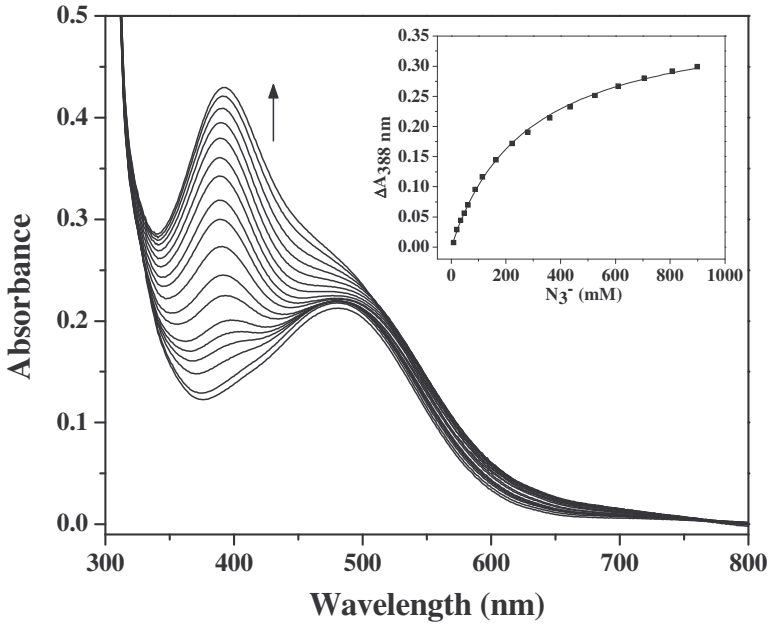

Figure 42: Azide coordination to Cu(II) in AGAO. Inset depicts the changes in absorbance of the LMCT band fit to a titration curve, yielding a K_d value for the Cu(II)-N_3^- complex.

Azide titrations for PPLO did not display the typical saturation behavior observed for the other CuAO enzymes (Figure 43). Once azide levels reach ~ 200 mM, ionic strength effects complicated analysis of the titration data. These effects are most likely a consequence of the greater degree of solvent accessibility in the active site environment of PPLO [44]. Subsequently, the reported K_d value of 153 ± 16 mM was estimated by fitting only the absorbance changes associated with azide additions up to 200 mM (Figure 43, inset).

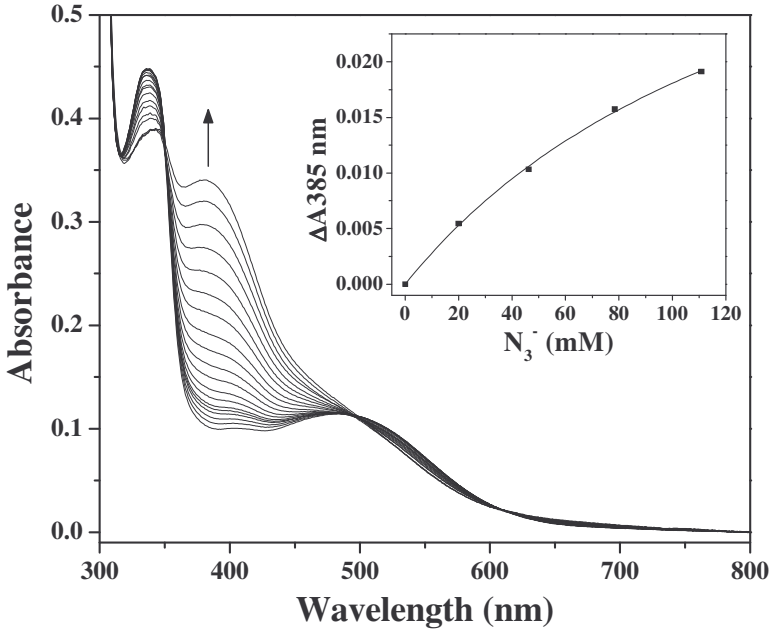

Figure 43: Azide coordination to Cu(II) in PPLO. Inset depicts the changes in absorbance of the LMCT band fit to a titration curve, yielding a K_d value for the Cu(II)-N_3^- complex.

Azide Titrations of Substrate-Reduced Amine Oxidases

In order to examine the affinity of azide for Cu(II) in the substrate-reduced forms of AGAO and PPLO, the enzymes were reduced with benzylamine under anaerobic conditions and the azide titrations were carried out as previously described for PSAO [107]. The experimentally determined K_d value for the substrate-reduced AGAO was 34 ± 5 mM (ε_{430} = ~ 2000 $M^{-1}cm^{-1}$) (Figure 44). Notably, there is a 6-fold increase in the affinity of azide for Cu(II) in the substrate-reduced form of the enzyme and the λ_{max} of the LMCT band for the Cu(II)-N_3^- complex is red-shifted 42 nm with respect to the oxidized, resting enzyme. The shift in the energy of the LMCT transition suggests that the redox state of the TPQ cofactor perturbs the electronic structure of the Cu(II) center in AGAO. For substrate-reduced PPLO, the approximate K_d for the Cu(II)-N_3^- complex

was determined to be 87 ± 21 mM with the λ_{max} of the LMCT band at 379 nm (Figure 45). Although the affinity of azide for substrate-reduced PPLO is greater than that for the oxidized enzyme, it is important to note that the anaerobic titration was subject to the same ionic strength effects as described above.

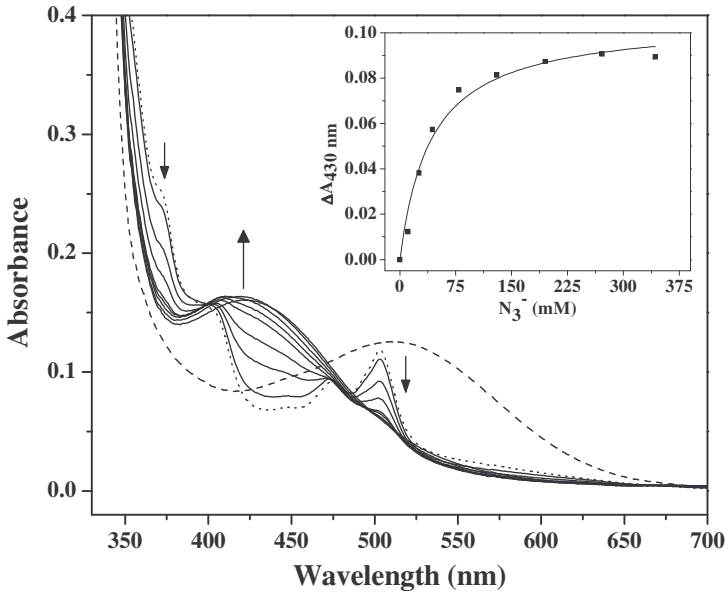

Figure 44: Azide coordination to Cu(II) in substrate-reduced AGAO. Dashed spectrum (---) represents the oxidized, resting protein sample. Dotted spectrum (· · ·) represents the substrate reduced protein prior to addition of azide. Arrows represent the spectral changes associated with the addition of azide. Inset depicts the second order fit used for the determination of K_d for the Cu(II)-N_3^- complex.

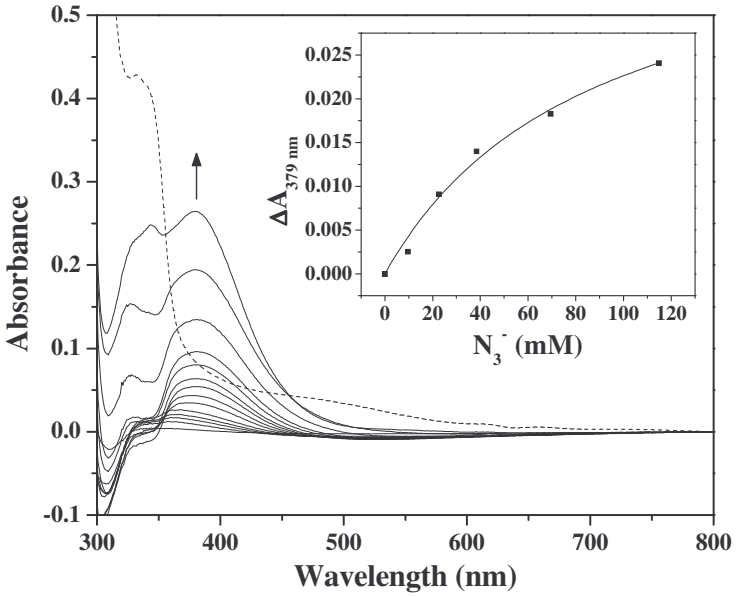

Figure 45: Difference spectra of azide coordination to Cu(II) in substrate-reduced PPLO. Dashed spectrum (---) represents the substrate reduced protein prior to addition of azide. Arrow represents the spectral change associated with the addition of azide. Inset depicts the second order fit used for the determination of K_d for the Cu(II)-N_3^- complex.

Azide Inhibition of the Reductive Half-reaction

The effects of azide on the reductive half-reaction (Eq. 1) were determined by analyzing the kinetic parameters of each enzyme for a given amine substrate in the presence of increasing amounts of azide, at saturating O_2 levels. The control kinetic parameters for substrates amine and O_2 for each enzyme examined are listed in Table 4. The mode of azide inhibition with respect to substrate amine varied depending on the enzyme source. For AGAO, azide was found to exhibit cleanly noncompetitive inhibition at lower azide concentrations (0-10 mM) with respect to substrate β-phenylethylamine, however, a mixed-type mode of inhibition cannot be ruled out at higher concentrations of azide (45 mM). For this reason, the 45 mM azide point has been excluded from the $K_{Mapp}/V_{max}(i)$ versus azide concentration plot for noncompetitive

inhibition (Figure 47). It should be noted that the relatively low K_M (1.4 μM) and high k_{cat} (44 sec^{-1}) for β-phenylethylamine contribute to the inherent difficulty of accurately determining initial rates of amine oxidation for this enzyme at low substrate concentrations, due to the rapid oxidation of β-phenylethylamine upon initiation of the assay. Substrate inhibition for AGAO with β-phenylethylamine was similar to that observed for rhDAO using histamine and putrescine [21] with one notable exception; *while increasing ionic strength abolishes substrate inhibition of rhDAO* [31]*, ionic strength has little to no effect on substrate inhibition of AGAO*. While no substrate inhibition was observed (up to 75 μM β-phenylethylamine) in the absence of azide, substrate inhibition appeared to increase at lower substrate concentrations in the presence of azide (Figure 46). This same effect was seen for the inhibition of PSAO by azide and cyanide with respect to substrate amine [107,150]. In order to exclude the complicating effects of substrate inhibition, kinetic fits were generated by utilizing only the points where substrate inhibition was not observed. Nonetheless, it can be said with confidence that the dominant mode of inhibition is noncompetitive with a calculated K_i value of 7.0 ± 1.5 mM (Figure 47).

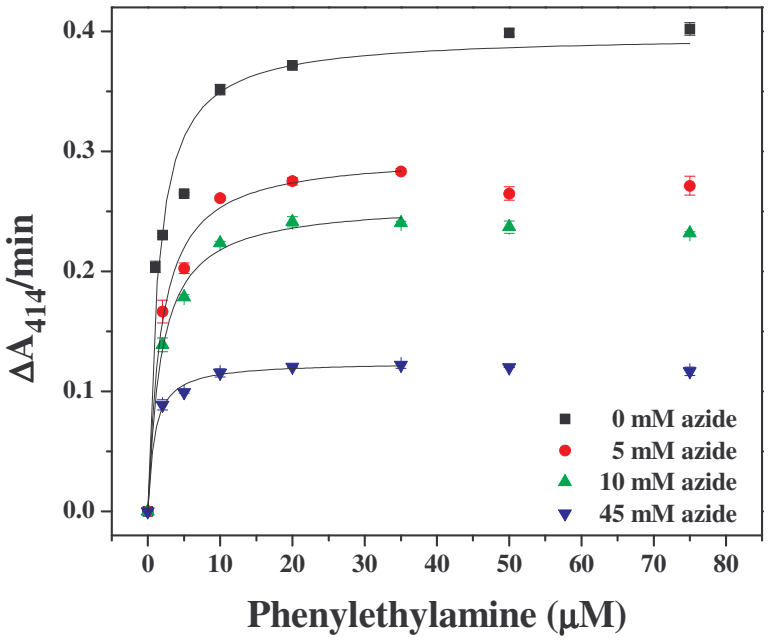

Figure 46: Azide inhibition of the reductive half reaction of AGAO. (a) Experimental data with Michaelis-Menten kinetic fits in the presence of 0 (■), 5 (●), 10 (▲), and 45 (▼) mM azide.

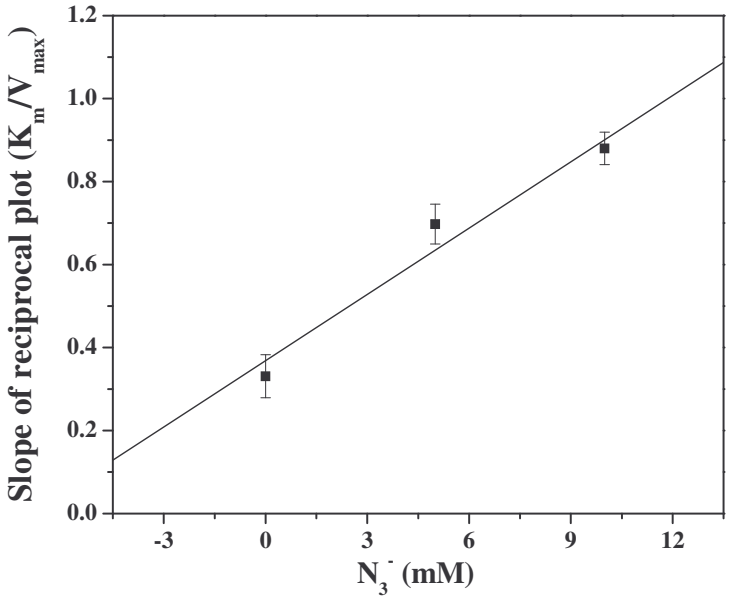

Figure 47: The $K_{Mapp}/V_{max}(i)$ versus azide concentration plot for treatment of noncompetitive inhibition of AGAO with respect to substrate amine.

Azide Inhibition of the Oxidative Half-reaction

The effects of azide on the oxidative half-reaction (Eq. 2) were determined by analyzing the kinetic parameters of each enzyme (Table 5) with saturating amine substrate (at least 10 × K_M) in the presence of increasing amounts of azide, while O_2 levels were varied from ~ 10 – 180 μM. The mode of azide inhibition with respect to substrate amine varied depending on the enzyme source. For the enzyme AGAO, the effects of azide on the oxidative half-reaction can be interpreted as a purely noncompetitive mode of inhibition (Figure 48). Due to the observation that substrate inhibition decreases the maximum rate of amine oxidation at levels of *β*-phenylethylamine substrate in excess of 75 μM, assays were performed at two fixed concentrations of amine substrate to exclude possible effects of substrate inhibition on the mode of azide inhibition. Rates of oxygen consumption collected in the presence of both 50 μM (~ 35 × K_M; data not shown) and 200 μM (~ 140 × K_M; Figure 48) *β*-phenylethylamine are both consistent with noncompetitive inhibition. The inhibition constants at 50 μM and 200 μM *β*-phenylethylamine substrate were determined to be 5 ± 2 mM and 20 ± 2 mM (Figure 49), respectively. Interestingly, these values are in close agreement with the inhibition constant determined for inhibition of the reductive half-reaction by azide (K_i = 7.0 ± 1.5 mM). The kinetic constants ($K_{Mapparent}$ and $V_{maxapparent}$) for all enzymes studied are reported in Table 5. This table includes data for rhDAO and PSAO for comparative purposes and to aid in interpretation of the discussion below.

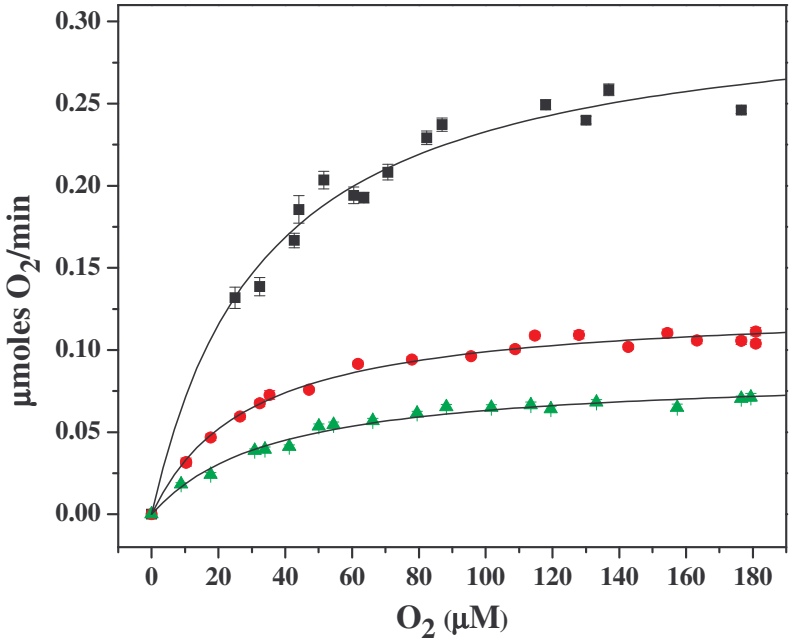

Figure 48: Azide inhibition of the oxidative half reaction of AGAO. Experimental data with Michaelis-Menten kinetic fits in the presence of 0 (■), 25 (●), and 50 (▲) mM azide.

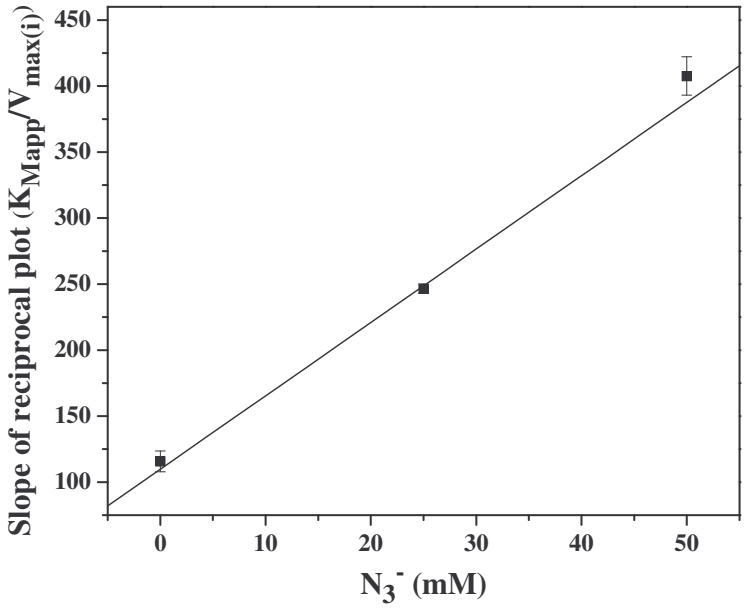

Figure 49: The $K_{Mapp}/V_{max}(i)$ versus azide concentration plot for treatment of noncompetitive inhibition of AGAO with respect to substrate dioxygen.

In the case of PPLO, azide exhibited noncompetitive inhibition at lower azide concentrations (5 and 15 mM), with the mode of inhibition shifting to mixed-type at higher azide concentrations (30 and 45 mM), as clearly seen in Figure 50. Kinetic constants for oxygen consumption at all azide concentrations are reported in Table 5. Treatment of the data at 5 and 15 mM azide levels for noncompetitive inhibition [109] yields a K_i value from the reciprocal plot of 38 ± 3 mM (Figure 51). Linear mixed-type inhibition may be considered a mixture of pure noncompetitive inhibition and partial competitive inhibition [109]. Accordingly, inhibition arises from the inhibitor binding to both free enzyme (K_i) and enzyme bound to substrate (αK_i), with the resulting ESI complex being inactive. Mathematical treatment of the 30 and 45 mM azide curves in a manner consistent with mixed-type inhibition reveals a K_i value of 23 ± 3 mM and an αK_i value of 108 ± 12 mM (data not shown). As in the case with AGAO, these values are in relatively good agreement with the calculated K_i from the reductive half-reaction (18 ± 0.3 mM) and the K_d (87 ± 21 mM) for the Cu(II)-N_3^- complex in substrate-reduced PPLO.

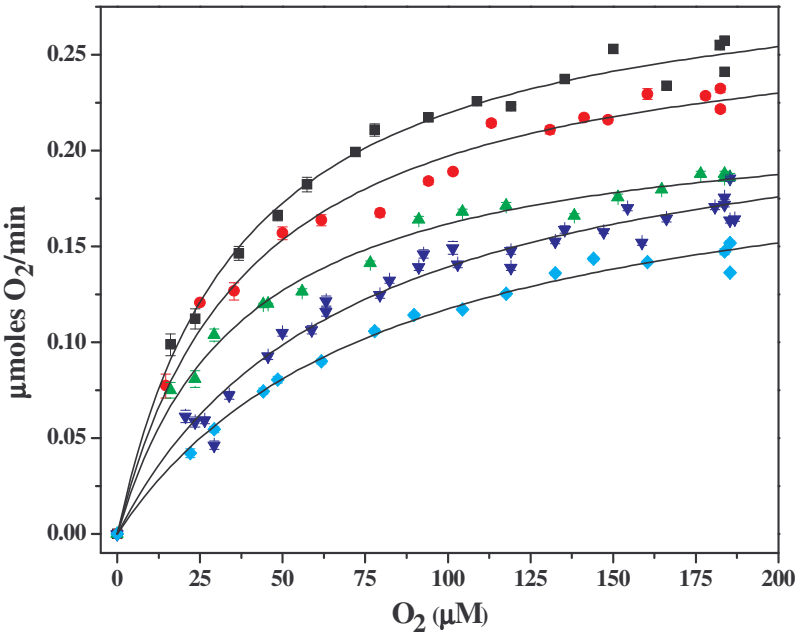

Figure 50: Azide inhibition of the oxidative half reaction of PPLO. Experimental data with Michaelis-Menten kinetic fits in the presence of 0 (■), 5 (●), 15 (▲), 30 (▼), and 45 (◆) mM azide.

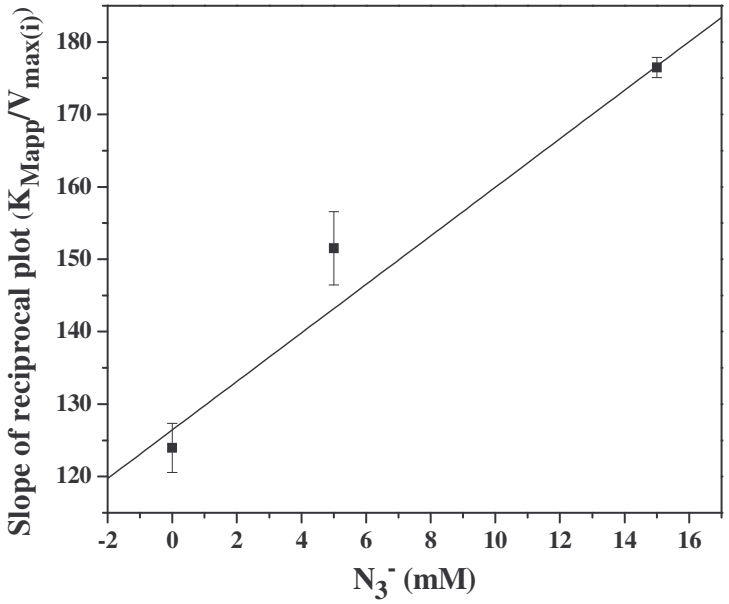

Figure 51: The $K_{Mapp}/V_{max}(i)$ versus azide concentration plot for treatment of noncompetitive inhibition of PPLO with respect to substrate dioxygen. Only 0, 5, and 15 mM azide points are plotted as the mode of inhibition shifts to mixed at 30 mM azide (see text).

Table 4: Properties of Copper Amine Oxidases

Enzyme	TPQ[a]	K_M (μM)		k_{cat} dimer (s^{-1})		K_d Cu(II)-N_3^- (mM)	
		Amine	O_2	Amine	O_2	Oxidized	Reduced
PSAO	1.8	420 ± 18[b]	49 ± 4	252 ± 3	308 ± 9	53 ± 5	59 ± 10[f]
rhDAO	1.4	20 ± 1[c]	6 ± 1	7.9 ± 0.2	2.9 ± 0.1	38 ± 3	ND
AGAO	1.4	1.4 ± 0.3[d]	38 ± 5	44 ± 2	53 ± 2	213 ± 18	34 ± 5
PPLO	1.6	38 ± 3[e]	37 ± 3	11.2 ± 0.3	12.6 ± 0.3	153 ± 16	87 ± 21

[a]Values are reported as TPQ content per protein dimer. [b]Amine substrate putrescine; 100 mM KPO_4, pH 7.2 at 30 °C with *I* = 540 mM (KCl). [c]Amine substrate putrescine; 50 mM HEPES, pH 7.2 at 37 °C with *I* = 250 mM (KCl). [d]Amine substrate β-phenylethylamine; 100 mM KPO_4, pH 7.2 at 30 °C with *I* = 440 mM (K_2SO_4). [e]Amine substrate benzylamine; 50 mM HEPES, pH 7.0 at 30 °C with *I* = 150 mM (KCl). [f]Value reported in ref [128].

Table 5: Kinetic Parameters for the Oxidative Half Reaction

Enzyme	Azide (mM)	$K_{M\ apparent}$ (μM)	$V_{max\ apparent}$ (μmoles O_2/min)
PSAO	0	49 ± 4	0.43 ± 0.01
	25	70 ± 5	0.39 ± 0.01
	55	104 ± 7	0.39 ± 0.01
	90	172 ± 23	0.42 ± 0.03
rhDAO	0	6 ± 1	— [a]
	50	23 ± 2	0.110 ± 0.003
	100	32 ± 4	0.100 ± 0.004
	200	38 ± 4	0.090 ± 0.004
AGAO	0	34 ± 2	0.310 ± 0.010
	25	29 ± 2	0.130 ± 0.002
	50	36 ± 4	0.090 ± 0.003
PPLO	0	37 ± 3	0.30 ± 0.01
	5	40 ± 3	0.28 ± 0.01
	15	38 ± 3	0.22 ± 0.01
	30	71 ± 6	0.24 ± 0.01 [b]
	45	82 ± 11	0.21 ± 0.01

[a] Oxygen kinetics for control curve were performed using a different stock of protein, thus the V_{max} value does not allow for direct comparison to the values obtained in the presence of inhibitor. The K_M reported herein is the average obtained from two independent control curves, both providing values within error of one another. The fact that K_M is independent of protein concentration allows for the inclusion of this value. [b] An inspection of the kinetic parameters for PPLO suggests a shift in kinetic inhibition patterns from noncompetitive to mixed-type at this azide concentration.

Discussion

The monodentate ligands azide and cyanide are known to displace the equatorial water ligand of copper and inhibit both half-reactions of copper amine oxidase catalysis (Eqs. 1 and 2) [107,128,151,152]. Therefore, investigations of the electronic and mechanistic effects of these ligand-substitution reactions can provide insight into the active site structures and the catalytic mechanisms of copper containing enzymes. Although these ligands have been used extensively in the study of CuAOs, significant variations in the methodology, as well as the quality, and reproducibility of the data, have led to ambiguities in interpretation. Furthermore, comparisons among CuAOs are necessary, as it has become increasingly clear that significant differences may exist in the interaction of CuAOs with these ligands [107,128,129]. The data presented herein are part of the first comparative study that analyzes the effects of azide on both half-reactions of multiple amine oxidases (AGAO, PPLO, PSAO and rhDAO), and includes bacterial, yeast, plant, and mammalian enzymes.

Azide as a Cu(II)-Directed Ligand

Variations in the binding affinity of azide to Cu(II) among resting, oxidized CuAOs have been previously described [60,84,127,128,146,147]. The data herein extend these findings as K_d values for Cu(II)-N_3^- complexes in the oxidized enzyme range from 38 – 213 mM (Table 4). In addition, it has been reported that the oxidation state of the quinone cofactor in some amine oxidases may affect the affinity of azide for Cu(II). A marked increase in affinity of N_3^- for Cu(II) has been reported for APAO when TPQ is in the reduced aminoquinol state, relative to the oxidized state, however, no difference in

affinity was noted between these two enzymatic states in PKAO, PPAO, or PSAO [84,85,128,147]. Results obtained for BPAO indicated a slightly higher binding affinity for azide in the resting form of the enzyme [127]. The present results indicate that N_3^- binds to Cu(II) with higher affinity in the substrate-reduced forms of AGAO and PPLO, compared to the oxidized (resting) states. Moreover, the LMCT λ_{max} red shifts by ~ 42 nm in substrate-reduced AGAO (relative to oxidized enzyme), which correlates with K_d decreasing from 213 ± 18 mM (oxidized enzyme; Figure 42) to 34 ± 5 mM (substrate-reduced enzyme; Figure 44). The binding affinity of azide in PPLO was observed to only slightly increase from a K_d of 153 ± 16 mM (oxidized enzyme; Figure 43) to 87 ± 21 mM (substrate-reduced enzyme; Figure 45). It should be noted that the binding affinity of azide has been measured only for the two forms of these enzymes that are easily trapped (Cu(II)–TPQ_{ox} and Cu(II)–TPQ_{amr}), while in actuality this small anion may bind with varying affinity to any of the remaining Cu(II) states during enzymatic catalysis (Figure 6). These differences in the binding affinities and energies of the LMCT transitions for azide coordination to different enzymatic forms reinforce the concept that changes in the chemical state of the quinone cofactor or in the active site environment can influence copper site reactivity and electronic structure, for which there is substantial precedence in the literature [107,127,128,134].

Steady State Kinetic Interpretation of Azide Inhibition of CuAOs

In order to gain insight into the effects of azide on the mechanism of CuAOs, kinetic parameters were determined for both the reductive and oxidative half-reactions in the presence and absence of azide. Specifically, we wished to survey the effects of azide

on the turnover kinetics of multiple amine oxidases in order to test the previously articulated hypothesis that azide competes with O_2 for a copper binding site during enzymatic reoxidation. Owing to an intrinsic property of the amine oxidase Ping-Pong Bi Bi mechanism, the two half-reactions (i.e. substrate amine oxidation and substrate O_2 reduction) may be kinetically independent [81,153-155]. In an attempt to cleanly dissect the effects of azide during each half-reaction, kinetic experiments were performed with variable concentrations of one substrate (either amine or O_2), while the other substrate was kept at saturating (steady-state) concentrations. By definition, steady-state conditions are maintained when the effective concentration of the ES complex remains relatively unaltered during turnover in the presence of saturating substrate [156]. For a Ping-Pong Bi Bi mechanism (Eqs. 1 and 2), this directly translates to the steady-state concentration of either E_{red} or E_{ox} depending on which substrate is saturating. Henceforth, the opposite half-reaction that is kept under conditions of saturating substrate during a kinetic experiment may be referred to as the "steady-state half-reaction". Due to the kinetic independence of each half-reaction, the effects of azide on either amine oxidation or O_2 reduction can be differentiated as long as the opposite half-reaction is kept under steady-state conditions and the reaction velocity (V_{max}) for this opposite half-reaction remains largely unperturbed in the presence of the inhibitor. In the present case, this implies that the inhibitor cannot affect the rate of steady-state formation of either E_{red} or E_{ox} without affecting the kinetics of the opposite half-reaction. It should be noted that V_{max} of the steady-state half-reaction can only remain unaltered if the rate constants leading up to and including the rate limiting step are not perturbed by the inhibitor [157].

Using the notation of Cleland, there are two enzyme-substrate complexes, EA and FB, for a Ping-Pong Bi Bi mechanism [156]. A reduction in reaction velocity of the steady-state half-reaction will occur if an inhibitor serves to decrease the effective concentration of the enzyme-substrate complex (EA or FB), via formation of a catalytically inactive ESI complex (uncompetitive or noncompetitive inhibition) or through formation of a catalytically inactive EI complex (competitive inhibition). However, the reaction velocity for the steady-state half-reaction in the presence of inhibitor may be close to the same as the rate in the absence of inhibitor (i.e. $V_{max(i)} \approx V_{max}$) if either ESI is not formed in appreciable amounts, or the concentration of the steady-state enzyme-substrate complex (ES) can be largely maintained as the concentration of inhibitor is increased (competitive inhibition) [157,158].

Azide Inhibition of the Reductive Half-reaction

The inhibition of PPAO by azide with respect to substrate amine has previously been described as uncompetitive [146,147] while inhibition patterns for BPAO have been reported as mixed at low amine concentrations with a shift to uncompetitive at higher substrate concentrations [127]. In this study, azide was discovered to exhibit a range of inhibition patterns (competitive, uncompetitive, or noncompetitive) during the reductive half-reaction (Eq. 1), depending on enzyme source. The inhibition of AGAO and PPLO by azide with respect to substrate β-phenylethylamine and benzylamine, respectively, was observed to be noncompetitive in nature. These results indicate that the inhibition arises from azide binding to multiple forms of the enzyme, independent of the binding of substrate. Our current results suggest that the affinity of azide for Cu(II) is higher in the

substrate-reduced (TPQ_{amr}) forms of AGAO and PPLO than the oxidized enzymes, however, nothing is known about the stability of the Cu(II)-N_3^- complex during any of the other stages of catalysis. For AGAO, the determined inhibition constant of 7.0 ± 1.5 mM is lower than the calculated K_d for both oxidized (213 ± 18 mM) and substrate-reduced forms (34 ± 5 mM) of AGAO. A similar trend is observed in PPLO for which the K_i of 18.0 ± 0.3 mM is lower than the experimentally determined K_d values for the Cu(II)-N_3^- complex in both the oxidized (153 ± 16 mM) and substrate-reduced forms (87 ± 21 mM) of the enzyme. Comparisons of the dissociation constants (K_d) determined for both resting (oxidized) and substrate-reduced forms of CuAOs indicate that the chemical state of TPQ influences copper site reactivity, and more importantly shows that azide can bind to multiple forms of the enzyme with varying affinities. Due to these active site specific variations, it is reasonable to assume that the affinity of azide for Cu(II) may be higher in one of the three catalytic states for which this complex is not easily characterized (TPQ_{SSB}, TPQ_{PSB}, or TPQ_{imq}). The data suggest that inhibition arises from azide binding to Cu(II) at discrete steps during the catalytic cycle. Given the noncompetitive nature of azide binding in AGAO and PPLO, it is essential to note that once azide levels approach or exceed the calculated K_i values (vs. substrate amine) *a substantial decrease in reaction velocity ($V_{max(i)}$) will result during the reductive half-reaction* of these enzymes. The significance of this becomes apparent when discussing the oxidative half-reaction (see below).

The result that azide acts as a competitive inhibitor in rhDAO [31,150] with respect to substrate putrescine was surprising and can rationalized in one of two ways: 1) azide binds directly to the substrate binding site, thus competing directly with substrate

amine for binding to the free enzyme; or 2) azide binding to copper in the free enzyme perturbs the active site of the free enzyme in such a way as to produce a complex that is catalytically inactive. In light of the clear evidence for azide binding to copper and the complete lack of evidence for azide reacting with TPQ, the latter possibility was considered more likely. One possibility is that azide binding to Cu(II) at the equatorial position disrupts the active-site hydrogen bonding network and thereby alters the orientation of the reactive TPQ C5 carbonyl, rendering it inaccessible to substrate amines. Hydrogen bonding has been shown to play an essential role in positioning the TPQ cofactor during both biogenesis and amine oxidation [66,68,159-161]. This hypothesis was further supported by the nearly identical values determined for the K_d (38 ± 3 mM) of the Cu(II)-N_3^- complex and the calculated K_i (37 ± 3 mM) for azide inhibition with respect to substrate putrescine [150].

In the case of PSAO, azide displayed uncompetitive inhibition towards substrate amine with a calculated K_i value of 740 ± 200 mM [150]. This indicates that azide binds to PSAO only after putrescine has bound, meaning that azide binds to the enzyme-substrate complex (ES or E_{red}). Therefore, the uncompetitive nature of azide's inhibition of amine oxidation with the relatively high K_i value of 740 ± 200 mM may represent N_3^- complexing Cu(II) at either the TPQ_{PSB}, TPQ_{amr}, or TPQ_{imq} stage of catalysis (Scheme 1). Inhibition by azide at the TPQ_{PSB} stage of catalysis would be expected to arise from an effect on hydrolysis of the Schiff base adduct, thereby generating product aldehyde. Along these lines, it has been reported that the steady-state species in the closely related amine oxidase from lentil seedlings (LSAO) was identified as TPQ_{PSB} with the subsequent formation of TPQ_{amr} and release of aldehyde product being the rate limiting

step [162]. Uncompetitive inhibition would also be expected if azide binding to Cu(II) at the TPQ_{amr} stage of catalysis prevented the first electron transfer to O_2. In addition, this mode of inhibition could also arise from Cu(II)-N_3^- complexation at the TPQ_{imq} stage of catalysis, thereby preventing either hydrolysis of TPQ_{imq} to TPQ_{ox} or the direct reaction of substrate with the iminoquinone. In any case, significant inhibition of the reductive half-reaction does not occur at the concentrations of azide used during the oxidative half-reaction experiments (see below).

Azide Inhibition of the Oxidative Half-reaction

Considerable disagreement exists with regard to the observations and the interpretation of the effects of exogenous Cu(II) ligands on the oxidative half-reaction (Eq. 2). Two independent studies with PPAO concluded that azide was a *competitive inhibitor with respect to substrate dioxygen*, with calculated inhibition constants being consistent with measured K_d values for the Cu(II)-N_3^- complex [84,85]. These results implicated the copper site as having a direct role in O_2 binding. A subsequent study with HPAO found the inhibition by azide to be noncompetitive with respect to substrate dioxygen during the oxidative half-reaction [60]. The results of this latter study are viewed as consistent with the proposal that oxygen binds to an off-metal site in close proximity to TPQ prior to its reduction, with the rate determining step being initial electron transfer from TPQ_{amr} to O_2 [51,60,72,80-82]. In HPAO, this hypothetical dioxygen binding site is situated ~ 3 Å from TPQ and ~ 4.7 Å from Cu and is lined by the residues Y407, L425, and M639 [87]. Recently, we have experimentally identified a hydrophobic pocket in AGAO, PPLO, and PSAO by utilizing xenon as a probe for

potential dioxygen-binding sites [87]. The crystal structures of these enzymes revealed one common xenon binding pocket in close proximity to the active site (~ 7 Å from Cu; ~ 9 Å from TPQ). Xenon was subsequently shown to bind in this exact site in BPAO [45]. It is important to note that the potential dioxygen binding site in these Xe-CuAO structures is distinct from the proposed site in HPAO. Xenon was not observed to bind in the site previously proposed by Klinman *et al.* in any of the CuAO – Xe structures. While the experimental identification of a consensus Xe binding site does not rule out dioxygen binding in the site proposed by Klinman et al. [81], it is clear that the most direct trajectory for O_2 from the experimentally observed Xe binding site towards the active site would involve initial close approach to the copper center (Figure 52).

The results obtained with PSAO and rhDAO clearly show that azide exhibits competitive inhibition against substrate O_2 with K_i values of 45 ± 7 mM and, 35 ± 5 mM respectively [150]. These values are in excellent agreement with the measured K_d values for the Cu(II)-N_3^- complexes of 53 ± 5 mM (PSAO) and 38 ± 3 mM (rhDAO) (Table 4). As mentioned previously, a critical component of analyzing the oxidative half-reaction concerns the ability to maintain a largely unaltered reaction velocity ($V_{max(i)} \approx V_{max}$) during the reductive half-reaction, while the concentration of azide is progressively increased. This was not an issue with PSAO since the K_i value obtained for the uncompetitive inhibition of substrate amine oxidation by azide is ~15 times greater than the affinity of azide for Cu(II) in either the oxidized, resting state or the substrate-reduced TPQ_{amr} state [128,150]. It has been proposed that the kinetic expectation for a Ping-Pong Bi Bi enzymatic reaction is that an inhibitor which is competitive with respect to substrate B will display uncompetitive behavior with respect to substrate A [154].

Interestingly, this is what is observed in PSAO, most likely due to the fact that azide has a minimal effect on the rate of the reductive half-reaction while amine is saturating ($10 \times K_M$) and O_2 is varied.

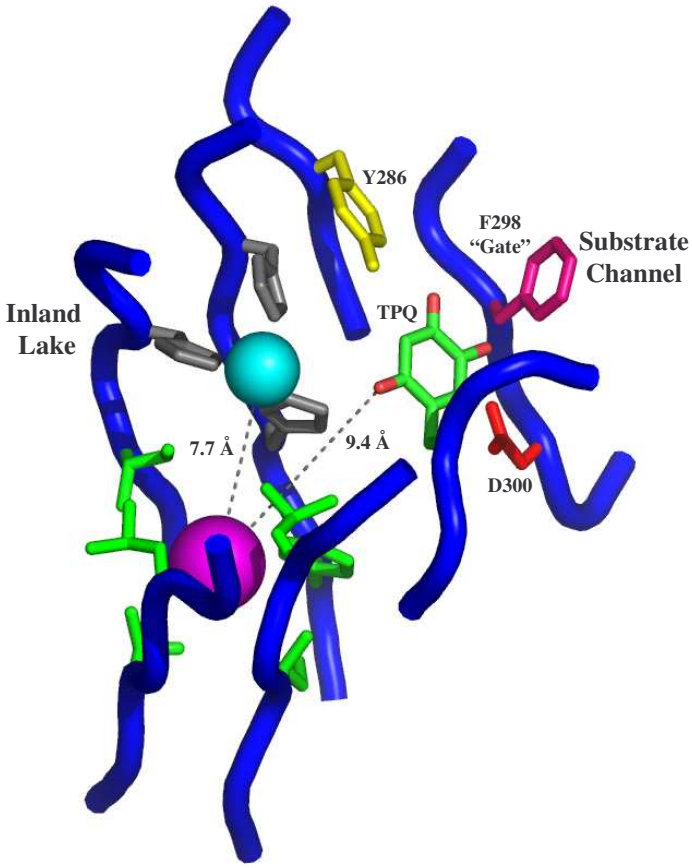

Figure 52: Xenon binding pocket in PSAO (PDB coordinates 1W2Z). Both Xe (purple) and Cu(II) (cyan) are represented as van der Waals spheres. Residues of interest are labeled. The productive orientation of TPQ is shown colored by atom (oxygen, red; carbon, green). The copper ligands (H442, H444, H603; gray) and the residues forming the xenon binding pocket (I405, L407, Y446, I601, L616, T618; green) are not labeled for clarity. The approximate locations of the substrate channel and the inland lake are given (see ref *18*). Xenon to Cu(II) and xenon to TPQ(O2) distances are also shown (see ref *81*). This figure was generated by E. M. Shepard using PyMOL [164].

Perturbations in steady-state conditions, where the concentration of the enzyme-substrate complex (E_{red}) can be expected to change over time, complicate the interpretation of kinetic results from turnover experiments. This was experimentally observed for the oxygen kinetics of PSAO obtained at 1 mM putrescine ($2 \times K_M$) where the mode of inhibition exerted by azide with respect to substrate O_2 was found to shift from *competitive* (at steady-state) to *noncompetitive* (non steady-state) [150]. The noncompetitive mode of inhibition observed under non steady-state conditions is an erroneous result, most likely originating from the more pronounced effects of azide on the reductive half-reaction when not at steady-state conditions.

In the case of rhDAO, both K_i values for the reductive and oxidative half-reactions are within error of the calculated Cu(II)-N_3^- K_d value, and competitive inhibition results in both cases [150]. While the observation that azide is a competitive inhibitor with respect to substrate amine is unprecedented for this class of enzyme, the fact that V_{max} remains relatively unaltered in the presence of a competitive inhibitor when substrate is saturating suggests that it is still possible to drive the reaction velocity ($V_{max(i)}$) to a level comparable with the control V_{max} in the reductive half-reaction. By increasing substrate amine concentrations to a level where any inhibition by azide with respect to amine is negligible ($100 \times K_M$ at 0 azide; $14 \times K_{Mapp}$ at 200 mM azide) it was possible to ensure maximum reaction velocity in this half-reaction, thereby allowing the true effects of azide on the oxidative half-reaction to be observed. Collectively, the results for PSAO and rhDAO demonstrating the competitive nature of inhibitor azide with respect to substrate dioxygen and the close agreement of the K_i and K_d values is

strong evidence in support of the hypothesis that O_2 reacts with or binds to copper during enzymatic reoxidation.

Azide was observed to exhibit noncompetitive and mixed-type (pure noncompetitive and mixed partial competitive) inhibition with respect to O_2 in AGAO and PPLO, respectively (Figures 48 and 50). Thus, the interpretation of these results is more complicated than for PSAO and rhDAO, where the competitive nature of inhibition allows for a more straightforward interpretation. The differences in the inhibition patterns displayed by AGAO and PPLO, compared to PSAO and rhDAO, may be rationalized by considering the effects of azide on the velocity of the reductive half-reaction while O_2 concentration is varied. While, at least to a good approximation, maximum reaction velocity could be maintained for the first half-reaction (Eq. 1) in the cases of PSAO and rhDAO, such kinetic conditions could not be sustained for either AGAO or PPLO in the presence of azide. Given the calculated K_i values for azide inhibition with respect to substrate amine, which are significantly lower than the K_d values for Cu(II)-N_3^- complexes in the substrate-reduced enzymes, substantial inhibition in the reductive half-reaction occurs at the concentrations of azide used during the oxidative half-reaction experiments. Moreover, since the mode of inhibition with respect to substrate amine in both of these enzymes is noncompetitive, the inhibition will be manifested as a decrease in V_{max} through formation of a catalytically inactive ESI complex. Thus, the resulting noncompetitive (AGAO) or mixed-type inhibition (PPLO) patterns in the oxidative half-reaction are likely a consequence of the effects of azide on the velocity ($V_{max(i)}$) during the reductive half-reaction. Despite the kinetic independence of each half-reaction in principle, the specific rate reduction in the rate of formation of

E_{red} may influence the kinetics of the oxidative half-reaction. Consequently, we suggest that inhibition by azide with respect to dioxygen is intrinsically competitive in AGAO and PPLO, but that this effect cannot be deconvoluted experimentally from the effects of azide on the reductive half-reaction. This might be the case for HPAO as well [60].

Although it is not possible to unambiguously determine the effects of azide on the oxidative half-reaction in AGAO and PPLO, it is worthwhile to address the mechanistic implications of the competitive nature of this inhibition in PSAO and rhDAO, with regard to the different mechanistic proposals discussed in the introduction. We believe the results with PSAO and rhDAO are most consistent with mechanistic proposals placing Cu(I) on-pathway in these enzymes, with the Cu(I)-TPQ_{sq} moiety principally involved in O_2 activation (Figure 7, A $\rightarrow$ D). Despite the fact that azide binds Cu(II) and O_2 reacts with Cu(I), ligation of Cu(II) by azide should appear competitive towards O_2 for the following reasons: 1) Cu(II)-TPQ_{amr} is in direct equilibrium with Cu(I)-TPQ_{sq} with an intramolecular electron transfer rate in PSAO of ~ 20,000 s^{-1} [77,79]; and 2) tetragonal Cu(II) complexes are known to display facile ligand substitution and therefore the reversible coordination by N_3^- should be rapid [127,152]. In addition, azide is known to stabilize Cu(II) in substrate-reduced CuAOs [128]. Further evidence of this was observed during the azide titration of substrate-reduced AGAO in this study, with rapid disappearance of the Cu(I)-TPQ_{sq} bands observed to occur upon addition of azide (Figure 44; Table 4). It can be expected that during the oxidative half-reaction the binding of azide to Cu(II)-TPQ_{amr} shifts the Cu(II)-TPQ_{amr} $\leftrightharpoons$ Cu(I)-TPQ_{sq} equilibrium in favor of

the former species, thereby preventing electron transfer to Cu(II) from TPQ_{amr}, in a manner consistent with competitive inhibition.

Kishishita *et al*. [89] consider their results in terms of mechanisms in which copper reduction is not required (O_2 is reduced via the TPQ_{amr} with Cu(II) simply acting as a site for superoxide binding) and in which the Cu(I)-TPQ_{sq} moiety is a catalytic intermediate. Indeed, they indicate that the rate enhancement in wild-type AGAO (relative to metal-substituted forms) is consistent with kinetically significant reduction of Cu(II). In the former mechanism, for which copper reduction is not required, azide would exert competitive inhibition towards O_2 only if it affected the rate constant for superoxide binding to Cu(II) in a manner that would be experimentally detected as a rise in the apparent K_M for O_2, assuming that no other step becomes rate limiting in the presence of azide. While possible, this does not seem not likely given the fact that both azide and superoxide are anions, and Cu(II) is known to undergo facile ligand substitution.

If CuAOs operated through the scheme proposed by Klinman and coworkers (Figure 7, A2 $\rightarrow$ D) [72], we can conceive of two possibilities for azide to exhibit what could be experimentally detected as competitive inhibition towards substrate dioxygen: (1) azide coordination to copper directly perturbs the affinity of dioxygen for the off-metal, hydrophobic dioxygen binding pocket as described in HPAO (shown in species A2, Figure 7) [81]; or (2) the binding of azide to copper prevents direct electron transfer from TPQ_{amr} to O_2. In regards to the former possibility, it has been argued that, comparing the kinetics of the Cu(II)–OH^- and Co(II)–H_2O forms of HPAO, the increased net charge at the metal center has a direct effect on the affinity of dioxygen for this

hydrophobic binding site, which was manifested as an increase in $K_M(O_2)$ in Co(II) substituted HPAO [83]. Therefore, the first possibility above appears unlikely since the presence of azide at the copper center would result in the same net charge as copper-bound hydroxide. For the second possibility to occur, it seems azide coordination to copper would have to disrupt the position of the reduced cofactor in a manner that would prevent electron transfer from TPQ_{amr} to O_2. It is not clear why this would be the case. Furthermore, the results reported for rhDAO and PSAO are difficult to reconcile with the proposed role of the paramagnetic copper center advocated by Prabhakar and Siegbahn [145]. Since the coordination of azide to Cu(II) has been shown not to significantly perturb the spin-orbit coupling of the copper center [84,127], it seems unlikely that the paramagnetic metal center in the Cu(II)–N_3^- complex would be unable to facilitate the spin conversion ($T \rightarrow S$) of the cofactor, as postulated by Prabhakar and Siegbahn, for electron transfer to dioxygen. Finally, while it could be argued that azide binding to Cu(II) effects either the pK_a of the axial water (implicated in the hypothetical formation of a catalytically active metal bound hydroxide) or the ability of superoxide to effectively migrate from the hydrophobic pocket towards the metal center, neither effect should be expected to generate the competitive mode of inhibition observed in the enzymes PSAO and rhDAO.

Conclusions

Despite the fact azide ligand-substitution reactions have been extensively studied in multiple CuAOs over the last 30 years, no detailed kinetic comparison among CuAO enzymes has previously been performed. In all probability, inhibition of CuAOs by azide

arises from azide coordinating Cu(II) at discrete steps during enzymatic turnover. Complicating the inhibition patterns is the fact that for several CuAOs, azide has varying affinity for Cu(II), depending on the redox state of the quinone cofactor. We have found that a comparative study of azide's effects on the *reductive and oxidative* half-reactions is necessary to clearly interpret the inhibition results for each half-reaction. Not surprisingly, our results illustrate the critical importance of maintaining steady-state conditions and keeping the maximum reaction velocity near constant levels in one half-reaction of an enzyme operating through a Ping-Pong Bi Bi mechanism, while performing kinetic inhibition studies on the opposite half-reaction. This can be easily performed for enzyme systems in which the inhibitor of interest has an effect with respect to only one substrate, however, when a single inhibitor induces substantial inhibition in both half-reactions, maintaining a consistent reaction velocity (V_{max}) may not be possible. This is illustrated in the case of AGAO and PPLO for which azide is a potent noncompetitive inhibitor (low K_i values) with respect to substrate amine so the presence of this inhibitor decreases the maximum reaction velocity for this half-reaction. This result may complicate deconvolution of the effects of azide on the reoxidation reaction. It is clear that it is critical to maintain consistent $V_{max(i)}$ for the reductive half-reaction as inhibitor concentration is increased in order to accurately discern effects of azide on O_2 reduction.

The fact that azide exhibits competitive inhibition with respect to substrate dioxygen in PSAO and rhDAO, with inhibition constants equivalent to the K_d values for Cu(II)-N_3^-, is strong evidence in support of O_2 reacting directly with Cu(I) during the oxidative half-reaction. Competitive inhibition cannot readily be reconciled in terms of

oxygen prebinding to the off-metal proteinaceous site proposed by Klinman and coworkers (Figure 7, A2), with the subsequent rate limiting step being electron transfer from TPQ_{amr} to O_2. However, if the recently identified xenon binding pocket in AGAO, BPAO, PPLO, and PSAO truly represents a transient dioxygen binding site in these enzymes, then our results can be rationalized by the fact that migration of O_2 towards the active site would result in an initial close approach to copper, from which electron transfer should readily occur (Figure 7, A $\rightarrow$ B; Figure 52). This hypothesis is in reasonable accord with the results reported for PSAO and rhDAO [150]. In addition, our recent report with the enzyme PSAO provided additional support for the catalytic viability of the Cu(I)-TPQ_{sq} intermediate by illustrating the close agreement between the K_d for Cu(I)-CN^- and the K_i for inhibition of this anion with respect to substrate amine [107].

Collectively, the results concerning the competitive interaction of azide with respect to dioxygen in three CuAOs (rhDAO, PSAO, and PPAO) provide strong support for a direct interaction of dioxygen with the metal center during enzymatic reoxidation in these enzymes. Although we suspect this to be the case in AGAO and PPLO as well, the inability to maintain a consistent reaction velocity during the reductive half-reaction in the presence of azide obscures the behavior of this inhibitor in the oxidative half-reaction. With this in mind, a thorough characterization of the effects of azide on the reductive half-reaction of HPAO may be warranted; however, given the large body of evidence in support of a non-redox role of copper in this enzyme, mechanistic differences may exist between CuAOs. Although it is tempting to put forth a unifying mechanistic proposal for all CuAOs based on the similarities among the active sites, mounting evidence suggests

that copper amine oxidases from different sources may in fact utilize discrete mechanisms to reoxidize the reduced quinone species.

CONCLUDING REMARKS

Increased interest in copper amine oxidase mechanism and inhibition has developed in recent years with the revelation that human vascular adhesion protein (HVAP-1) is of the same enzyme class (E.C. 1.4.3.6). With the potential for therapeutic applications, substantial efforts have been made to determine the molecular factors which govern inhibitor sensitivity and selectivity for copper amine oxidases. Since the human CuAOs have proven much more difficult to isolate, the majority of our understanding of CuAO structure, mechanism, and inhibition has come through the characterization of bacterial and yeast CuAOs. The similarity in active site structure of the seven crystallographically characterized CuAOs lends credibility to using this approach for mechanistic studies. Despite these similarities, considerable disagreement still exists concerning the precise role of copper during oxygen activation and enzymatic reoxidation. To address these mechanistic uncertainties and expore the potential for a recently introduced series of inhibitors, the phenylethylamine oxidase from *Arthrobacter globiformis* was chosen as a model CuAO for this work owing to its ease in purification and the availability of a high resolution X-ray structure.

In an attempt to explore the molecular recognition of inhibitors and define the factors that control inhibitor potency and selectivity, a series of Ruthenium based, fluorescent compounds containing a tertiary amine that binds in the active site channel of AGAO were screened for their ability to inhibit amine oxidation in AGAO. These compounds, which are some of the most potent CuAO inhibitors studied to date, bind reversibly with inhibition constants in the mid to low nanomolar range and are considered

excellent leads for the development of highly potent CuAO inhibitors. It is believed that the potency of these compounds is governed by the extent of favorable van der Waals and hydrophobic interactions between the inhibitor and the residues lining the active site channel of AGAO. Characterization of the interaction of these compounds with other CuAOs, however, is warranted in order to test the generality of these findings.

Inhibition studies were expanded from substrate analogues to the use of the small molecule copper ligands cyanide and azide. These copper ligands were characterized with regards to their effects on catalysis in order to probe the role of copper during enzymatic reoxidation. This work demonstrates the first evidence of cyanohydrin derivitization of the TPQ cofactor in AGAO and presents a general mechanism of CuAO inhibition by cyanide. It is believed that the primary mode of inhibition by cyanide is the stabilization of the Cu(I)-TPQ_{sq} species thereby preventing electron transfer to dioxygen. Although not definitive, these results lend support to the hypothesis that oxygen activation in CuAOs is facilitated by reaction with Cu(I) during enzymatic reoxidation. The results of inhibition by azide are considerably more complex and their interpretation must consider the inhibition with respect to both substrate amine and dioxygen. Unlike the enzymes rhDAO and PSAO, in which the minimal effect of azide on the velocity of the reductive half-reaction allows for a straightforward analysis of the inhibition observed during enzymatic reoxidation, azide was shown to have a pronounced effect on the velocity of the reductive half reaction in AGAO and PPLO. This effect abolishes the kinetic independence of each half-reaction in AGAO and PPLO and precludes an accurate examination of azide's inhibition with respect to substrate dioxygen in these latter two enzymes. Thus the observed noncompetitive inhibition by azide in these

enzymes is possibly an erroneous result. Although it is likely that copper plays a redox role during catalysis in all copper amine oxidases, definitive proof of whether initial electron transfer to dioxygen originates from reduced quinone or from Cu(I) in AGAO and PPLO remains elusive. Currently, efforts are underway to establish whether the Cu(I)-TPQ_{sq} moiety is a catalytically viable intermediate during enzymatic reoxidation in AGAO by means of temperature jump relaxation measurements. Using this procedure, the electron transfer rate between the organic cofactor and the copper center (k_{ET}) can be determined. The possibility of a direct reaction of dioxygen with Cu(I) can be explored by determining whether this electron transfer is kinetically competent with respect to the overall rate limiting step during catalysis.

APPENDIX A

During the purification of AGAO that has been expressed in *E. coli* cells, care must be taken to separate the AGAO from a catalase expressed by the host *E. coli* cells. The presence of catalase can be readily identified by an intense absorption feature at 410 nm. To minimize the amount of catalase contamination, two (*katG* and *katE*) of the three catalase genes found within the chromosome of the host *E. coli* BL21 (DE3) strain were disrupted by the P1 phage-mediated transduction and homologous recombination. This catalase deficient strain of *E. coli* was generously provided to us by Professor Katsu Tanizawa (Osaka University, Japan). A complete summary of the engineering of this cell strain can be found in [89]. In summary, the *katE* gene was first disrupted using the phage lysate obtained from a catalase-deficient *E. coli* mutant UM120 (*thi-1 HfrH katE12::Tn10*) and the *katG* gene was then disrupted from the chromosome of the *katE*-deleted *E. coli* BL21 (DE3) using the phage lysate obtained from another catalase-deficient *E. coli* mutant SN0027 (*supE44 hsdR endA1 pro thi katG::Tn5*). The resulting *katGE* disrupted *E. coli* BL21 (DE3) cells (designated CD03) produced AGAO as efficiently as the original strain upon transformation with the expression plasmid pAGAO2 (described in Chapter 2).

REFERENCES CITED

1. Binda, C, Mattevi, A, Edmondson, DE (2002) Journal of Biological Chemistry 277:23973-23976.

2. Knowles, PF ,Dooley, DM (1994) Amine Oxidases, In: *Metal Ions in Biological Systems*. Singel, H and Singel, A (eds) Marcel Dekker, Inc., New York, pp. 361-403.

3. McIntire, WS ,Hartmann, C (1993) Copper-Containing Amine Oxidases, In: *Principles and Applications of Quinoproteins.* Davidson, VL (eds) Marcel Dekker, Inc., New York, pp. 97-171.

4. Janes, SM, Klinman, JP (1995) Methods Enzymol. 258:20-34.

5. Tanizawa, K (1995) J.Biochem.(Tokyo) 118:671-678.

6. Morris, NJ, Ducret, A, Aebersold, R, Ross, SA, Keller, SR, Lienhard, GE (1997) J.Biol Chem 272:9388-9392.

7. Bono, P, Salmi, M, Smith, DJ, Jalkanen, S (1998) J. Immunol. 160:5563-5571.

8. Salminen, TA, Smith, DJ, Jalkanen, S, Johnson, MS (1998) Protein Eng. 11:1195-1204.

9. Okeley, NM, van der Donk, WA (2000) Chemistry and Biology 7:159-171.

10. Ostermeier, C, Harrenga, A, Ermler, U, Michel, H (1997) Proc. Natl. Acad. Sci., U.S.A 94:10547-10553.

11. Das, TK, Pecoraro, C, Tomson, FL, Gennis, RB, Rousseau, DL (1998) Biochemistry 37:14471-14476.

12. Janes, SM, Mu, D, Wemmer, D, Smith, AJ, Kaur, S, Maltby, D, Burlingame, AL, Klinman, JP (1990) Science 248:981-987.

13. Cai, D, Klinman, JP (1994) J. Biol. Chem. 269:32039-32042.

14. Matsuzaki, R, Fukui, T, Sato, H, Ozaki, Y, Tanizawa, K (1994) FEBS Lett. 351:360-364.

15. Ruggiero, CE, Smith, JA, Tanizawa, K, Dooley, DM (1997) Biochemistry 36:1953-1959.

16. Bollinger, JA, Brown, DE, Dooley, DM (2005) Biochemistry (Submitted).

17. Pearson, AR, Jones, LH, Higgins, LA, Ashcroft, AE, Wilmot, CM, Davidson, VL (2003) Biochemistry 42:3224-3230.

18. Satoh, A, Kim, JK, Miyahara, I, Devreese, B, Vandenberghe, I, Hacisalihoglu, A, Okajima, T, Kuroda, S, Adachi, O, Duine, JA, Van Beeumen, J, Tanizawa, K, Hirotsu, K (2002) J. Biol. Chem. 277:2830-2834.

19. Wilce, MCJ, Dooley, DM, Freeman, HC, Guss, JM, Matsunami, H, McIntire, WS, Ruggiero, CE, Tanizawa, K, Yamaguchi, H (1997) Biochemistry 36:16116-16133.

20. Carter, SR, McGuirl, MA, Brown, DE, Dooley, DM (1994) J.Inorg.Biochem. 56:127-141.

21. Elmore, B, Bollinger, JA, Dooley, DM (2002) J. Biol. Inorg. Chem. 7:565-579.

22. McGuirl, MA, McCahon, CD, McKeown, KA, Dooley, DM (1994) Plant Physiol. 106:1205-1211.

23. Green, J, Haywood, GW, Large, PJ (1983) Biochem. J. 211:481-493.

24. Rangachari, PK (1992) Am. J. Physiol. 262:G1-13.

25. Gupta, MK, Gupta, P, Rezai, F (2001) Clin. Cardiol. 24:258-259.

26. Kumagai, H ,Yamada, H (2000) *Structure and Function of Amine Oxidases*. Mondovi, B (eds) CRC Press, Boca Raton, Florida.

27. Bachrach, U, Heimer, Y (1985) *The Physiology of Polyamines*. Bachrach, U, Heimer, Y (eds) CRC Press, Boca Raton, Florida.

28. Seiler, N (2000) Neurochem. Res. 25:471-490.

29. Nilsson, BO (1999) Inflamm. Res. 48:509-515.

30. Grillo, MA, Colombatto, S (2004) Amino Acids 26:345-351.

31. Elmore, B0 (2002) *Characterization of Recombinant Human Kidney Diamine Oxidase and Equine Plasma Amine Oxidase*, PhD Thesis, Montana State University, Bozeman.

32. Lyles, GA (1996) Int. J. Biochem. Cell Biol. 28:259-274.

33. Langford SD, Trent MB, Balakumaran A, Boor PJ (1999) Toxicol. Appl. Pharmacol. 155:237-244.

34. Matyus, P, Dajka-Halasz, B, Foldi, A, Haider, N, Barlocco, D, Magyar, K (2004) Curr. Med. Chem. 11:1285-1298.

35. O'Sullivan, J, Unzeta, M, Healy, J, O'Sullivan, MI, Davey, G, Tipton, KF (2004) Neurotoxicology 25:303-315.

36. Yu, PH, Wright, S, Fan, EH, Lun, ZR, Gubisne-Harberle, D (2003) Biochim. Biophys. Acta 1647:193-199.

37. Jaakkola, K, Jalkanen, S, Kaunismaki, K, Vanttinen, E, Saukko, P, Alanen, K, Kallajoki, M, Voipio-Pulkki, LM, Salmi, M (2000) J. Am. Coll. Cardiol. 36:122-129.

38. Jaakkola, K, Nikula, T, Holopainen, R, Vahasilta, T, Matikainen, MT, Laukkanen, ML, Huupponen, R, Halkola, L, Nieminen, L, Hiltunen, J, Parviainen, S, Clark, MR, Knuuti, J, Savunen, T, Kaapa, P, Voipio-Pulkki, LM, Jalkanen, S (2000) Am. J. Pathol. 157:463-471.

39. Enrique-Tarancon, G, Castan, I, Morin, N, Marti, L, Abella, A, Camps, M, Casamitjana, R, Palacin, M, Testar, X, Degerman, E, Carpene, C, Zorzano, A (2000) Biochem Journal 350 (Pt 1):171-180.

40. Kamsler, A, Segal, M (2004) Mol. Neurobiol. 29:167-178.

41. Kumar, V, Dooley, DM, Freeman, HC, Guss, JM, Harvey, I, McGuirl, MA, Wilce, MCJ, Zubak, VM (1996) Structure 4:943-955.

42. Li, RB, Klinman, JP, Mathews, FS (1998) Structure 6:293-307.

43. Parsons, MR, Convery, MA, Wilmot, CM, Yadav, KDS, Blakeley, V, Corner, AS, Phillips, SEV, McPherson, MJ, Knowles, PF (1995) Structure 3:1171-1184.

44. Duff, AP, Cohen, AE, Ellis, PJ, Kuchar J.A., Langley, DB, Shepard, EM, Dooley, DM, Freeman, HC, Guss, JM (2003) Biochemistry 42:15148-15157.

45. Lunelli, M, Di Paolo, ML, Biadene, M, Calderone, V, Battistutta, R, Scarpa, M, Rigo, A, Zanotti, G (2005) J. Mol. Biol. doi:10.1016/j.jmb.2004.12.038

46. Nymalm, Y, Kidron, H, Soderholm, A, Viitanen, L, Kaukonen, K, Pihlavisto, M, Smith, D, Veromaa, T, Airenne, TT, Johnson, MS, Salminen, TA (2003) Acta Crystallogr. D. Biol. Crystallogr. 59:1288-1290.

47. Dove, JE, Klinman, JP (2001) Adv. Protein Chem. 58:141-174.

48. Dawkes, HC, Phillips, SEV (2001) Curr. Opin. Struct. Biol. 11:666-673.

49. Halcrow, M, Phillips, S, Knowles, P (2000) Amine Oxidases and Galactose Oxidase, In: *Subcellular Biochemistry*. Holzenburg, A. and Scrutton, N (eds) Kluwer Academic/Plenum Publishers, New York, pp. 183-231.

50. Wilmot, CM, Murray, JM, Alton, G, Parsons, MR, Convery, MA, Blakeley, V, Corner, AS, Palcic, MM, Knowles, PF, McPherson, MJ, Phillips, SEV (1997) Biochemistry 36:1608-1620.

51. Chen, ZW, Schwartz, B, Williams, NK, Li, RB, Klinman, JP, Mathews, FS (2000) Biochemistry 39:9709-9717.

52. Zhang, XP, McIntire, WS (1996) Gene 179:279-286.

53. Shepard, EM, Smith, J, Elmore, B, Kuchar J.A., Sayre, LM, Dooley, DM (2002) Eur. J. Biochem. 269:3645-3658.

54. O'Connell, KM, Langley, DB, Shepard, EM, Duff, AP, Jeon, HB, Sun, G, Freeman, HC, Guss, JM, Sayre, LM, Dooley, DM (2004) Biochemistry 43:10965-10978.

55. Brown, DE, McGuirl, MA, Dooley, DM, Janes, SM, Mu, D, Klinman, JP (1991) J. Biol. Chem. 266:4049-4051.

56. Ruggiero, CE, Dooley, DM (1999) Biochemistry 38:2892-2898.

57. Kim, M, Okajima, T, Kishishita, S, Yoshimura, M, Kawamori, A, Tanizawa, K, Yamaguchi, H (2002) Nature Struct. Biol. 9:591-596.

58. Dove, JE, Schwartz, B, Williams, NK, Klinman, JP (2000) Biochemistry 39:3690-3698.

59. Schwartz, B, Dove, JE, Klinman, JP (2000) Biochemistry 39:3699-3707.

60. Schwartz, B, Olgin, AK, Klinman, JP (2001) Biochemistry 40:2954-2963.

61. Brazeau, BJ, Johnson, BJ, Wilmot, CM (2004) Arch. Biochem. Biophys. 428:22-31.

62. Prabhakar, R, Siegbahn, PEM (2004) J. Amer. Chem. Soc. 126:3996-4006.

63. Matsunami, H, Okajima, T, Hirota, S, Yamaguchi, H, Hori, H, Kuroda, S, Tanizawa, K (2004) Biochemistry 43:2178-2187.

64. Nakamura, N, Matsuzaki, R, Choi, YH, Tanizawa, K, Sanders-Loehr, J (1996) J. Biol. Chem. 271:4718-4724.

65. Choi, YH, Matsuzaki, R, Suzuki, S, Tanizawa, K (1996) J. Biol. Chem. 271:22598-22603.

66. Schwartz, B, Green, EL, Sanders-Loehr, J, Klinman, JP (1998) Biochemistry 37:16591-16600.

67. Hevel, JM, Mills, SA, Klinman, JP (1999) Biochemistry 38:3683-3693.

68. Murray, JM, Kurtis, CR, Tambyrajah, W, Saysell, CG, Wilmot, CM, Parsons, MR, Phillips, SEV, Knowles, PF, McPherson, MJ (2001) Biochemistry 40:12808-12818.

69. Kuchar J.A., Dooley, DM (2001) J. Inorg. Biochem. 83:193-204.

70. Murray, JM, Saysell, CG, Wilmot, CM, Tambyrajah, WS, Jaeger, J, Knowles, PF, Phillips, SEV, McPherson, MJ (1999) Biochemistry 38:8217-8227.

71. Mure, M, Klinman, JP (1995) J. Am. Chem. Soc. 117:8707-8718.

72. Mure, M, Mills, SA, Klinman, JP (2002) Biochemistry 41:9269-9278.

73. Coleman, AA, Scaman, CH, Kang, YJ, Palcic, MM (1991) J. Biol. Chem. 266:6795-6800.

74. Alton, G, Taher, TH, Beever, RJ, Palcic, MM (1995) Arch. Biochem. Biophys. 316:353-361.

75. Uchida, M, Ohtani, A, Kohyama, N, Okajima, T, Tanizawa, K, Yamamoto, Y (2003) Biosci. Biotechnol. Biochem. 67:2664-2667.

76. Plastino, J, Green, EL, Sanders-Loehr, J, Klinman, JP (1999) Biochemistry 38:8204-8216.

77. Dooley, DM, McGuirl, MA, Brown, DE, Turowski, PN, McIntire, WS, Knowles, PF (1991) Nature 349:262-264.

78. Dooley, DM, Brown, DE (1996) J. Bio. Inorg. Chem. 1:205-209.

79. Turowski, PN, McGuirl, MA, Dooley, DM (1993) J. Biol. Chem. 268:17680-17682.

80. Su, QJ, Klinman, JP (1998) Biochemistry 37:12513-12525.

81. Goto, Y, Klinman, JP (2002) Biochemistry 41:13637-13643.

82. Mills, SA, Klinman, JP (2000) J. Amer. Chem. Soc. 122:9897-9904.

83. Mills, SA, Goto, Y, Su, QJ, Plastino, J, Klinman, JP (2002) Biochemistry 41:10577-10584.

84. Barker, R, Boden, N, Cayley, G, Charleton, SC, Henson, R, Holmes, MC, Kelly, ID, Knowles, PF (1979) Biochem. J. 177:289-302.

85. Olsson, B, Olsson, J, Pettersson, G (1978) Eur. J. Biochem. 87:1-8.

86. Wilmot, CM, Hajdu, J, McPherson, MJ, Knowles, PF, Phillips, SEV (1999) Science 286:1724-1728.

87. Duff, AP, Trambaiolo, DM, Cohen, AE, Ellis, PJ, Juda, GA, Shepard, EM, Langley, DB, Dooley, DM, Freeman, HC, Guss, JM (2004) J. Mol. Biol. 344:599-607.

88. Schoenborn, BP, Watson, HC, Kendrew, JC (1965) Nature 207:28-30.

89. Kishishita, S, Okajima, T, Kim, M, Yamaguchi, H, Hirota, S, Suzuki, S, Kuroda, S, Tanizawa, K, Mure, M (2003) J. Amer. Chem. Soc. 125:1041-1055.

90. Hirota, S, Iwamoto, T, Kishishita, S, Okajima, T, Yamauchi, O, Tanizawa, K (2001) Biochemistry 40:15789-15796.

91. Padiglia, A, Medda, R, Pedersen, JZ, Finazzi-Agro, A, Lorrai, A, Murgia, B, Floris, G (1999) J. Bio. Inorg. Chem. 4:608-613.

92. Medda, R, Padiglia, A, Bellelli, A, Sarti, P, Santanche, S, Agro, AF, Floris, G (1998) Biochem. J. 332:431-437.

93. Tanizawa, K, Matsuzaki, R, Shimizu, E, Yorifuji, T, Fukui, T (1994) Biochem. Biophys. Res. Commun. 199:1096-1102.

94. Shimizu, E, Ohta, K, Takayama, S, Kitagaki, Y, Tanizawa, K, Yorifuji, T (1997) Biosci. Biotechnol. Biochem. 61:501-505.

95. Skerra, A, Schmidt, TGM (1999) Biomolecular Engineering 16:79-86.

96. Szutowicz, A, Kobes, RD, Orsulak, PJ (1984) Anal. Biochem. 138:86-94.

97. Janes, SM, Klinman, JP (1991) Biochemistry 30:4599-4605.

98. Neumann, R, Hevey, R, Abeles, RH (1975) J. Biol. Chem. 250:6362-6367.

99. Tabor, CW, Tabor, H, Rosenthal, SM (1954) J. Biol. Chem. 208:645-661.

100. Dooley, DM, Brown, DE (1995) Methods Enzymol. 258:132-140.

101. Steinebach, V, Benen, JAE, Bader, R, Postma, PW, De Vries, S, Duine, JA (1996) Eur. J. Biochem. 237:584-591.

102. Cai, DY, Williams, NK, Klinman, JP (1997) J. Biol. Chem. 272:19277-19281.

103. DuBois, JL, Klinman, JP (2005) Arch. Biochem. Biophys. 433:255-265.

104. Juda, GA, Bollinger, JA, Dooley, DM (2001) Protein Expression and Purification 22:455-461.

105. Shepard, EM, Heggem, H, Juda, GA, Dooley, DM (2003) Biochim. Biophys. Acta Protein Struct. Mol. Enzymol. 1647:252-259.

106. Hess, CR, Juda, GA, Dooley, DM, Amii, RN, Hill, MG, Winkler, JR, Gray, HB (2003) J. Amer. Chem. Soc. 125:7156-7157.

107. Shepard, EM, Juda, GA, Ling, KQ, Sayre, LM, Dooley, DM (2004) J. Biol. Inorg. Chem. 9:256-268.

108. Mure, M, Klinman, JP (1993) J. Am. Chem. Soc. 115:7117-7127.

109. Segel, IH (1975) *Enzyme Kinetics: Behavior and Analysis of Rapid Equilibrium and Steady-State Enzyme Systems*. John Wiley and Sons, New York, New York.

110. Zhang, Q, Mashima, Y, Noda, S, Imamura, Y, Kudoh, J, Shimizu, N, Nishiyama, T, Umeda, S, Oguchi, Y, Tanaka, Y, Iwata, T (2003) Gene 318:45-53.

111. O'Sullivan, J, Unzeta, M, Healy, J, O'Sullivan, MI, Davey, G, Tipton, KF (2004) Neurotoxicology 25:303-315.

112. Stanek, J, Caravatti, G, Capraro, HG, Furet, P, Mett, H, Schneider, P, Regenass, U (1993) J. Med. Chem. 36:46-54.

113. Hall JE, Kerrigan JE, Ramachandran K, Bender BC, Stanko JP, Jones SK, Patrick DA, Tidwell RR (1998) Antimicrob. Agents Chemother. 42:666-674.

114. Francesconi I, Wilson WD, Tanious FA, Hall JE, Bender BC, Tidwell RR, McCurdy D, Boykin DW (1999) J. Med. Chem. 42:2260-2265.

115. Stanek, J, Caravatti, G, Frei, J, Furet, P, Mett, H, Schneider, P, Regenass, U (1993) J. Med. Chem. 36:2168-2171.

116. Paridaens, R, Uges, DR, Barbet, N, Choi, L, Seeghers, M, Van der Graaff, W, Groen, HJ, Dumez, H, Buuren, IV, Muskiet, F, Capdeville, R, Oosterom, AT, deVries, EG (2000) Br. J. Cancer 83:594-601.

117. Dorhout, B, Odink, MF, deHoog, E, Kingma, AW, van der Veer, E, Muskiet, FA (1997) Biochim Biophys Acta 1335:144-152.

118. Tomasi, S, Le Roch, M, Renault, J, Corbel, JC, Uriac, P, Carboni, B, Moncoq, D, Martin, B, Delcros, JG (1998) Bioorg. Med. Chem. Lett. 8:635-640.

119. Queener, SF (1995) J. Med. Chem. 38:4739-4759.

120. Van Voorhis, WC (1990) Drugs 40:176-202.

121. Tidwell, RR, Kilgore Jones, S, Geratz, JD, Ohemeng, KA, Cory, M (1990) J. Med. Chem. 33:1252-1257.

122. Perrine, D, Chenu, JP, Georges, P, Lancelot, JC, Saturnino, C, Robba, M (1995) Antimicrob. Agents Chemother. 39:339-342.

123. Bitonti, AJ, Bush, TL, McCann, PP (1989) Biochem. J. 257:769-774.

124. Pegg, AE, Hu, RH (1995) Cancer Lett. 95:247-252.

125. Lee, Y, Ling, KQ, Lu, XL, Silverman, RB, Shepard, EM, Dooley, DM, Sayre, LM (2002) J. Amer. Chem. Soc. 124:12135-12143.

126. Dooley, DM, Golnik, KC (1983) J. Biol. Chem. 258:4245-4248.

127. Dooley, DM, Cote, CE (1985) Inorg. Chem. 24:3996-4000.

128. McGuirl, MA, Brown, DE, Dooley, DM (1997) JBIC 2:336-343.

129. He, Z, Zou, Y, Greenaway, FT (1995) Arch. Biochem. Biophys. 319:185-195.

130. Steinebach, V, De Vries, S, Duine, JA (1996) J. Biol. Chem. 271:5580-5588.

131. Imanaga, Y (1989) Investigations on the Active Site of Glucose Dehydrogenase from *Pseudomonas fluorescens*, In: *PQQ and Quinoproteins*. Jongejan, JA, Duine JA (eds) Kluwer Academic Publishers, Boston, MA.

132. Finazzi-Agro, A, Rinaldi, A, Floris, G, Rotilio, G (1984) FEBS Lett. 176:378-380.

133. Dooley, DM, Cote, CE, McGuirl, MA, Bates, JL, Perkins, JB, Moog, RS, Singh, I, Knowles, PF, McIntire, WS (1989) Copper-PQQ Interactions in Amine Oxidases, In: *PQQ and Quinoproteins*. Jongejan, JA, and Duine, JA (eds) Kluwer Academic Publishers, Boston, MA, pp. 307-316.

134. Dooley, DM, McIntire, WS, McGuirl, MA, Cote, CE, Bates, JL (1990) J. Am. Chem. Soc. 112:2782-2789.

135. Agostinelli, E, De Matteis, G, Sinibaldi, A, Mondovi, B, Morpurgo, L (1997) Biochem. J. 324:497-501.

136. De Matteis, G, Agostinelli, E, Mondovi, B, Morpurgo, L (1999) J. Bio. Inorg. Chem. 4:348-353.

137. Segel, IH (1976) *Biochemical Calculations 2nd Edition*. John Wiley & Sons, New York, NY.

138. Douglas, B, McDaniel, D, Alexander, J (1994) *Concepts and Models of Inorganic Chemistry 3rd Edition*, John Wiley and Sons, Inc., New York, NY.

139. Murthy, NN, Karlin, KD (1995) *Mechanistic Bioinorganic Chemistry*, (Thorp, H.H., Pecoraro, V.L., Eds.), pp 165-193, Amer. Chem. Soc., Washington D.C..

140. Karlin, KD, Tyekl'ar, Z (1993) *Bioinorganic Chemistry of Copper*. Chapman & Hall, New York.

141. Whittaker, JW (1999) Essays Biochem 34:155-172.

142. Fry, HC, Scaltrito, DV, Karlin, KD, Meyer, GJ (2003) J. Am. Chem. Soc. 125:11866-11871.

143. Ho, RYN, Liebman, JF, Valentine, JS (1995) Overview of the Energetics and Reactivity of Oxygen, In: *Active Oxygen in Chemistry.* Foote, C. S., Valentine, JS, Greenberg, A, and Liebman, JF (eds) Blackie Academic and Professional, New York, pp. 1-23.

144. Padiglia, A, Medda, R, Bellelli, A, Agostinelli, E, Morpurgo, L, Mondovi, B, Finazzi-Agrò, A, Floris, G (2001) Eur. J. Inorg. Chem. 1:35-42.

145. Prabhakar, R, Siegbahn, PEM, Minaev, BF (2003) Biochim. Biophys. Acta Protein Struct. Mol. Enzymol. 1647:173-178.

146. Dooley, DM, Cote, CE, Golnik, KC (1984) Journal of Molecular Catalysis 23:243-253.

147. Lindstrom, A, Olsson, B, Pettersson, G (1974) Eur. J. Biochem. 48:237-243.

148. Kuchar J.A. (2001) *Cloning, Sequence Analysis, and Characterization of the "Lysyl Oxidase" from Pichia pastoris*, PhD. thesis, Montana State University, Bozeman, MT.

149. Meites, L, Meites, T (1948) Anal. Chem 20:984-985.

150. Juda, GA, Shepard, EM, Elmore, B0, Dooley, DM (2005) Biochemistry (Submitted).

151. Dooley, DM, McGuirl, MA (1986) Inorg. Chim. Acta 123:231-236.

152. Dooley, DM, McGuirl, MA, Cote, CE, Knowles, PF, Singh, I, Spiller, M, Brown, RD, III, Koenig, SH (1991) J. Amer. Chem. Soc. 113:754-761.

153. Oi, S, Inamasu, M, Yasunobu, KT (1970) Biochemistry 9:3378-3383.

154. Nordlie, R (1982) Kinetic Examination of Enzyme Mechanisms INvolving Branched Reaction Pathways-A Detailed Considerations of Multifunctional Glucose-6-phosphatase, In: *Methods and Enzymology*, (Purich, D.L., Ed.), pp 319-323, Academic Press, New York.

155. Webb, BC, Todhunter, JA, Purich, DL (1976) Archives of Biochemistry and Biophysics 173:282-292.

156. Cleland, WW (1963) Biochimica et Biophisica Acta 67:104-137.

157. Cleland, WW (1963) Biochimica et Biophisica Acta 67:173-187.

158. Cleland, WW (1963) Biochimica et Biophisica Acta 67:188-196.

159. Cai, DY, Dove, J, Nakamura, N, Sanders-Loehr, J, Klinman, JP (1997) Biochemistry 36:11472-11478.

160. Mure, M, Brown, DE, Saysell, C, Rogers, MS, Wilmot, CM, Kurtis, CR, McPherson, MJ, Phillips, SE, Knowles, PF, Dooley, DM (2005) Biochemistry 44:1568-1582.

161. Mure, M, Kurtis, CR, Brown, DE, Rogers, MS, Tambyrajah, WS, Saysell, C, Wilmot, CM, Phillips, SE, Knowles, PF, Dooley, DM, McPherson, MJ (2005) Biochemistry 44:1583-1594.

162. Medda, R, Padiglia, A, Pedersen, JZ, Rotilio, G, Finazzi-Agro, A, Floris, G (1995) Biochemistry 34:16375-16381.

163. Oi, S, Inamasu, M, Yasunobu, KT (1970) Biochemistry 9, #17:3378-3383.

164. Delano, W.L. (2002) Delano Scientific, San Carlos, CA.